The Hong Kong Polytechnic University

Department of Applied Physics

Electrospinning of Conducting Polymer Blend and Composite Nanofibers for Sensor Applications

LI Wai Kit

A thesis submitted in partial fulfillment of the requirements for the degree

of Master of Philosophy

August 2009

CERTIFICATE OF ORIGINALITY

I hereby declare that this thesis is my own work and that, to the best of my knowledge and belief, it reproduces no material previously published or written, nor material that has been accepted for the award of any other degree or diploma, except where due acknowledgement has been made in the text.

LI Wai Kit

Abstract

Study of electrospinning of polymer nanofibers for this project has spread into three areas: investigation of the electrospinning process, electrical properties of Polyethylene oxide (PEO)/carbon black nanofibers, and PMMA/PANi(AMPS) for alcohol sensing.

In order to optimize the fiber size and suppress the bead formation, different electrospinning conditions and solutions of PMMA have been investigated. Highly aligned electrospun nanofibers have been made successfully by using a high speed rotating collector with the surface velocity beyond 6 ms^{-1}. On the other hand, aligned PEO/carbon black nanofibers has been electrospun. Characterization of the fibers has been done by using SEM, TEM and FTIR. As revealed by the polarized FTIR, the nanofibers produced are mainly in trans configuration where the helix structure were suppressed. With the present of carbon black inclusion, the conductivity of PEO nanofibers decreases significantly. This indicates that the conducting phase of the electrospun composite nanofibers would not help to raise the conductivity of the composite fiber, which is contrary to the conventional concept.

Lastly, the study of PMMA/PANi(AMPS) nanofibers is performed, which is aimed to investigate the nanofibers response with respect to various alcohol molecules: such as the methanol, ethanol and isopropanol, respectively. The electrical conduction of the samples respond to various concentrations of alcohol and their repeatability of the signals were studied, and two mechanisms that responsible to the resistance change are suggested. As the PANi is the essential component responsible to the alcohol sensing but it will also hinder the formation of fiber forming in the electrospinning process, an optimum fraction of the PANi has been determined in this part of investigation.

Publications

Li, Wai-Kit, & Wong, Yuen-Wah (2009), Electrical properties of electrospun nanofibers of PEO/carbon black composite. *Solid State Phenomena, 151*, 67-71.

Acknowledgements

I would like to acknowledge the support of my supervisor Dr. Y. W. Wong for his excellent guidance, constant encouragement and invaluable advice throughout the project. I would also like to thank my family, and my research companions: Mr. H. K. Lau, Ms. W. F. Fong, Mr. H. F. Wong, Ms. C. Y. Lam, Mr. K. H. Chau, Mr. Y. K. Chan, Mr. S. M. Mok and Ms. M. K. Lee for their spiritual support and encouragement. Special thanks should be given to Mr. C. S. Lo and Mr. M. N. Yeung for their assistance in experiment.

I would like to acknowledge the Research Committee of The Hong Kong Polytechnic University of the provision of a research grant (project no. G-RP0C).

Table of Contents

Chapter 1

Introduction

1.1 Background

Electrospinning is a convenient and versatile process for the purpose of producing ultrafine fibers of materials which can be prepared in liquid form, for instance the dissolved polymers or ceramics in sol-gel form. The size of the solidified fibers can be in the order of sub-microns or even down to the nanometer scale. Throughout the decades, significant progress has been made in this process and the resultant nanoscaled fibers have been subjected to a wide range of applications. Although there are other methods to fabricate polymer nanofibers, electrospinning is the most simple and cost effective. It can be used for mass production. As the nanofibers possess the large surface area to volume ratio, they are desirable for gas sensing application.

Polyethylene oxide (PEO) is a well known polymer electrolyte. The charge movement inside PEO is due to the ion migration driven by the applied electric field. Carbon black is a kind of conducting powder of which the majority charge carrier is the electrons. It has been widely used for blending with polymers to form a composite in order to enhance the electrical conduction of the polymers, as well as the mechanical properties. Although PEO is an electrolytic polymer, its conductivity may be further improved by the introduction of carbon black powders for the benefit of applications in secondary battery. In addition, due to the different electrical conduction mechanisms of PEO and carbon black, the electrospun nanoscaled PEO/carbon black composite fibers would show some interesting electrical properties in the quasi-one-dimensional structure.

Other than the polymer electrolytes, there are some polymers so called intrinsic conducting polymers of which the majority charge carriers are electrons or holes. They have been found many applications from electronic devices; metallic interconnects in circuits, chemical sensors, electromagnetic radiation shielding and rust prevention of metals etc. Polyaniline (PANi) is one of the intrinsic conducting polymers which have been investigated the most. It is a stable polymer with good electrical properties with suitable doping. PANi is sensible to alcohol molecules and thus has been electrospun for alcohol sensing investigation in this project. Since the electrospun fibers have a huge surface area to volume ratio, a fast responding time compared to the thin film type sensor is expected. In this thesis, the first part will discuss the influence of polymer solutions and electrospinning setup on the morphology of fibers. This work is aimed at producing smooth and oriented fibers.

After that, discussion will be carried out on the composite fibers of PEO and carbon black. It will focus on their electrical characteristics to observe whether this kind of composite fibers (electrolyte polymer/electronic conductive particles) is suitable for sensing application.

The last part will be followed by the discussion on AMPS doped PANi blended with PMMA. AMPS helped to enhance the conductivity and PMMA act as a carrier of the PANi. The PMMA molecular chain has sufficiently high molecular weight which helps to form smooth and thin fibers with electrospinning.

1.2 Electrospinning

1.2.1 Introduction

In general, the diameter of polymer fibers produced by various methods ranges from micrometer to nanometer. The smaller the diameter the larger is the surface area to volume ratio. This ratio of a nanoscaled fiber can be a thousand times larger than a microscaled fiber. Together with the flexibility in surface functionalities and superior mechanical performance such as stiffness and tensile strength make the polymer nanofibers to be the optimal candidates of many important applications such as the gas sensing.

In recent decade, a number of processing techniques have been used to prepare polymer nanofibers, such as drawing (Ondarçuhu & Joachim, 1998), template synthesis (Feng et al., 2002; Martin, 1996), phase separation (Ma & Zhang, 1999), self-assembly (Liu et al., 1999; Whitesides & Grzybowski, 2002) and electrospinning (Deitzel, Kleinmeyer, Hirvonen, & Beck Tan, 2001b; Fong & Reneker, 2001).

Among those methods, electrospinning is the most attractive one as the technique is simple and convenient to process and cost effective. Long and continuous nanofibers can be produced by electrospinning and mass production of one-by-one continuous nanofibers can be achieved by further development.

The term “electrospinning” was derived from “electrostatic spinning”. It is a process that had been patented several decades ago (Formhals, 1934), describing an experimental setup for the production of polymer filaments using electrostatic force. Polymer filaments were formed from the solution between two electrodes that carrying electrical charges of opposite polarity. In other words, electrospinning is a process that creates fibers through an electrically charged jet of polymer solution; details of electrospinning setup are introduced in Chapter 2.

After that, the technique was kept advancing and developing. In 1952, Vonnegut and Neubauer invented a simple apparatus for the electrical atomization, they were able to produce streams of highly electrified uniform droplets of about 0.1 mm in diameter by using water or other liquid (Vonnegut & Neubauer, 1952). In 1955, Drozin found that for certain liquids and under suitable conditions, liquid was issued as a highly dispersed aerosol with droplets in relatively uniform size (Drozin, 1955). In 1966, Simons found that fibers produced from more viscous solutions were relatively continuous (Simons, 1966). In 1971, Baumgarten achieved acrylic fibers of 0.05-1.1 μm (Baumgarten, 1971). Since 1980s and up to now, investigations of the process are continuously performed by many researchers. It becomes a surge of interest since the rise of nanotechnology because fibrous structures of polymers with diameters down to nanometers can be fabricated with this process, and the technique is being advanced continuously (Chen et al., 2001; Dalton, Grafahrend, Klinkhammer, Klee, & Möller, 2007; Fong & Reneker, 1999; Huang, Zhang, Kotaki, & Ramakrishna, 2003; Larrondo & St. John Manley, 1981a; Larrondo & St. John Manley, 1981b; Larrondo & St. John Manley, 1981c; Reneker & Chun, 1996; Reneker, Yarin, Fong, & Koombhongse, 2000b; Theron, Zussman, & Yarin, 2004; F. Yang, Murugan, Wang, & Ramakrishna, 2005).

1.2.2 Solution Property

The property of solution is an essential characteristic in electrospinning process. During the process, the polymer solution will be ejected from the tip of a needle. The surface tension, viscosity and electrical property of the solution determine the resultant fiber morphology.

Surface Tension

Since surface tension can be attributed to the formation of beads on electrospun fibers, it is important to understand the role of surface tension in a fluid. When a small drop of water falls in air, it becomes a spherical shape due to the surface tension. For molecules at the surface of the liquid will experience, a net force pulled towards the droplet which is produced by the inner liquid molecules exerting a greater attractive force than the gas molecules outside the liquid as shown in Fig. 1.1. Therefore, contraction of surface of the solution induced by the tension of surface is balanced by repulsive forces from the collision of the interior liquid molecules (Ramakrishna, Fujihara, Teo, Lim, & Ma, 2005).

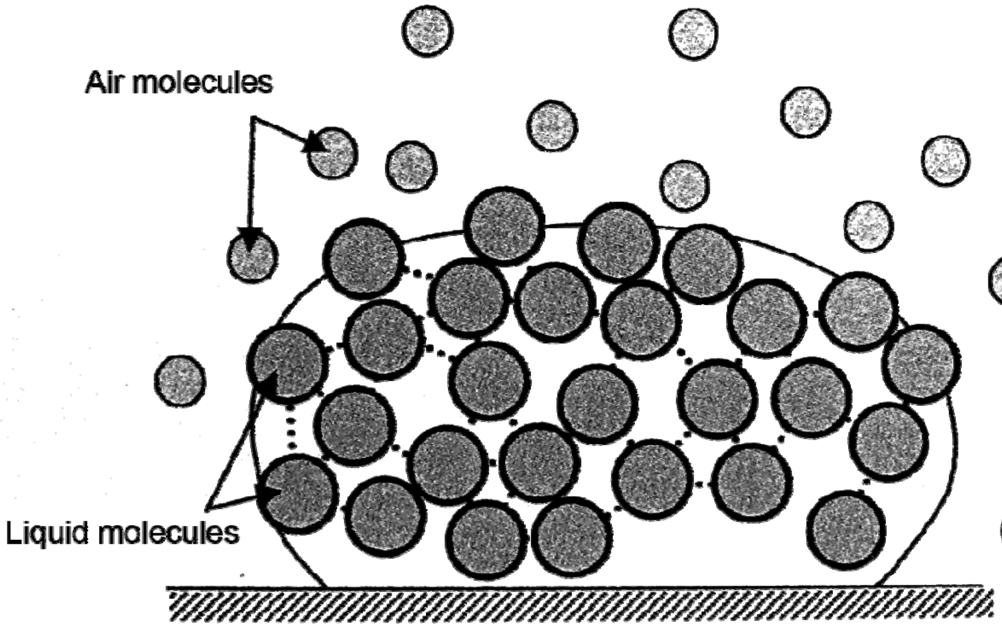

Fig. 1.1 Attractive forces between the liquid molecules are stronger than the attractive forces of the air molecules (Ramakrishna et al., 2005).

Viscosity

Viscosity is a measure of the resistance of a material of the flow. It has a key effect on the resultant electrospun fiber morphology. Usually, viscosity is related to the degree of polymer molecule chain entanglement within the solution.

In polymer solutions, the configuration of polymer chains affects the intrinsic viscosity of the solution. The extended or uncurled configuration of polymer chain molecules will be associated with higher intrinsic viscosity. Otherwise, if polymer chains adopt curled configuration will cause a drop of viscosity (Gurtovenko & Blumen, 2005).

In addition, for a polymer of long chain hydrocarbons, the effect of solvent on the intrinsic viscosity can be illustrated in a relatively simple way. The intrinsic viscosity is high in “good” solvents versus in “poor” solvents (Alfrey, 1947), as the long chain molecules are surrounded by continuous, energetically similar solvent molecules. This reduces contacts between polymer chains and thus favors the uncurled configurations.

In poor solvents, polymer segments attract each other in the solution and squeeze out the solvent. The flexibility of the polymer chain is also a factor, if the chain is rigid, the solvent effect on the intrinsic viscosity is less (Alfrey, Bartovics, & Mark, 1942).

In other words, a higher viscosity means greater interaction between the solvent and polymer molecules. Solvent molecules will tend to spread over the entangled polymer molecules and avoid the solvent molecules to come together under the effect of surface tension (Fig. 1.2).

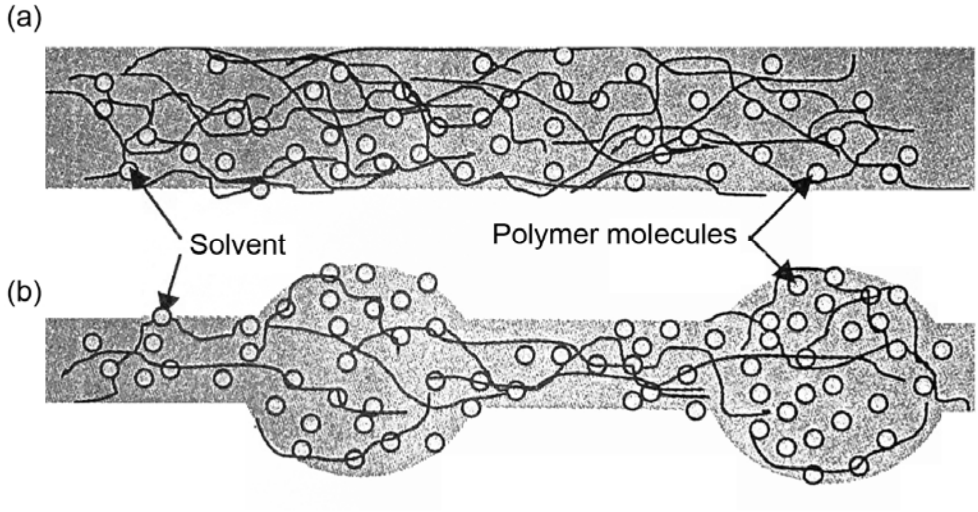

Fig. 1.2 (a) At high viscosity, solvent molecules are distributed over the entanglement of polymer molecules. (b) At low viscosity, solvent molecules start to congregate under surface tension (Ramakrishna et al., 2005).

Conductivity of Solution

In electrospinning process, the solution has to gain enough charges in order to gain sufficient repulsive forces to overcome the surface tension. The abilities of the solution to stretch and draw depend on the ability of the solution to carry charges.

Generally, the electrical conductivity of solvents is very small, typically ranges from 0.1 to 10^{-7} Scm^{-1} as they contain few free ions. Acids, bases, salts and dissolved carbon dioxide may increase the conductivity of the solvent. Mixing chemically non-interacting components including mineral salts, mineral acids, carboxylic acids, some complexes of acids with amines, stannous chloride and some tetraalkylammonium salts, can enhance the conductivity of the solvent significantly. Furthermore, for organic acid solvents, small amount of water will greatly increase the conductivity, which is due to the ionization of the solvent molecules (Ramakrishna et al., 2005).

1.2.3 Electrostatics

Electrospinning takes place when there is a potential difference between the solution and the collector. The charged electrospinning jet is controlled by an external electric field. The electric field surrounds the jet, the dissipation of charges on the fibers that are on the collector influence the electrospinning process. All those factors are related to electrostatics.

Electric Field

An essential element in electrospinning is a high voltage. When high voltage applied to the solution, it induces necessary charges and also the external electric field. The electric field will initiate the process when the solution overcomes the surface tension of the solution. Generally, 6 kV is enough to cause solution drop at the tip of the needle to distort; the shape is known as Taylor Cone (Taylor, 1964). Fig. 1.3 illustrates the initiation of a polymer jet and also the change of shape of the Taylor Cone.

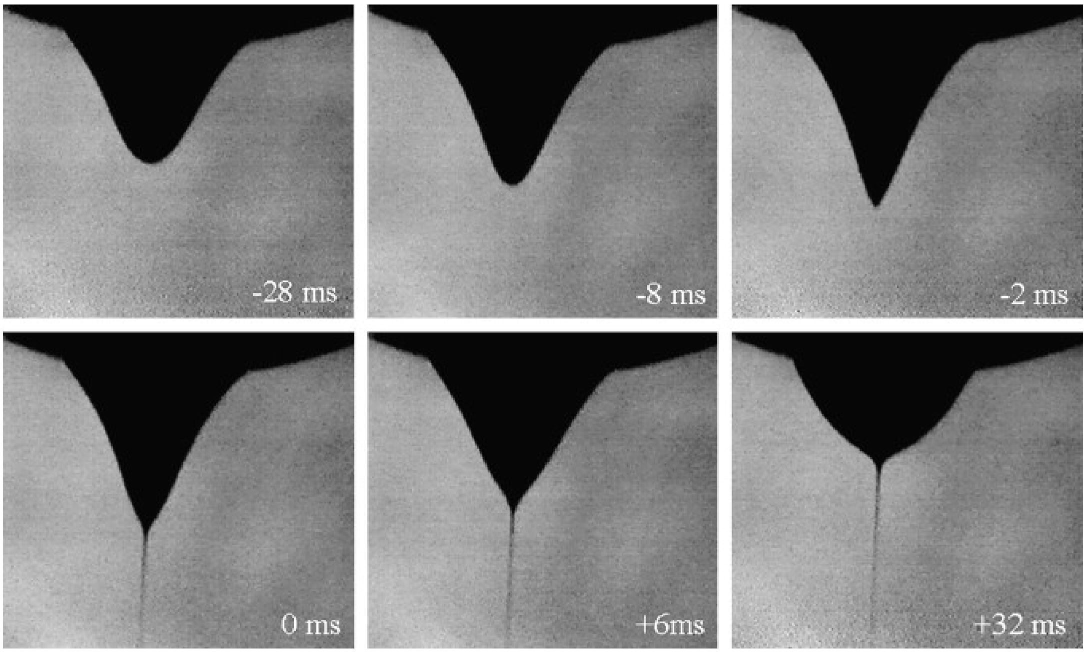

Fig. 1.3 The evolution of the shape of a fluid drop. The time zero was taken to be the frame in which the jet first appeared (Fong & Reneker, 2001).

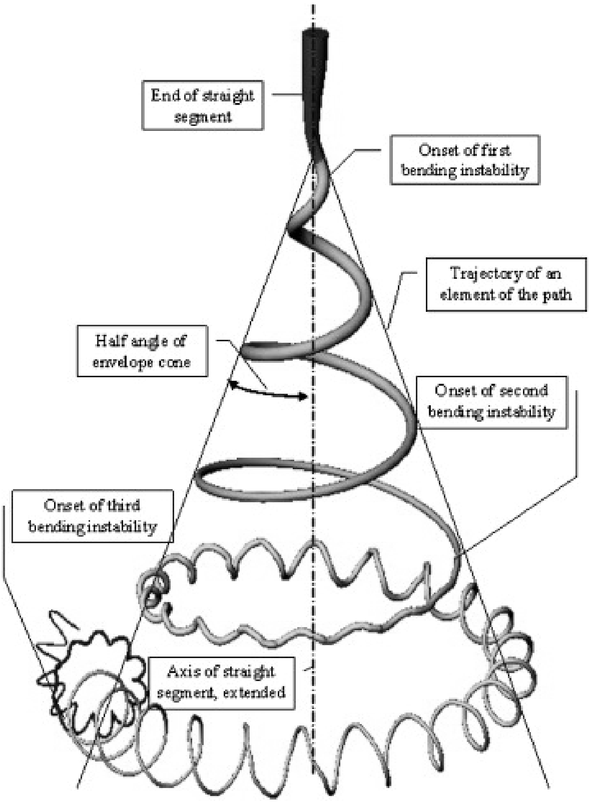

Fig. 1.4 Schematic diagram of an electrospinning jet that contained three successive electrical bending instabilities (Reneker & Fong, 2005).

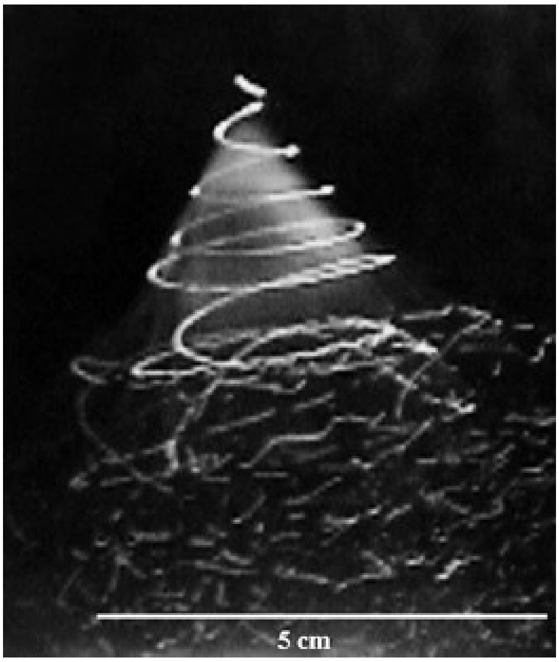

Fig. 1.5 Stroboscopic picture of a jet of polyethylene oxide during electrospinning (Reneker & Fong, 2005).

The repulsive force between charges of polymer jet is another important issue. The repulsive forces stretch the solution and reduce the diameter. Although straight segment is parallel to the axis of the jet and the flow direction, bending perturbations begins (Reneker, Yarin, Fong, & Koombhongse, 2000c; Spivak & Dzenis, 1999; Yarin, Koombhongse, & Reneker, 2001) and grows rapidly into a coil due to the influence of the charge carrier with the jet. By coiling, the electrical energy applied to the jet would elongate the jet efficiently, whether than losing much kinetic energy to keep the leading part ahead. The formation of the coiled path allowed the jet to elongate 10,000 times in common. The phenomenon is known as electrical bending instability. After several turns, a new electrical bending instability formed a smaller coil and so forth until the elongation stopped. Fig. 1.4 depicts the different stages of the formation of the jet and the bending of the coils (Reneker & Fong, 2005). Fig. 1.5 shows the picture of the way that electrical bending instability occurs during electrospinning (Reneker & Fong, 2005).

Field Ionization

Electrospinning is to make use of the repulsive forces between the charges on the polymer jet to stretch the solution. However, the ionized air molecules that would neutralize the charges will impact the process (Fong, Chun, & Reneker, 1999). For instance, electrons will be freed by natural radioactive ionization source, which will ionize the air molecules. The geometry of the electrodes will have an effect on the air breakdown field strength. For sharp electrode, even at a low applied voltage, the electric field at the tip is high enough to reach the air breakdown field which is called the corona discharge. The voltage required is about 5 kV to 6kV when the grounded object is meters away. On the other hand, the positive voltage required for ionization is 30% higher than negative voltage (Jonassen, 2002).

1.2.4 Fiber Alignment

Though the morphology of the nanofibers can be controlled in certain extent, only randomly aligned nanofibers can be achieved by simple electrospinning setup due to the electrical bending instability and the high travelling speed of the jet. However, the fiber architecture may have effects on their collective properties. Highly oriented fiber deposition thus is desirable which will greatly increase the potential applications.

Auxiliary Electrode/Electric Field

A patented method is to fabricate tubular products for blood vessel prosthesis and urinary and bile duct applications (Fig. 1.6a) (Bornat, 1987). The invention is to deposit fibers circumferentially oriented by employing an auxiliary electric field produced by the Aluminum grid in the proximity of the mandrel.

Another similar setup was reported that by asymmetrically placing rotating and charged mandrel between two charged plates (Fig. 1.6b) (Berry, 1990), electrospun fibers with larger diameter could be oriented circumferentially along the longitudinal axis of the tubular structure while small diameter fibers remain randomly oriented.

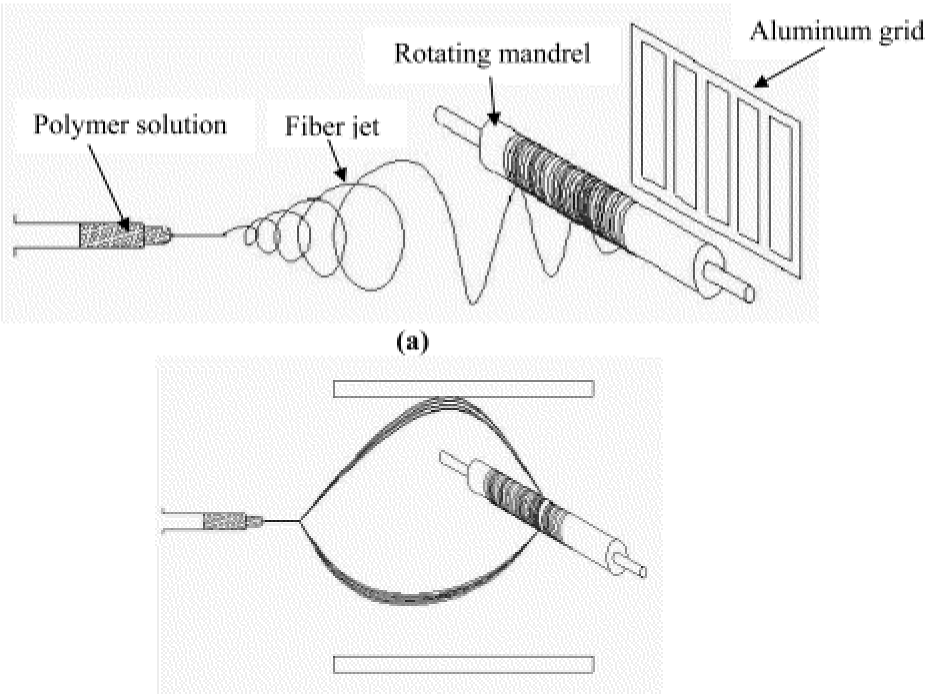

(a)

(b)

Fig. 1.6 Aligning electrospun fibers with an auxiliary electrical field (Huang et al., 2003).

Cylinder Collector with High Rotating Speed

By rotating a cylinder with a high speed up to thousands of rpm, electrospun nanofibers can be oriented circumferentially (Fig. 1.7). Many of researchers have used this technique to obtain aligned electrospun fibers, such as (Fennessey & Farris, 2004; Matthews, Wnek, Simpson, & Bowlin, 2002; Shin et al., 2008; Son, Youk, Lee, & Park, 2004). When the linear speed of the rotating cylinder surface matches the jet depositions, fibers can be placed in a circumferential manner and thus resulting in a good alignment. That speed is named as an alignment speed. If the rotating speed is slower than the alignment speed, fibers will be randomly deposited. One the other hand, if it is too fast, continuous fiber cannot be collected.

Although this method can only achieve the fiber alignments to some extent, it is popular due to its convenience. Besides, this type of collector has been modified as shown in (Fig. 1.8). Stepper motor was introduced to move the drum along its axis to increase the area of fiber collected. Still, the key to achieve good oriented fibers is the rotating speed and the flying speed of the fibers.

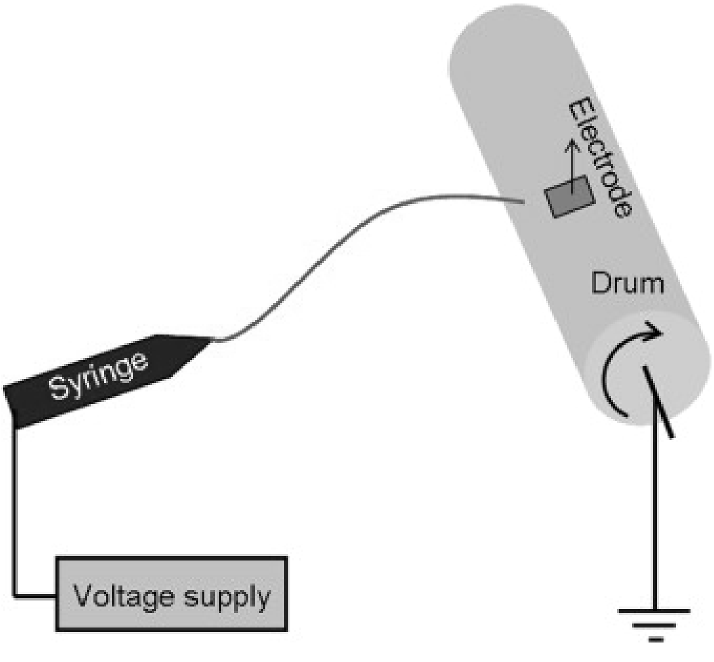

Fig. 1.7 A schematic diagram showing the electrospinning apparatus used to align nanofibers (Zong et al., 2002).

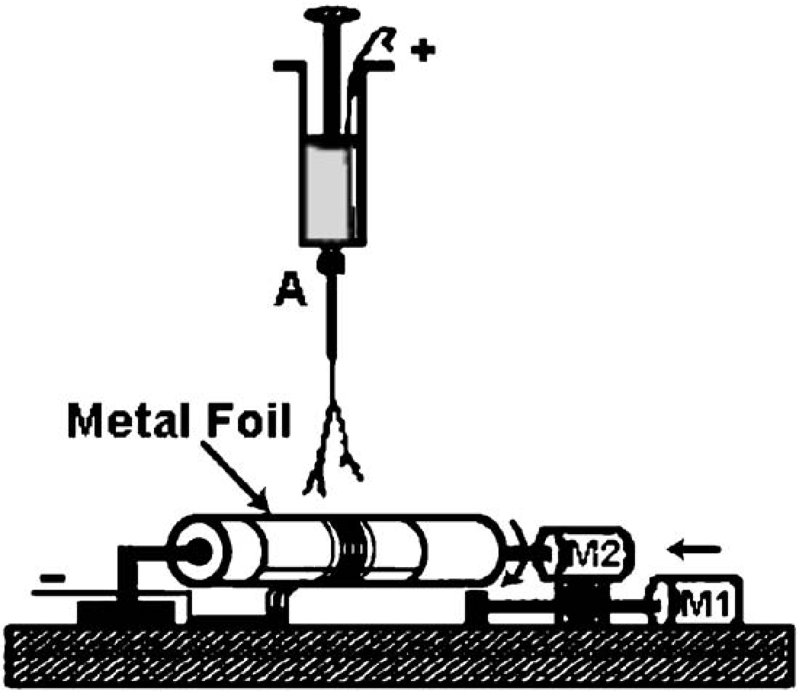

Fig. 1.8 A schematic diagram of the electrospinning setup. A polymer solution is taken inside a syringe (A). Motor M2 is a rotate the drum and M1 is a stepper motor (Sundaray, Subramanian, Natarajan, & Krishnamurthy, 2006).

Parallel Conducting Collector

A simple and versatile method to generate uniaxially aligned arrays of nanofibers was introduced by (Li, Wang, & Xia, 2004). The collector were alternately grounded, nanofibers with pattern was achieved (Fig. 1.9). In addition, it was observed that the substrate also important to achieve good alignment. Fig. 1.10 shows the results when different substrates were used.

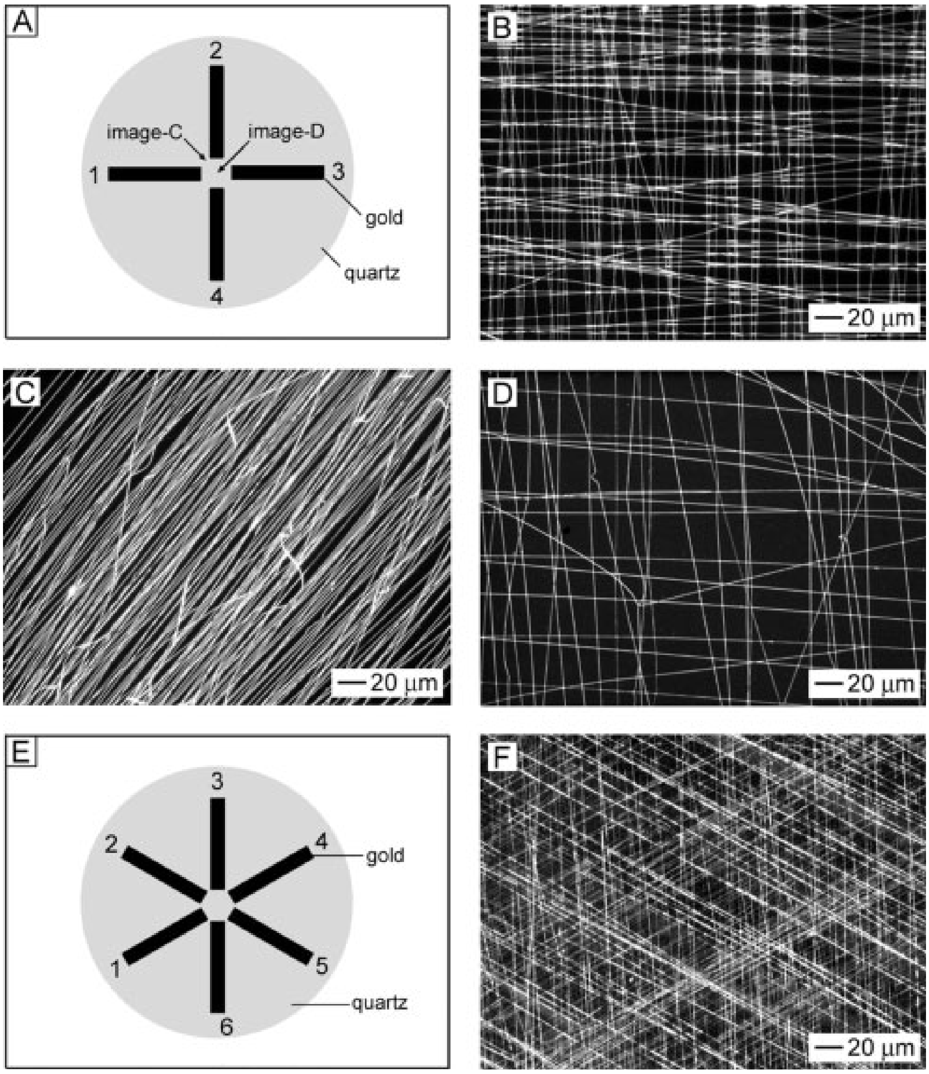

Fig. 1.9 (A,E) Schematic illustrations of test patterns of four (A) and six (E) electrodes deposited on quartz wafers. (B) Optical micrograph of a mesh of PVP nanofibers collected in the center area of the gold electrodes shown in (A). During collection, the electrode pairs of 1-3 and 2-4 were alternately grounded for ~5 s. (C,D) Optical micrographs of PVP nanofibers collected on the four-electrode pattern by grunding all four electrodes at the same time. The regions from which these images were captured are indicated in (A). (F) Optical micrograph of a tri-layer mesh of PVP nanofibers that was collected in the center area of the gold electrodes shown in (E). the electrode pairs

of 1-4, 2-5 and 3-6 were sequentially grounded for 5 s to collect alternating alyers with the orientations of their fibers rotated by ~ 60˚ (Li et al., 2004).

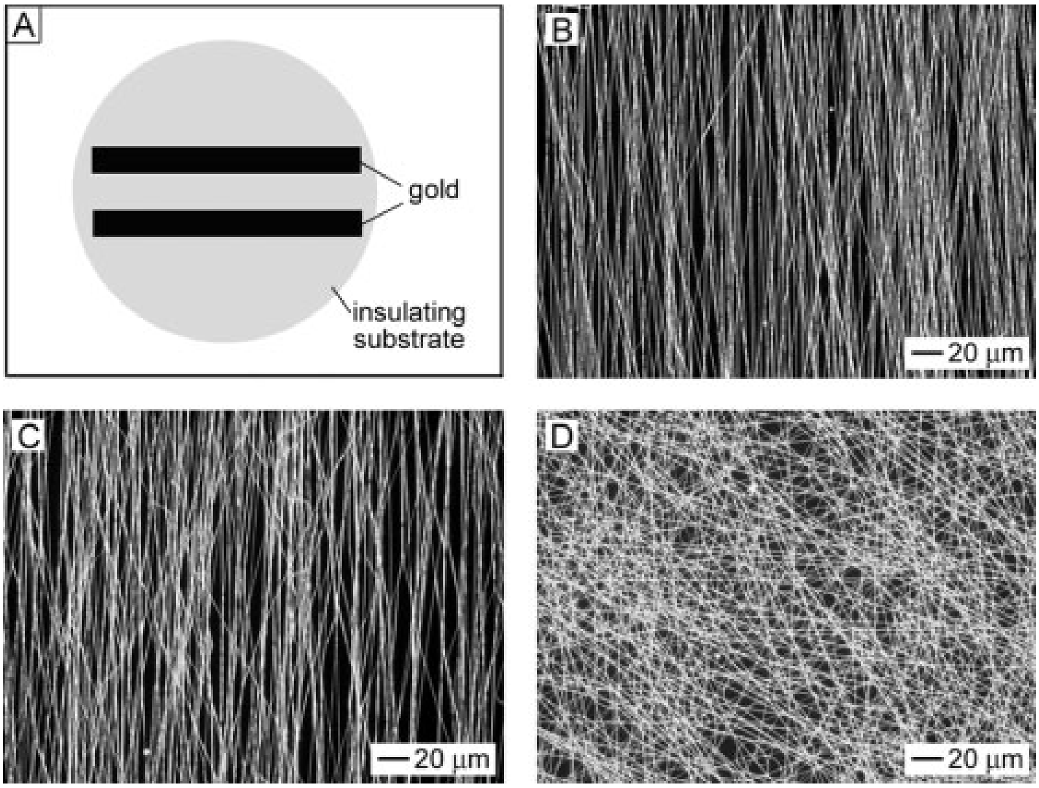

Fig. 1.10 (A) Schematic illustration of a test pattern that comprised two gold electrodes deposited on an insulating solid substrate. Optical micrographs of nanofibers collected between two gold electrodes patterned on various substrates: (B) quartz wafer, (C) polystyrene sheet and (D) glass slide (Li et al., 2004).

Tip Collector

A special technique to collect aligned fibers was reported by (Rafique et al., 2007) as shown in Fig. 1.11. Fibers were ejected individually and one by one, with the grounded tip collector, they were aligned due to the repulsive forces between each fiber. Though a large area of aligned fibers can be collected (Fig. 1.12), the requirement on the solution is complicated. The solution concentration is correlated to the needle diameter; specific needle diameter has to be achieved, unless the fibers will be electrospun continuously and cannot be aligned.

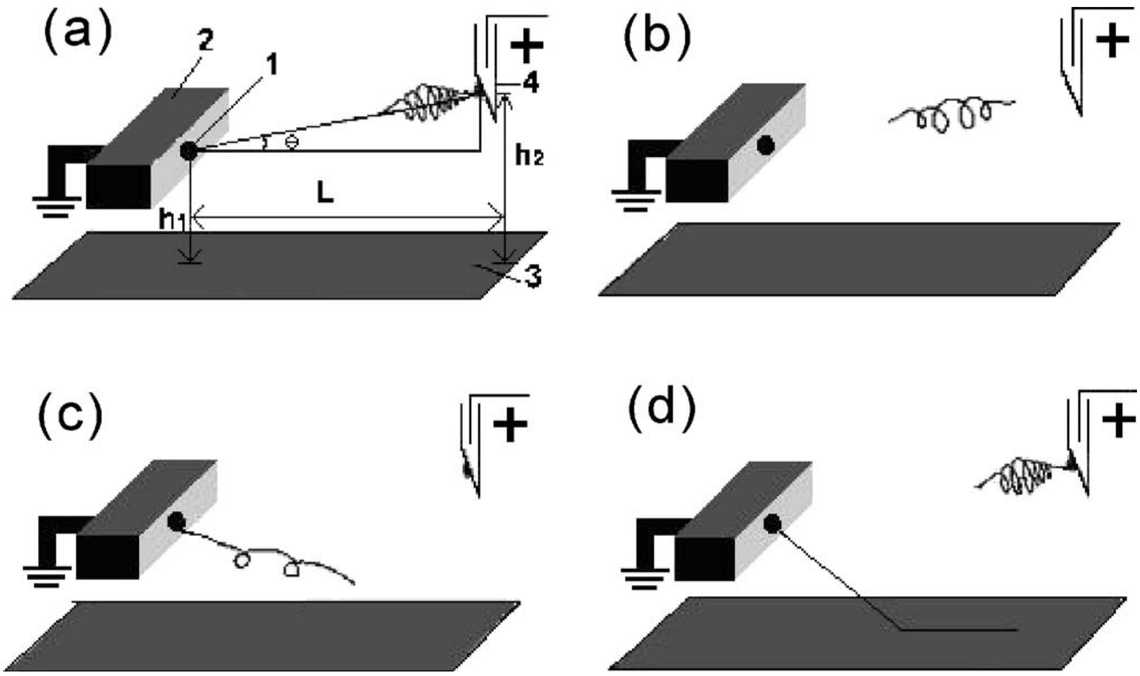

Fig. 1.11 Schematic drawings showing the modified electrospinning setup and aligning mechanism in different time. It comprises mainly of an ordinary syringe with needle (4), and assembled collector, and a support plate (3). The assembled collector consists of one grounded wire electrode (1) and its holder (2) (Rafique et al., 2007).

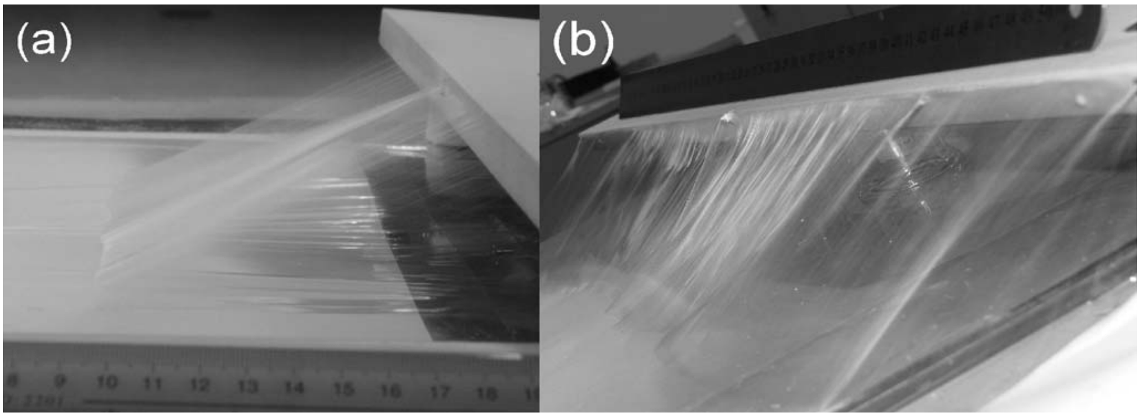

Fig. 1.12 Macroscopic image of the resultant highly aligned nanofibers collected by a 38 cm long wooden board (Rafique et al., 2007).

1.3 Materials

1.3.1 Polyethylene Oxide

Polyethylene oxide (PEO) is known as one of the polymer electrolytes, an ionic conducting solid material. The conductivity is produced by the movement of ionic species assisted by the motion of macromolecule (Gary, 1997; Scrosati, 1993). As polymer electrolytes are solid at room temperature, they have been used to replace liquid electrolyte in lithium-reversible battery to achieve all-solid-state rechargeable lithium batteries. PEO is the most commonly used solid electrolyte because of its chemical stability and is water solvable (Armand, 1987; Croce, Appetecchi, Persi, & Scrosati, 1998; Manuel Stephan & Nahm, 2006).

Regarding electrospinning, due to the relatively high molecular weight of 1,000,000 and good solubility in many solvents, PEO has been widely used for studying electrospinning, including the study of electrospinning process and conditions(Theron et al., 2004), morphology and structure of its electrospun fibers, and the applications of its composites (Deitzel, Kleinmeyer, Hirvonen, & Beck Tan et al., 2001b; Hamlett, Jayasinghe, & Preece, 2008; Reneker & Yarin, 2008; Theron et al., 2004; Tripatanasuwan, Zhong, & Reneker, 2007; Uyar & Besenbacher, 2009).

1.3.2 Carbon Black

Carbon black is a kind of graphite powders of which the conductivity is between 0.1 and 100 Scm^{-1} depending on the size and structure of the particles. It is one of the most versatile fillers used in compounding polymers. It serves as effective and moderately low-cost fillers with varying levels of conductivity. Carbon black was widely used to replace metallic particles due to its light weight and cheaper price.

Carbon black is usually produced by incomplete combustion of hydrocarbon vapors. Most of the carbon black particles are spherically shaped and non-discrete component of an aggregate. The carbon black used in this project has a conductivity of about 3 Scm^{-1} and the average diameter is about 50nm as shown in Fig. 1.13. Carbon black has seldom been applied on electrospinning. However, it has been used to increase the conductivity of electrospun fibers for sensing applications (Kessick & Tepper, 2006). According to the article, 20 wt% of carbon black in the fibers are able to form percolation, it is noted that the diameter of fibers is in micron size range.

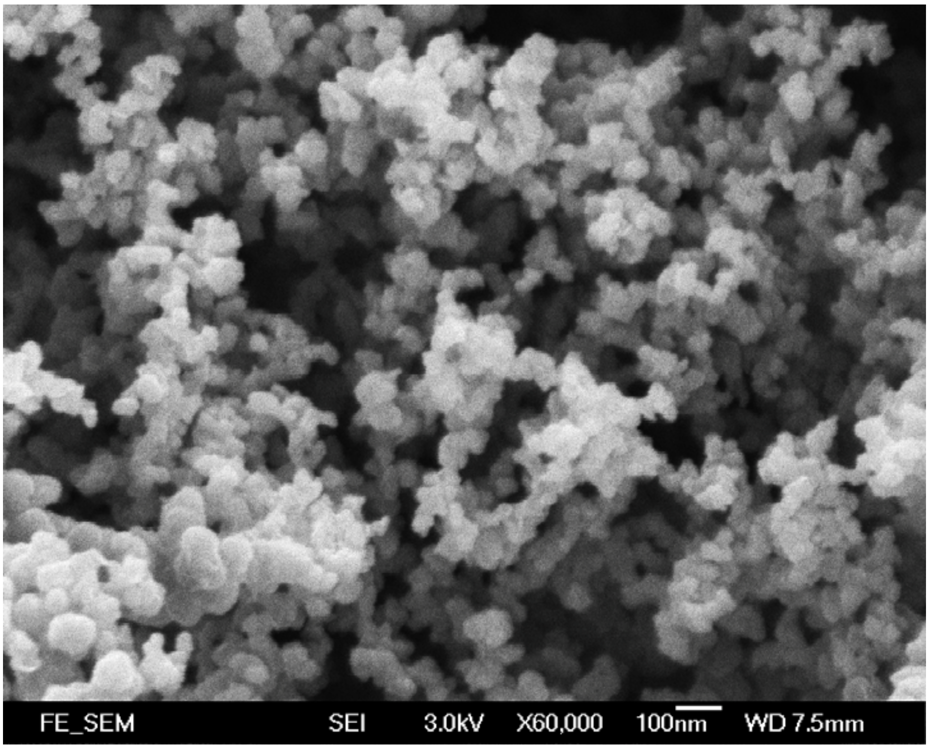

Fig. 1.13 SEM picture of carbon black shows the aggregation of carbon black particles.

1.3.3 Polyaniline

Conducting polymers have been studied extensively since the early eighty, which include polypyrrole, polythiophene and polyaniline.

Polyaniline is a conjugated polymer which exhibits intrinsic conduction by doping. This conducting polymer has been found extensive applications in various fields including the micro-sensors and micro-actuators, which provide cheaper, accurate and faster alternatives to devices already on the market. Chemical sensors and biosensors based on polyaniline with remarkable specifications have been also developed.

To become conductive, the conjugated polymers have to be disturbed either by removing electrons (oxidation) or by inserting electrons (reduction); this process is known as doping.

The dopant ions play an important role in balancing charge distribution and influence the distribution of positive charge on the polymer backbone. They create extra closely spaced electronic levels to form within the band gap.

Polyaniline was noticed as electrically conductive in 1968, but only after 1980, its physical, chemical and electrical characterization became intensively study. Polyaniline is the first dispersible inherently conductive polymer and commercialized by Zipperling Kessler and Co.

Polyaniline can be switched between insulating and conductive forms very quickly when exposed to an acidic or alkaline environment. There is an advantage in polyaniline, it can be doped into its conductive state using carious protonic, anorganic and organic acids. When the organic acid has a macromolecular structure, a conductive compound can be obtained (Wilson et al., 2007). According to Nicholas (Pinto, Ramos, Rojas, Wang, & Johnson Jr., 2008), the same molar mass of polyaniline and dopant can make polyaniline be fully doped.

Commonly, the polymer chains of polyaniline are short to be electrospun into fine fibers; carrier (other polymer with sufficient chain length for electrospinning) is required to blend with polyaniline (Norris, Shaker, Ko, & MacDiarmid, 2000; Pinto et al., 2008).

It is found that polyaniline is also sensitive to vapors of aliphatic alcohols, and it is still being studied intensively (Ji, Li, & Yang, 2008; Pinto et al., 2008; Segal, Tchoudakov, Narkis, Siegmann, & Yen, 2005).

1.4 Alcohol Sensing

There are many potential applications of electrospun polymer nanofibers (Fig. 1.14). Chemical sensor is one of the applications. It can be achieved by blending functional materials into the fibers. For instance, polyaniline is blended with other polymers to form conducting composites (Chipara et al., 2003; Segal et al., 2005).

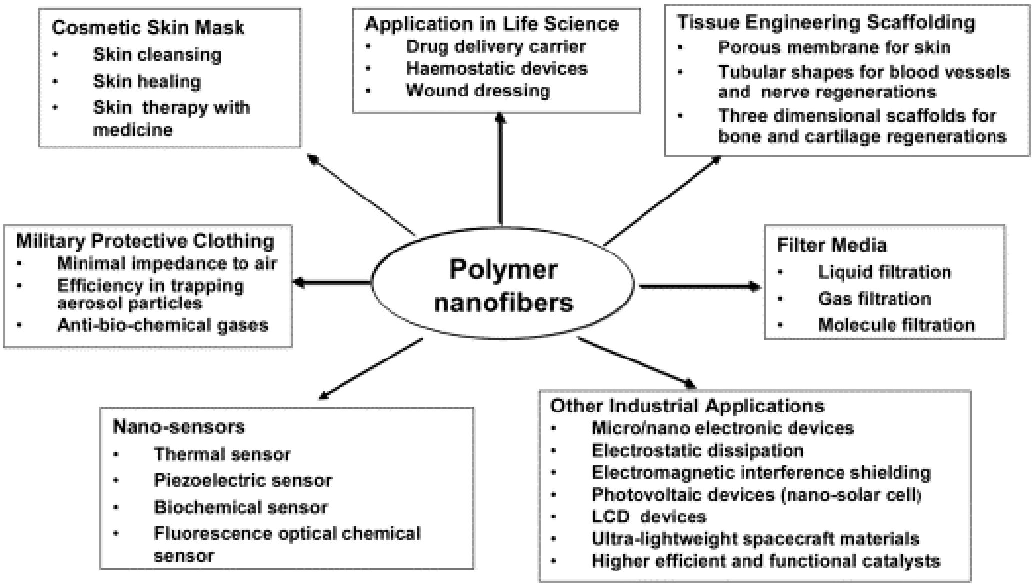

Fig. 1.14 Potential applications of electrospun polymer nanofibers (Huang et al., 2003).

Regarding to the chemical sensing capability of polyaniline, it has been used to detect alcohols in particular. Resistance of neat PANi systems (without excess dopant) will decrease on exposure to different polar and hydrogen bonding molecules including alcohols. There have been a number of mechanisms proposed to explain this phenomenon (Athawale & Kulkarni, 2000; Matveeva, 1996; Svetlicic, Schmidt, & Miller, 1998; Tan & Blackwood, 2000). It can be summarized as a result of the crystallinity change of the doped PANi (Kinlen, Liu, Ding, Graham, & Remsen, 1998), the increase in crystallinity due to gradual removal of excess dopant molecules during the exposure to the various alcohols (Segal et al., 2005) is responsible for the reisistance decreasing. It is suggested that hydrogen bonding between the polar molecules and the PANi chains facilitates conformation changes of the chains, and thus increases their electrical conduction (Athawale & Kulkarni, 2000; Matveeva, 1996; Tan & Blackwood, 2000). Also, it has been shown that polar molecules can also contribute to a reduced scattering cross-section of defects created by the polarization effects of the dopant anion and thus enhance conductivity (Shacklette, 1994).

However, when dealing with the composite or blend of polyaniline, the change of resistance cannot be simply explained by the crystallinity change as it has been found that the crystallinity of the blend does not change on exposure to alcohols (Segal et al., 2005). Further discussion is in Chapter 5 together with the discussion of the results.

1.5 Outline of Thesis

The main objective of this project is to study the electrospinning process and using this technique to fabricate nanoscaled PEO/carbon black fibers and PMMA/PANi fibers. In particular the fabrication of the latter system is for alcohol sensing application.

This thesis will report the work and the results obtained and it is divided into six chapters. The first chapter gives the background and literature review on electrospinning, materials used and nanofibers for chemical sensing. In Chapter 2, the characterization methods used for the prepared samples are introduced. Following this, the experimental setup of electrospinning process and electrical measurements are described. As three different set of experiments have been involved in this project, details of the setup of each experiment is described in this chapter.

Chapter 3 is about the study of the processing condition for electrospinning. The focus is the optimization of the condition for electrospinning to produce nanofibers with desired morphology, smooth and highly aligned nanofibers. PMMA is the polymer used in this study.

Composite fibers is described in Chapter 4, PEO/carbon black nanofibers were fabricated. The concentration of carbon black in PEO would affect the fiber morphology, molecular chain conformation of the PEO and their electrical properties. The results will be reported in this chapter. Chapter 5 is the experiments of alcohol sensing. PANi is doped with AMPS at a fixed ratio and then blended with PMMA. Electrical response to various alcohols, including methanol, ethanol and isopropanol were examined. The response to different concentration of alcohol and the real time response to the alcohol flow will be discussed.

In the last chapter, we shall conclude the experimental results and important findings. With the suggestion of future investigation, the values of this project are objectively and fairly evaluated.

Chapter 2

Characterization and Experimental

In this chapter, the characterization methods for the samples will be introduced; and the setup of electrospinning and electrical measurements for this project will be described.

2.1 Characterization Methods

2.1.1 Fourier Transform Infrared (FTIR) Spectroscopy

Fourier Transform Infrared (FTIR) Spectroscopy is utilized for studying the molecular vibrations and rotations by infrared absorption. Many functional groups in organic molecules show characteristic vibrations of which the frequency is in the infrared (IR) region of the electromagnetic spectrum. Those molecular vibrations are localized within the functional groups, thus they can be identified by their absorption bands.

FTIR is a well developed technique for IR spectroscopy. It takes the advantages of microcomputer technology for fast Fourier transformation calculation, storage and processing of large amounts of data. In FTIR spectrometer, the IR beam is modulated by a Michelson interferometer and transmits through the sample; the signal waveform received by the IR detector is called interferogram and can be converted into the IR spectrum through Fourier transformation. Due to the simplicity of the measurement technique, FTIR has established itself as one of the standard method in characterization of polymer. (Hesse, Meier, & Zeeh, 1997)

In this project, Nicolet Magna-IR 760 spectrometer was used for analyzing the samples and other materials. In analyzing the aligned electrospun fibers, IR polarizer has been used. It allows the electric vector of the IR beam which is either parallel or perpendicular to the fiber direction goes to the sample. With the aid of the polarizer, the chemical bond orientation of the molecules with respect to the axis of the fibers can be identified.

2.1.2 Scanning Electron Microscopy (SEM)

Scanning electron microscope (SEM) is used for studying the morphologies of the specimens. It images the surface features of the specimens by scanning a focused beam of high energy electrons on the specimen surface from which a high magnification up to 250,000x can be achieved. The interaction of the primary electron beam with the specimens can be divided into two classes: elastic scattering affecting the trajectories of the beam of electrons within the specimens and inelastic scattering which result in a transfer of energy from the electrons to the specimen, such as secondary electrons, auger electrons) and backscattered electrons are able to emerge from the specimen surface (Reimer, 1998). Both of these two kinds of electron scattering can be made used in material analysis other than the microscopic imaging.

JEOL JSM-6335F field emission scanning electron microscope was used in this project. Secondary electrons were collected in imaging mode for the study of surface morphology of fibers. The applied voltage of the primary electrons was 3kV and the samples were coated with gold before for SEM observation.

2.1.3 Transmission Electron Microscopy (TEM)

Transmission electron microscope (TEM) is used for imaging specimen at significantly high resolution. A beam of electrons transmits through ultra-thin specimen and interacts with it as the beam passes through. The image is focused onto an imaging device, such as fluorescent screen or detected by a sensor such as a digital CCD camera.

TEM is able to reveal fine details of specimen up to the atomic resolution. As the electron beam passes through the sample, the energy of the electrons will be absorbed due to the interaction with different parts of the specimen, thus making the difference in electron intensity producing a contrast to form a TEM image.

JEOL 2010F TEM transmission electron microscope was used for imaging the carbon black particles in PEO fibers in this project. Small amount of fibers were electrospun onto a TEM copper-grid sample holder.

2.1.4 X-ray Diffraction (XRD) Analysis

X-ray diffraction (XRD) is a versatile, non-destructive technique to reveal details of the chemical composition and crystallographic structure information of materials. XRD in polymers is different from metallurgical or ceramic diffraction.

When x-rays irradiate on atoms in the crystal lattice, each atom scatters a small fraction of the incident beam. Thus the diffracted beams from all atoms in the crystal planes involved may interfere and the resultant diffracted beam is only enhanced if the path difference from successive planes is a whole number of wavelength of the incident x-ray radiation. The diffracted beam has a maximum intensity when

$$2d\sin\theta = n\lambda \tag{2.1}$$

where d is the distance between plans of the atoms, θ is the angle between the x-rays beam and the crystal plane, n is an integer and λ is the wavelength of the x-ray.

For polymeric materials, it is generally agreed that the observed x-ray diffractions arise as a result of the diffraction from the crystalline region as well as the amorphous region. As polymers own long chain structure that is highly susceptible to orientation, XRD is a primary tool for the determination of crystalline orientation through the Herman's orientation function (Kasai & Kakudo, 2005).

The Hermans' orientation parameter f represents the degree of orientation. If the angle between the vibration transition moment of the absorbing unit and the local chain axis, ψ, is 0° or 90° (Fig. 2.1), f is given by:

$$f = \frac{3\left\langle \cos^2 \alpha \right\rangle - 1}{2} \quad (\psi = 0^\circ) \tag{2.2}$$

and

$$f = 1 - 3\left\langle \cos^2 \alpha \right\rangle \quad (\psi = 90^\circ), \tag{2.3}$$

in which orientation distribution function $\left\langle \cos^2 \alpha \right\rangle$ is defined by:

$$\left\langle \cos^2 \alpha \right\rangle = \frac{\int_0^{\frac{\pi}{2}} I(\alpha) \sin \alpha \cos^2 \alpha d\alpha}{\int_0^{\frac{\pi}{2}} I(\alpha) \sin \alpha d\alpha} \tag{2.4}$$

where α is the angle between fiber axis and the director of orienting unit, and $I(\alpha)$ is the azimuthal intensity distribution. For perfect oriented fibers, the value of orientation parameter, f is 1, but f would be zero when the fibers are randomly oriented (Lin, Jho, & Yee, 1993; Mitchell & Windle, 1988; Windle, 1982).

In this project, Philips Xpert XRD System was utilized for analyzing crystalline polymer samples including fibers, mainly PEO fibers. Transmission experiment was used. The degree of orientation of the fibers was revealed by XRD Psi scan.

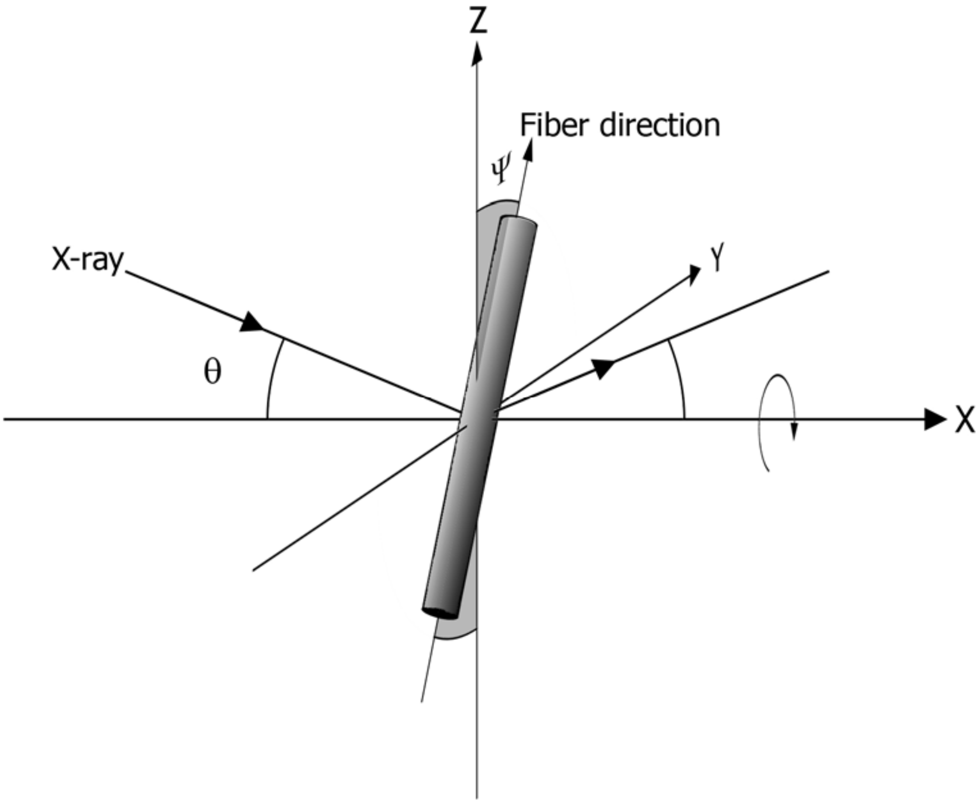

Fig. 2.1   Schematic diagram for orientation determination.

2.2 Experimental

2.2.1 Electrospinning Setup

The electrospinning setup consisted of a syringe to hold the polymer solution, two electrodes and a DC high voltage power supply in the kV range (Fig. 2.2). The polymer solution from the syringe is drawn out of the tip and split into fiber due to the high electrostatic field applied. The jet of fiber carried charges causes the fiber to bend in such a way that every time the polymer fiber looped, its diameter is reduced. The fiber is collected as a web on the surface of a grounded target.

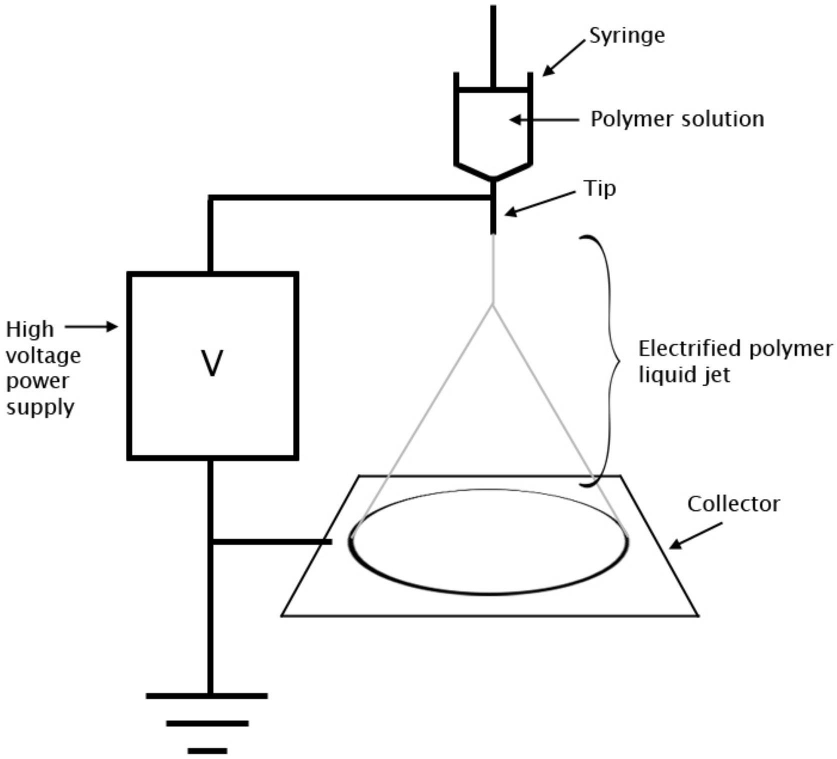

Fig. 2.2 Schematic diagram of the setup for electrospinning.

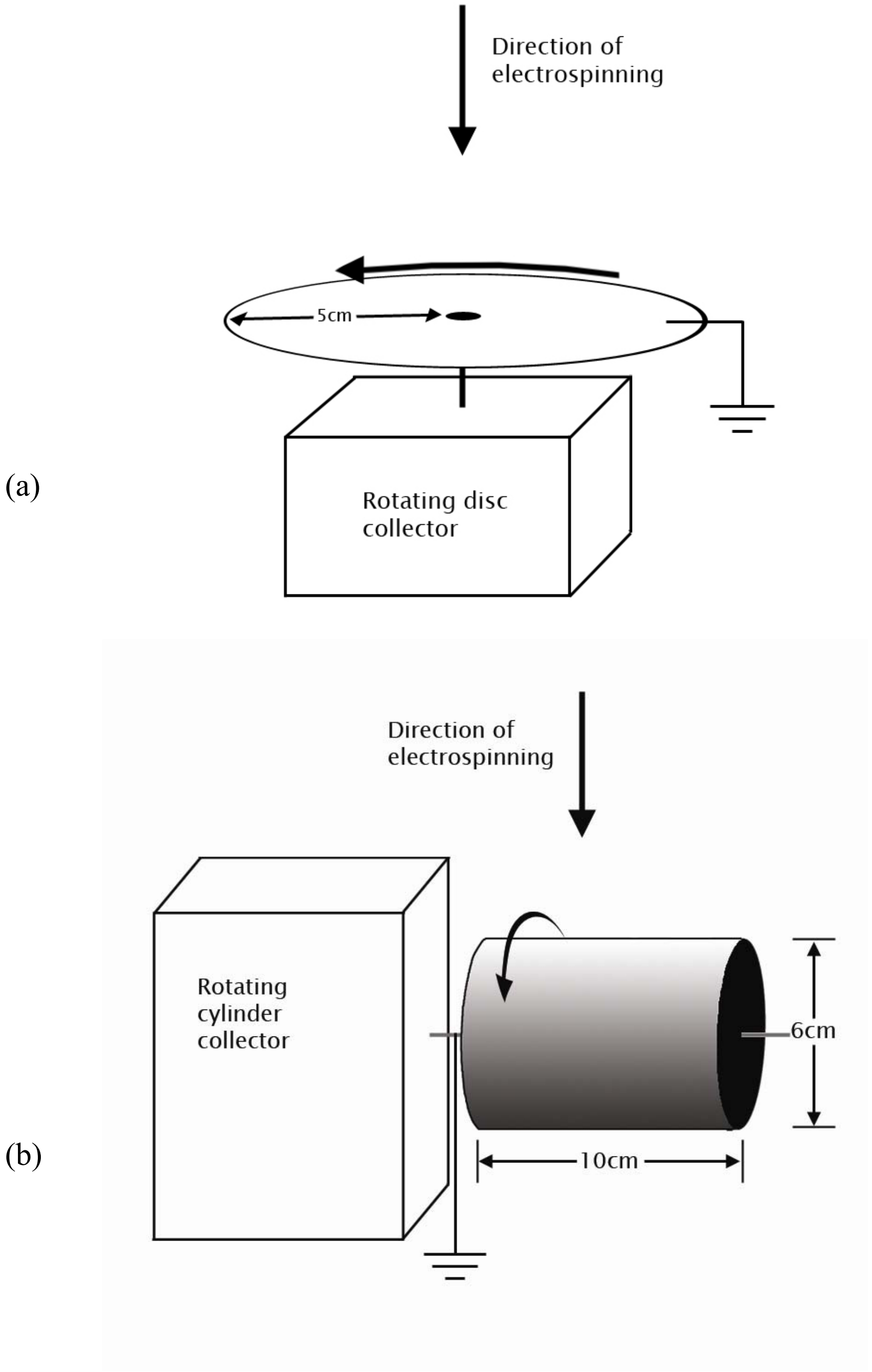

Fig. 2.3 Schematic diagrams of (a) rotating disc and (b) rotating cylinder collector.

The high voltage power supply was supplied by Phywe (Germany), which was able to give a maximum 25kV and 150mJ. Syringes (1cc) with capillary of 30-gauge were supplied by Becton, Dickinson and Company (USA); the sharp tips were grinded to have a flat opening before use. All electrospinning processes were carried out at room temperature in air.

Two kinds of rotating collector, disc and cylinder as shown in Fig. 2.3a and b respectively, have been used. The cylindrical one is used for unidirectional nanofibers collection. The rotation speed of the disc can be reached to a maximum of 4000 rpm, therefore the linear velocities of the collector surface change from zero at the centre to 21 ms^{-1} at the rim of the disc. The rotation speed of the cylinder can be reached to a maximum of 3500 rpm where the linear velocity is constant all over the collector surface to a maximum of 11 ms^{-1}. Aluminium foils of 18 μm thick were used to collect the deposited fibers and the samples were then dried at 45 °C for 12 hours before all measurements. Bundles of fibers collected were transferred from the aluminium foil to a polyethylene terephthalate (PET) sheet of 0.1 mm thick, which is a good polymeric insulator, as the sample holder for electrical measurement. Other kinds of sample holder were also made on demand which depends on the requirement of the measurements.

2.2.2 Electrical Measurements

D.C. measurement was carried out by the Keithley 6517A electrometer and A.C. electrical measurement was carried out by the Lock-in Amplifier (Stanford Research

Systems SR810).

Sample was placed on the PET sample holder and silver paste electrodes were applied at a separation of 1 mm at both ends of the sample and the width is 10 cm (Fig. 2.4). If the sample was a bundle of fibers, measurements would be carried out along the fiber direction.

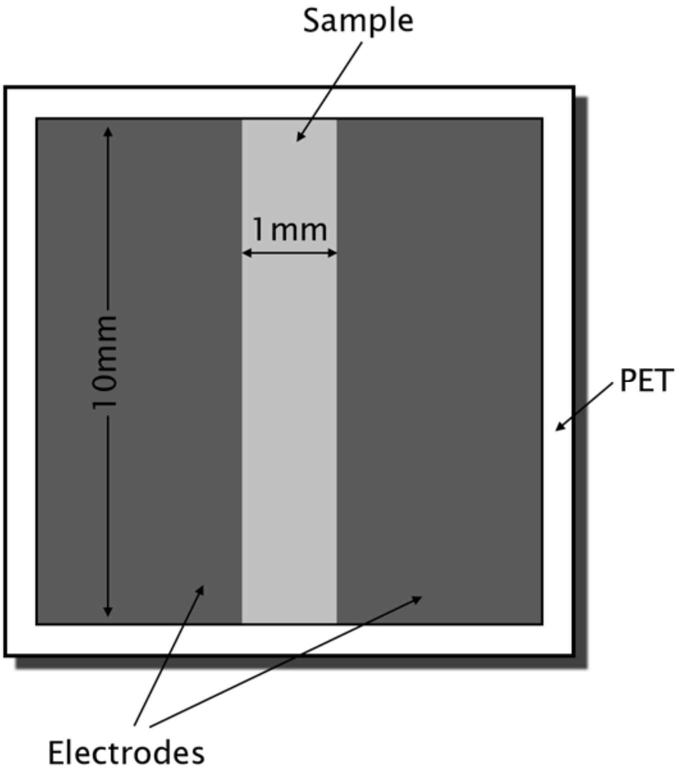

Fig. 2.4 Sample holder for electrical measurements.

Chapter 3

Study of Electrospinning

In the preparation of samples by electrospinning process, a mixture of polymer beads with the fibers is always formed. Since the focus of this project is concerned about the properties of nanofibers, the formation of beads is not favorable and therefore we attempted to find out the proper parameters to electrospin finest fibers without beads. There are numerous parameters affecting the electrospinning process outcome, some of them will be discussed in the following chapter. This investigation was carried out by using PMMA.

3.1 Experimental

3.1.1 Solution Preparation

PMMA with molecular weight (M_w) of 120,000 and 350,000 were purchased from Sigma-Aldrich. The solvent 1-Methyl-2-pyrrolidone (NMP) was purchased from International Laboratory USA. Dimethylformamide (DMF) and Methylethylketon (MEK) were supplied by Labscan Ltd. and Riedel-de Haën, respectively.

In order to examine the effect of solvents in electrospinning process, three organic solvents, DMF, NMP and mixture of NMP and MEK (1:1 in weight) have been used to dissolve 15 wt% of PMMA (M_w=120,000) at 40˚C and stirred for 12 hours.

Regarding the test of concentration variation of PMMA (M_w=120,000) solution, NMP was used and 10, 15 and 20 wt% of PMMA solution have been prepared. 7 wt% of PMMA (M_w=350,000) was dissolved in NMP for testing the effect on polymer molecular weight.

For examining the effect of different voltages and polarities, experiments were carried out by 20 wt% PMMA (M_w=120,000) in NMP and 20 wt% PMMA (M_w=120,000) in NMP/MEK (1:1 in weight). Lastly, 15 wt% PMMA (M_w=120,000) in NMP was employed for the test of the effect on the rotation speed of the collector.

3.1.2 Electrospinning Process

For the electrospinning process, different voltages (12 kV, 17 kV and 25 kV) and polarities (positive and negative 25 kV) had been applied to the tip to verify their effect upon the formation of fibers. The distance between the tip and collector is 21 cm. To investigate the effect on the rotating speed of the disc collector, it was set to 3360 rpm and positive 21 kV was applied on the tip. After electrospinning, the collected samples were dried at 40˚C for 24 hours.

3.2 Results and Discussion

3.2.1 Influence of Polymer Solution

The properties of the polymer solution would influence the electrospinning process and the resultant fiber morphology most significantly. By changing the solvent or concentration of polymer, various properties of fibers can be obtained.

Solvents

As solvent is required to dissolve polymer for electrospinning, its property is an essential factor. Fig. 3.1a, b and c shows fibers obtained from DMF, NMP and mixture of NMP and MEK respectively. The fibers obtained from DMF have much more beads than the rest; however the fibers are as fine as 70 nm. When fibers are dissolved by NMP solvents, they have less beads and more uniform in diameter of around 200nm. With the blend of NMP and MEK, fibers are thicker and the formation of beads was further reduced. The properties of solvents are the causes of the noticeable differences.

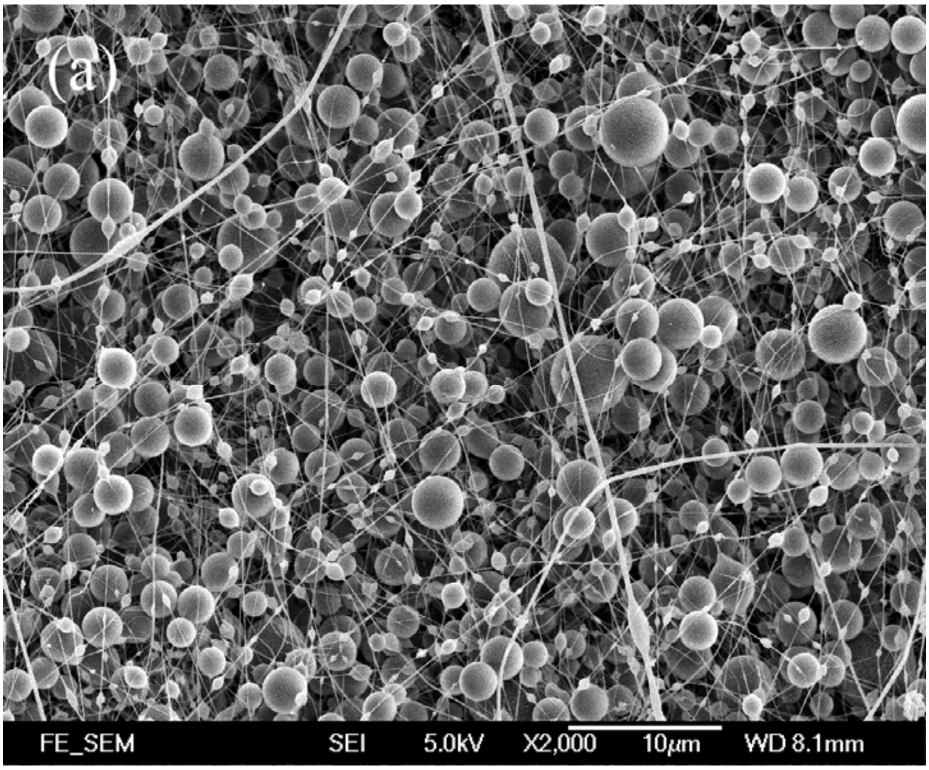
(a)
FE_SEM
SEI
5.0kV
X2,000
10μm
WD 8.1mm

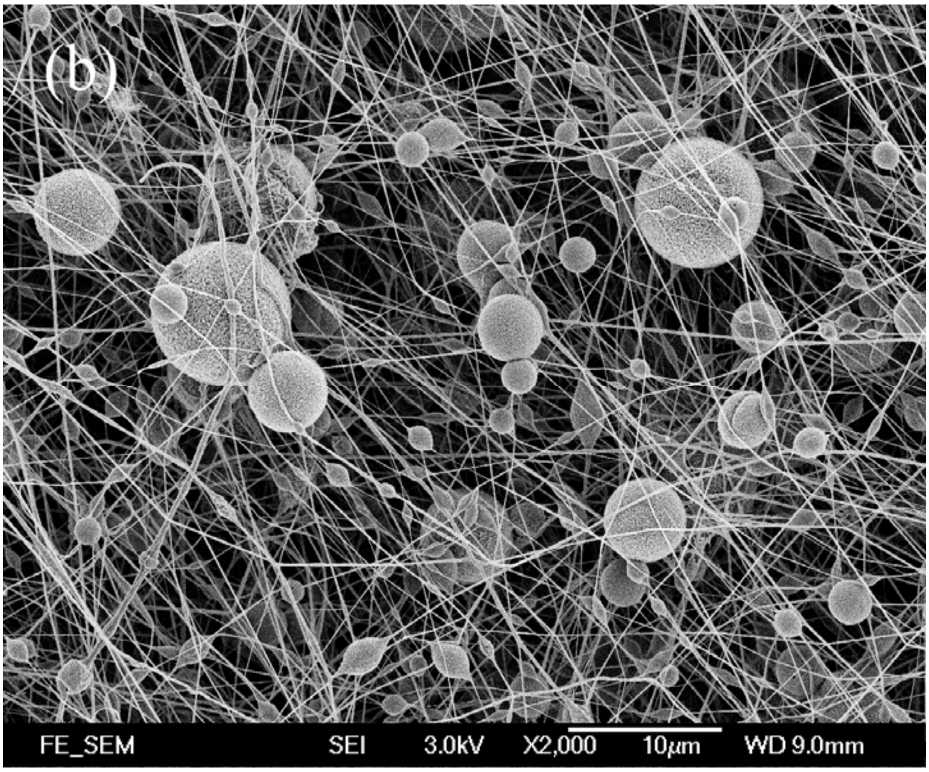
(b)
FE_SEM
SEI
3.0kV
X2,000
10μm
WD 9.0mm

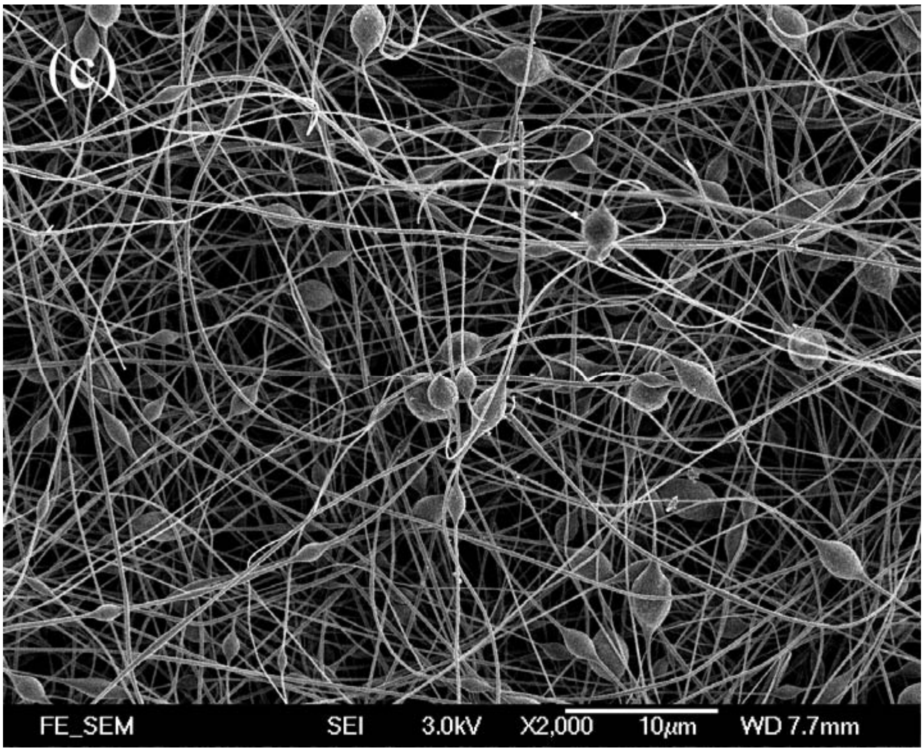

Fig. 3.1 15% PMMA (Mw=120,000) fibers in (a) DMF, (b) NMP and (c) mixture of NMP and MEK (1:1 in weight).

Conductivity and the contact angles on PET sheet of the PMMA solutions have been used to investigate the effect of the solutions. The conductivity of solutions was carried out at 1 kHz in a 1 cm^3 container. The contact angles were measured on PET sheet where 1 ml of solution was dropped on PET surface.

Table 3.1 shows the results of the solutions. Contact angles of different solutions are similar that ranging from 19.1° to 20.2°, the difference is minor that cannot explain the difference of fiber morphologies.

The conductivity of the solution with DMF is the highest; it is the reason that the solution obtained finest fiber. Higher conductivity means more charge carriers inside, when there is a high voltage applied on the solution, change density is higher and thus introduce bigger repulsive forces within the solution that makes the fibers thinner (Zong et al., 2002). Concerning the fibers from NMP solvent, as the conductivity of the solution is lower than the one of DMF, the fibers are not as thin as those from DMF.

On the other hand, many beads are found on the fibers from DMF solvent, this may due to poor interaction between PMMA and the solvent molecules, a research group (Wannatong, Sirivat, & Supaphol, 2004) found similar result in polystyrene (PS) solution.

Table 3.1 Measured parameters of 15 wt% PMMA solutions in DMF, NMP and blend of NMP and MEK.

	DMF	NMP	NMP/MEK
Contact Angle/°	20	19.1	20.2
Conductivity/Scm^{-1}	$7.99x10^{-6}$	$2.53x10^{-6}$	$3.23x10^{-6}$

Regarding the difference in the fiber morphologies from NMP and NMP/MEK solvents, the measured parameters are similar and seem not important issues to the difference in morphology. There were some other parameters affecting the morphology, which is the drying rate and viscosity of the solutions. As the viscosities of the solutions are considered as a minor factor, drying rate of the jet during electrospinning is considered. Table 3.2 shows the boiling points of the solvents. Lower Boiling points indicates higher vapor pressure and higher drying rate. As the boiling point of NMP is much higher than MEK, it is believed that the fibers in NMP/MEK solution were dried much faster than those in NMP, so the fibers in NMP/MEK have much less time to stretch before the solvent evaporates. This may be the reason of thicker fibers and fewer beads for the fibers from NMP/MEK solution.

Table 3.2 Boiling points of DMF, NMP and MEK solvents.

	DMF	NMP	MEK
Boiling point/˚C	153	202	80

Concentration and Molecular Weight of PMMA

Fig. 3.2 shows the effect upon the concentration of PMMA which changes the size and shape of the fibers. The influence came from the change of viscosity as it is increased with the concentration of PMMA. In Fig. 3.2a, it is 10 wt% of PMMA, the viscosity was not enough, that is, the polymer chain entanglements was not strong enough to withstand the electrostatic force, continuity of the jet could not be maintained during electrospinning and the jet turned into droplets eventually. Comparing to Fig. 3.2b and c of which the concentrations are 15 and 20 wt% respectively, fibers of 15 wt% is finer which is desirable for having larger surface area to volume ratio, however, less beads were formed and droplets disappeared in fibers of 20 wt%. These results indicate that a proper liquid viscosity is required to maintain the continuity of the jet during electrospinning. With higher viscosity, beads are not favorable to form, which had been reported by other research groups (Mit-uppatham, Nithitanakul, & Supaphol, 2004). However, when the viscosity is too high, it will make the solution very difficult to be drawn out through the syringe needle (Kameoka et al., 2003) and the solution may dries at the tip before the electrospinning begins (Zong et al., 2002).

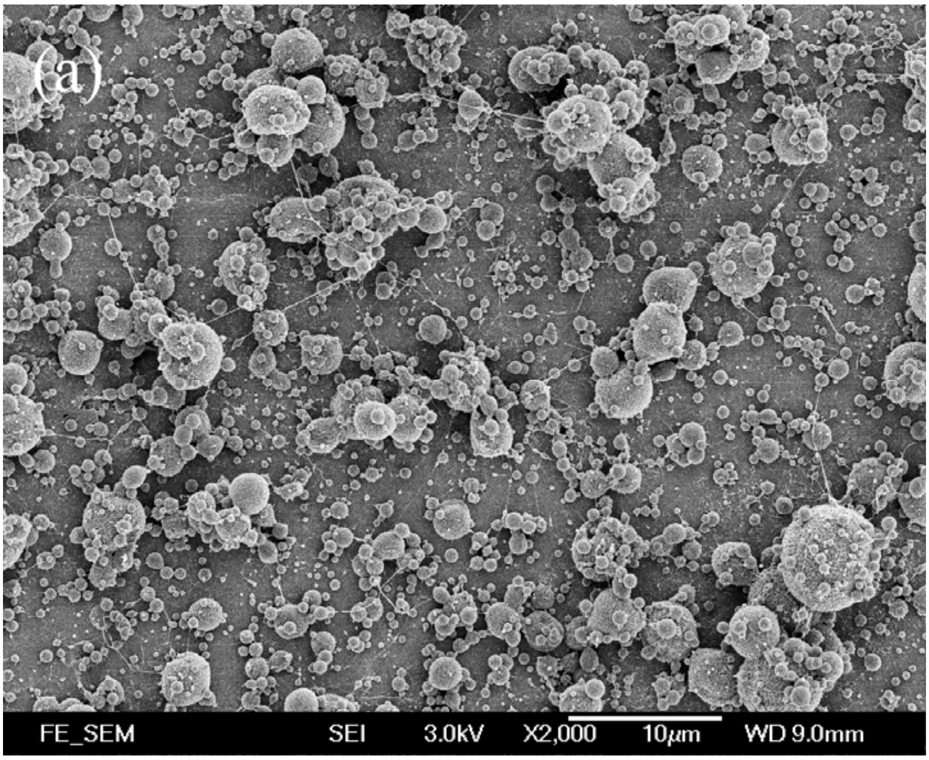

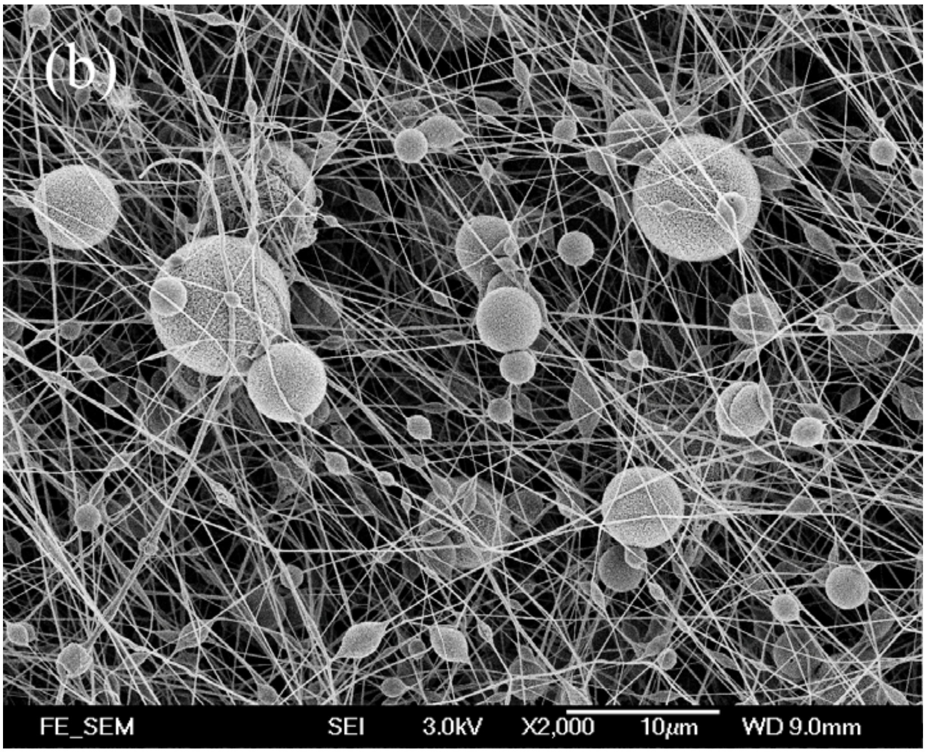

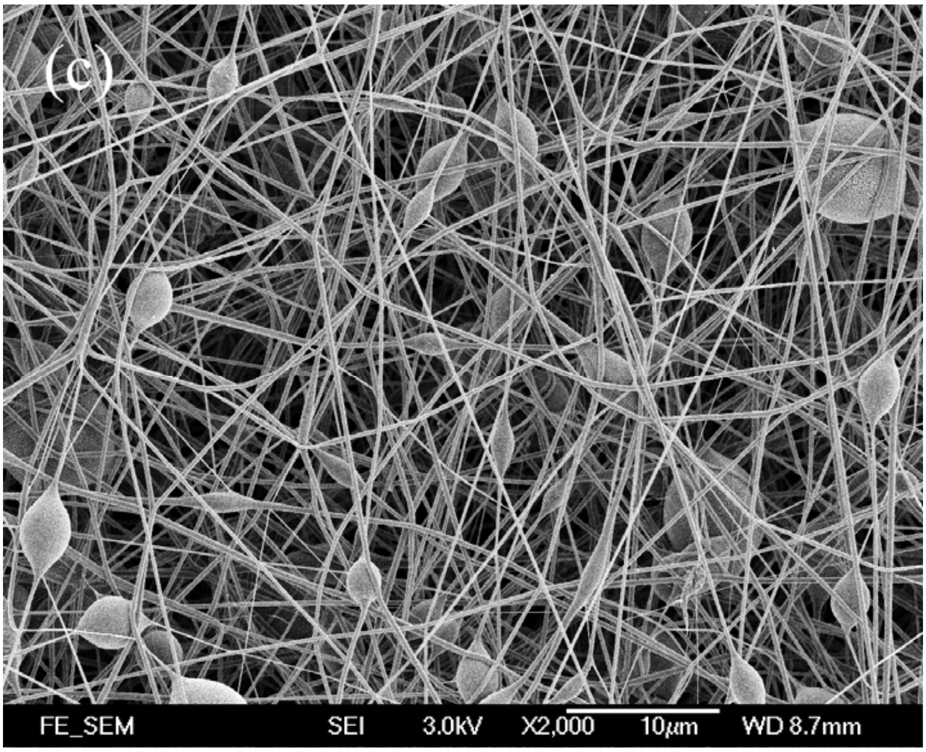

Fig. 3.2 SEM pictures of PMMA (M_w=120,000) fibers with different concentration: (a) 10%, (b) 15% and (c) 20% dissolved in NMP.

On the other hand, the diameter of the fiber also increases with viscosity, which is probably due to the greater resistance of the jet to be stretched by the electrostatic force (Jarusuwannapoom et al., 2005).

In order to minimize fiber diameter and suppress the formation of beads, PMMA with higher molecular weight has been tested. Fig. 3.3 reveals the fiber fabricated using PMMA of molecular weight M_w=350,000 which is about three times higher than the samples shown in previous sections. The average fiber diameter is about 150 nm and no bead is formed in this sample.

The molecular weight is a measure of the length of the polymer chain. It increases with the chance to form large amount of chain entanglement in the solvent, which increase the viscosity of the polymer solution. A polymer solution of higher viscosity favors the formation of long and thin fibers, which has been illustrated in previous section already. In summary, the molecular weight would affect the morphology of the electrospun fibers. Which higher molecular weight at proper concentration, finer and smooth fibers can be produced.

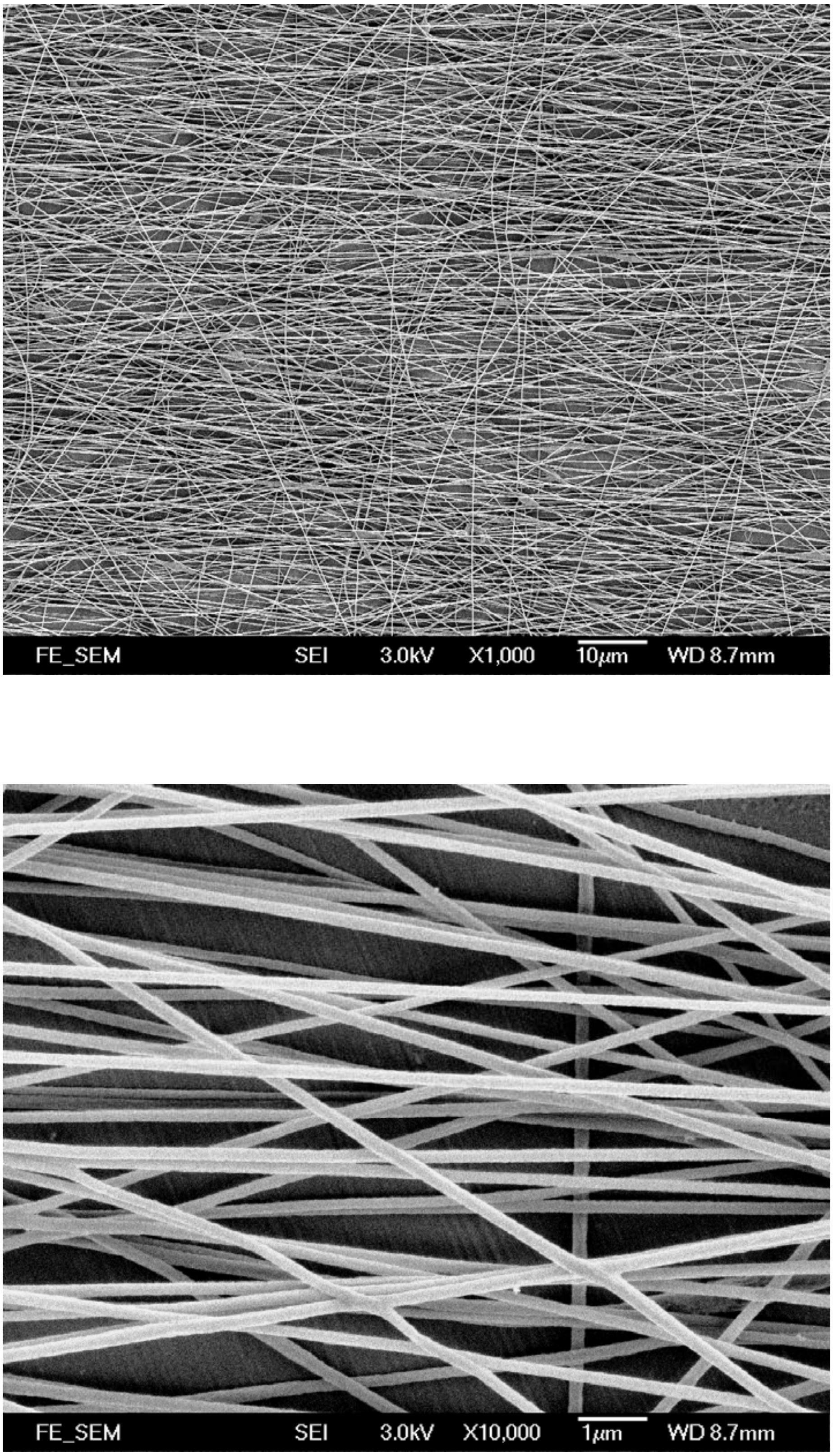

Fig. 3.3 SEM pictures of 7% PMMA (M_w=350,000) fibers dissolved in NMP.

3.2.2 Voltage and Charge Polarity

High electric field is as necessary to induce electrostatic charges of the polymer solution which facilitates the electrospinning process. Fig. 3.4 shows the PMMA fibers fabricated at different applied voltages. Fig. 3.4a shows the fibers electrospun at 12 kV, which was just enough to initiate the electrospinning process; therefore only a small amount of fibers could be deposited onto the collector. Considering in terms of fiber diameter and number of beads formed in Fig. 3.4b and c, it is found that in the case of the PMMA, the applied voltage did not influence the fiber properties much.

Nevertheless, the applied voltage thus the electric field should have an influence in stretching and accelerating the jet. Many research groups reported that higher voltage causes greater stretching due to the greater columbic forces and stronger electric field, which reduce the fiber diameter (Buchko, Chen, Shen, & Martin, 1999; Lee et al., 2004). Formation of secondary jets may also be a reason of the reduction of fiber diameter (Demir, Yilgor, Yilgor, & Erman, 2002).

Apart from reducing the diameter of fibers, some groups (Deitzel, Kleinmeyer, Harris, & Beck Tan, 2001; Demir et al., 2002; Zong et al., 2002) reported that higher voltage that higher voltage favor beads formation and also change the shape of the beads; which may due to the instability of the jet.

The electrospun PMMA fibers at different applied voltage have not much difference in our study may be limited by the high voltage used (0 to 25 kV) which is not enough to influence the morphology of fibers significantly for the PMMA/NMP solutions.

Regarding the polarity of applied voltage used for electrospinning, obvious changes on size of beads and diameter of fibers are discernible as shown in Fig. 3.5. Fibers electrospun with negative voltage (Fig. 3.5b) are accompanied by large spherical beads, on the contrary, those fiber electrospun with positive voltage (Fig. 3.5a) are thinner (around 70 nm) and the beads are smaller. Though the beads were everywhere, the result indicated positive voltage benefits fabrication of smooth fibers as separated, large spherical beads in negative voltage turns into little beads on fibers. One group (Varesano, Carletto, & Mazzuchetti, 2009) has observed the similar effect on negative voltage. Based on this observation, positive voltage has been used in this project for all of the rest of electrospinning process.

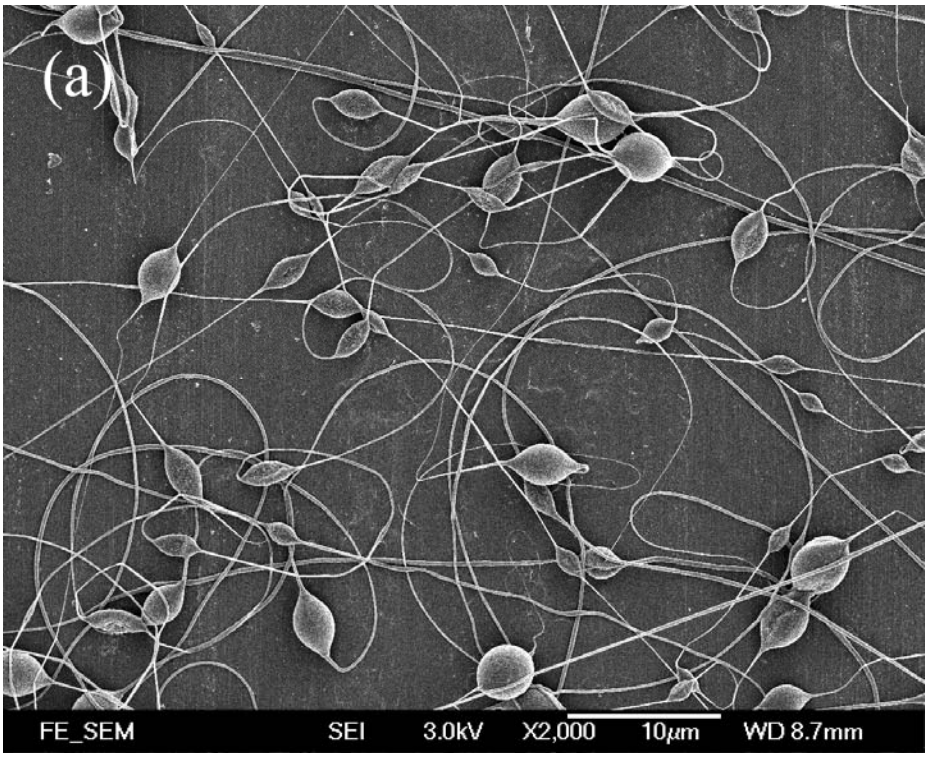
(a)
FE_SEM
SEI
3.0kV
X2,000
10μm
WD 8.7mm

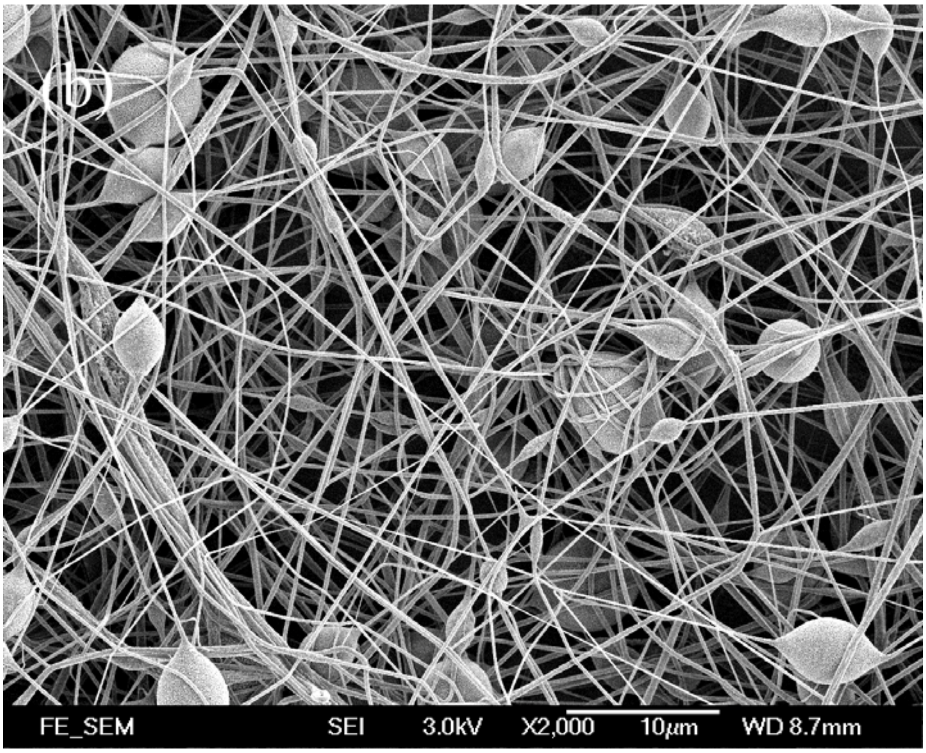
(b)
FE_SEM
SEI
3.0kV
X2,000
10μm
WD 8.7mm

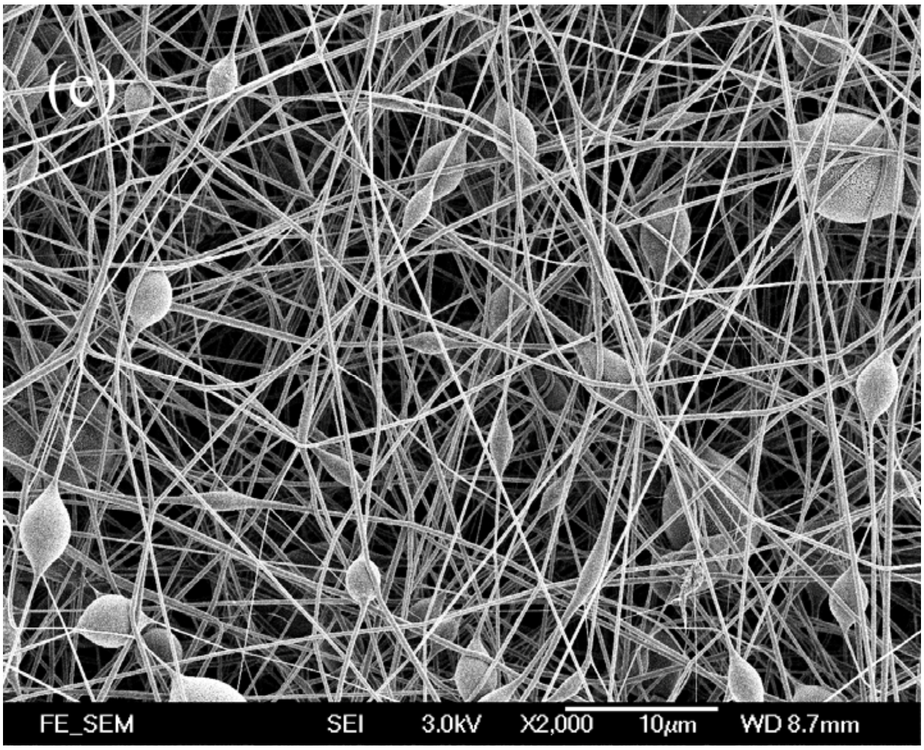

Fig. 3.4 SEM pictures of PMMA fibers electrospun at different voltages: (a) 12 kV, (b) 17 kV and (c) 25kV.

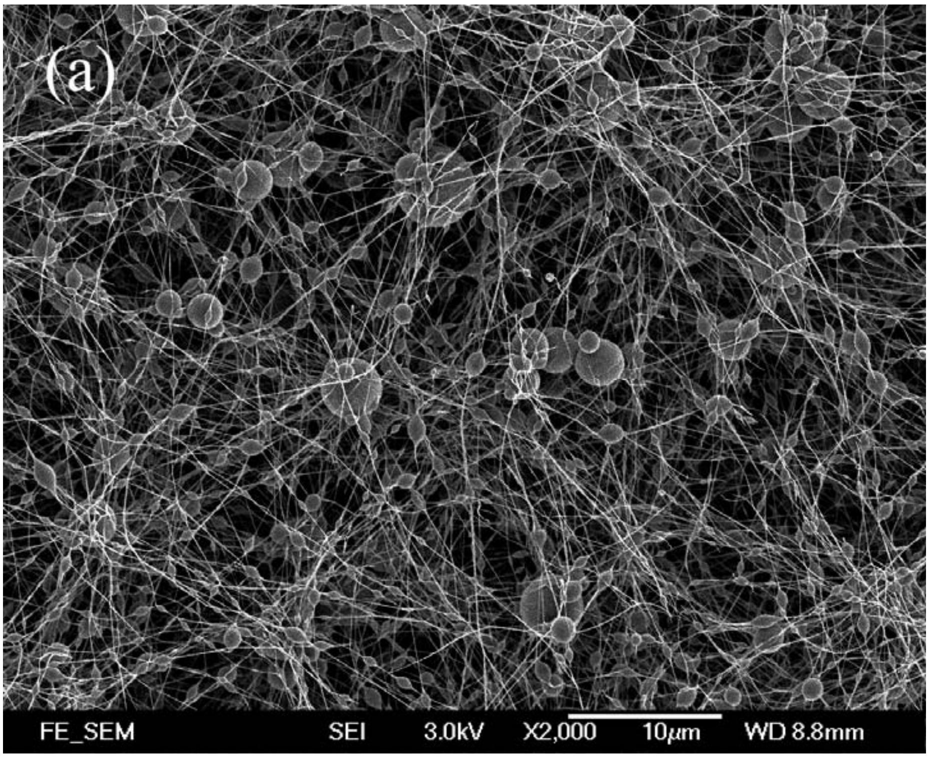

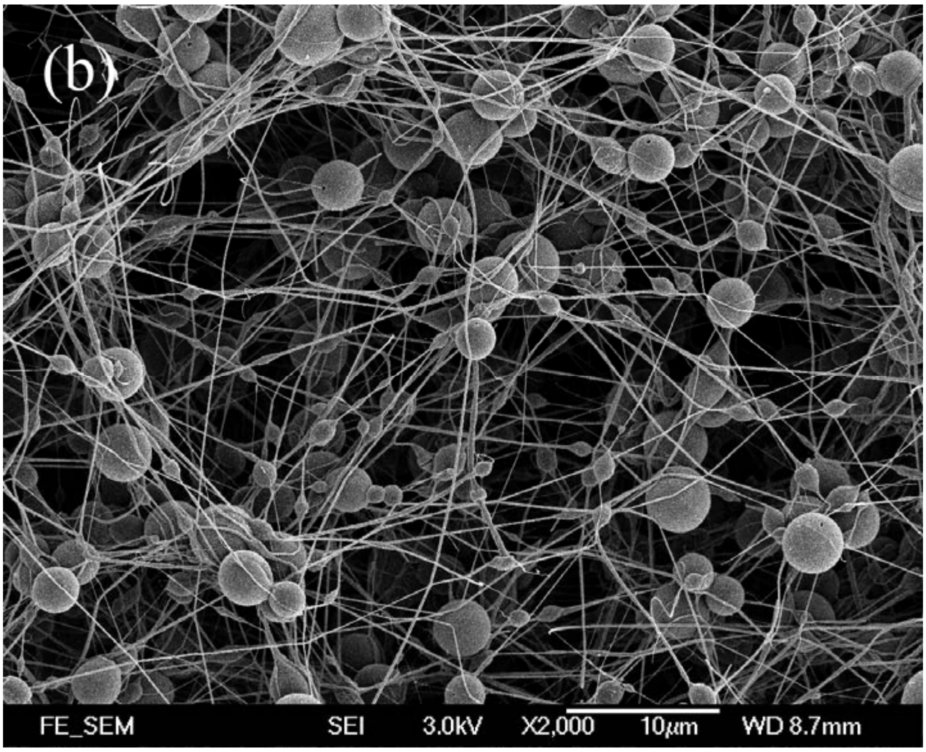

Fig. 3.5 SEM pictures of PMMA fibers electrospun at 25 kV with different polarities: (a) positive and (b) negative.

3.2.3 Rotating Collector

Rotating collector was utilized for collecting the electrospun fibers. The linear velocity of the collecting surface would have effect on the alignment of fibers. As a matter of fact, for most of the electrospinning setup, rotating collector of slow speed can only yield randomly aligned fibers. Fig. 3.6a to h illustrate the fiber which were collected at different locations, i.e. 1, 5, 8, 10, 15, 18, 25 and 35 mm respectively measured from the center of a collecting disc, the diameter of which is 100 mm and the rotating speed was 3600 rpm. This electrospinning process was done for a short period of time for clearly illustrating the fiber orientation. The fibers are about 170 nm in diameter. It can be seen that from Fig. 3.6a to e, the fibers are most randomly aligned. Starting from Fig. 3.6f, at 18mm from the center of the disc, the majority of fibers collected are aligned in the tangential direction to circumference of the disc; and at distance of 25 mm and 35 mm, fibers are aligned in the same direction and seems like reaching the limit of the orientation of this setup. This result shows that fibers started to align when the linear velocity is above 9 ms^{-1}.

It is known that to reach higher quality of orientation, closer distance between the tip and the collector is required (Sundaray et al., 2004); this is to prevent the flying jet from the bending perturbations (Reneker, Yarin, Fong, & Koombhongse, 2000a). However, massive quantity of fibers were required to collected in the same electrospinning process, flying distance of the polymer jet in electrospinning had to be enough for drying the fibers; as NMP required long time to evaporate, closer distance between the tip and collector implies a short jet flying time which is not preferred. Moreover, the degree of orientation presented in terms of Hermans' orientation factor will be illustrated in the next chapter; it can be measured by XRD and is benefited from the crystalline structure of the PEO fibers.

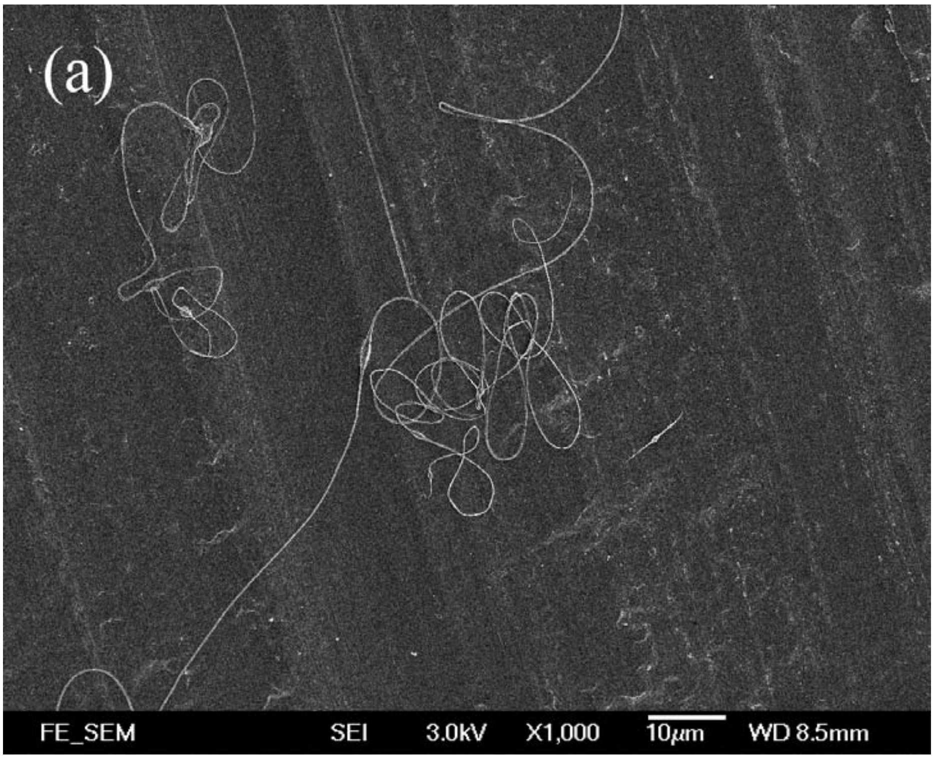
(a)
FE_SEM
SEI
3.0kV
X1,000
10μm
WD 8.5mm

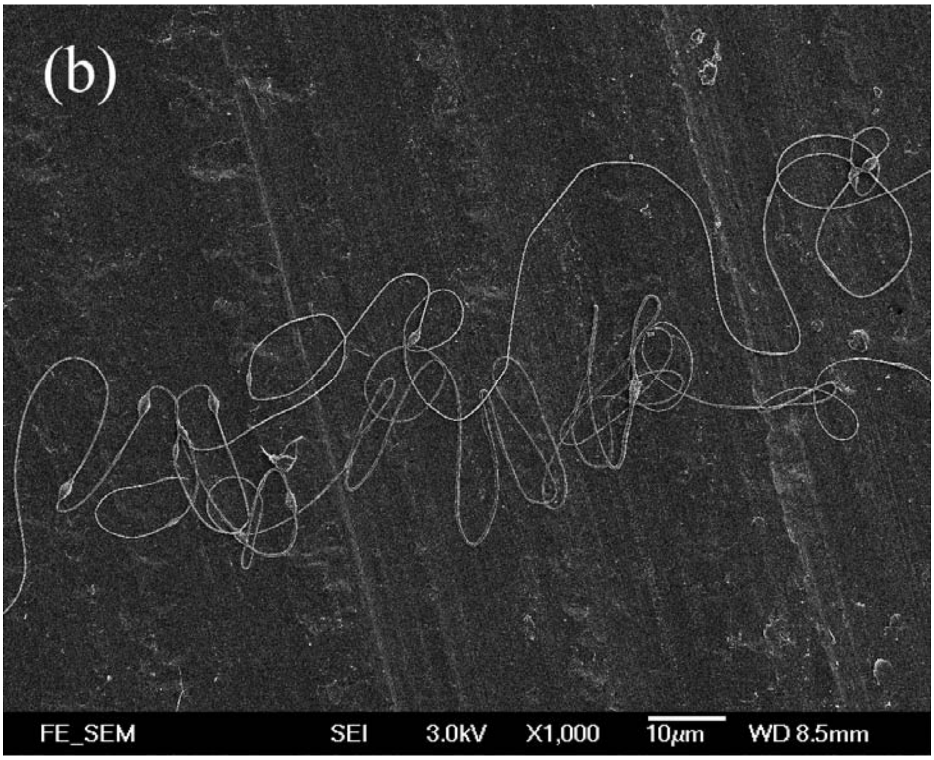
(b)
FE_SEM
SEI
3.0kV
X1,000
10μm
WD 8.5mm

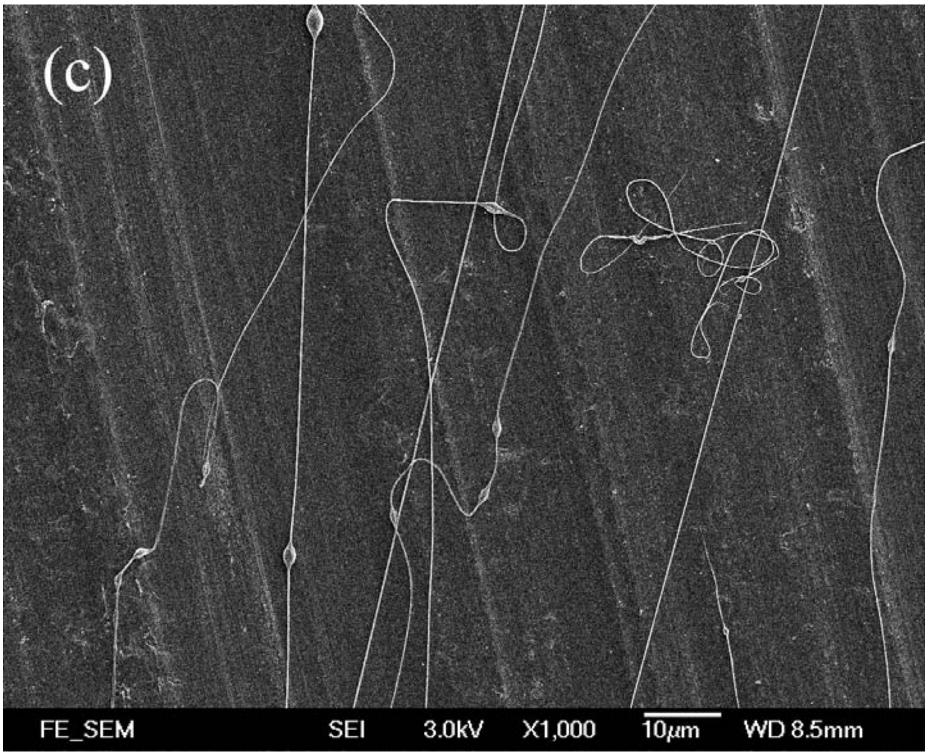
(c)
FE_SEM
SEI
3.0kV
X1,000
10μm
WD 8.5mm

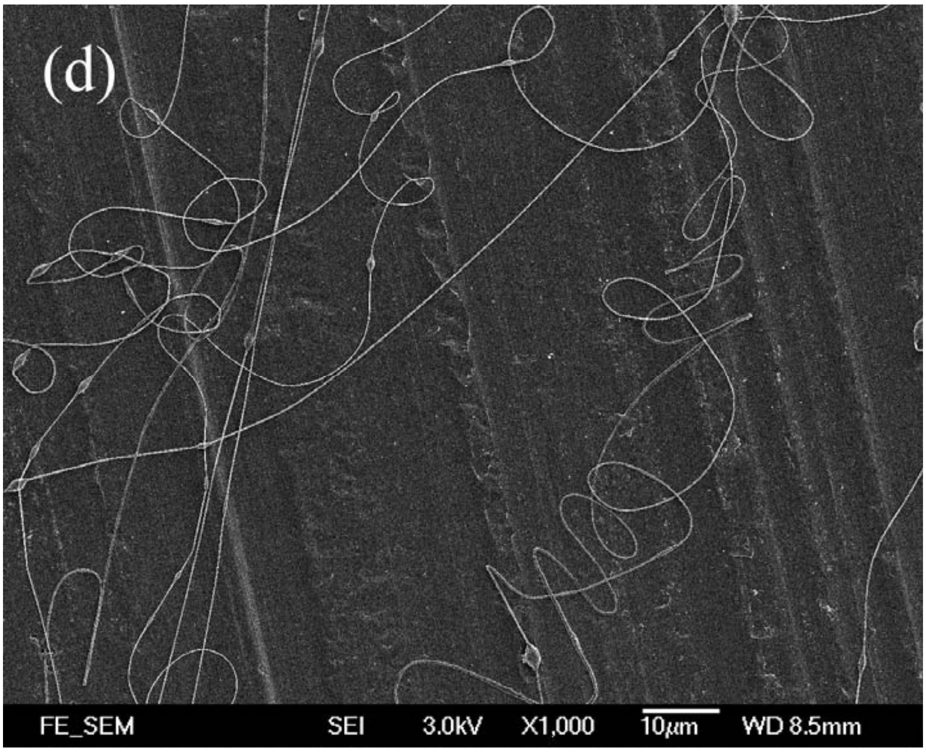
(d)
FE_SEM
SEI
3.0kV
X1,000
10μm
WD 8.5mm

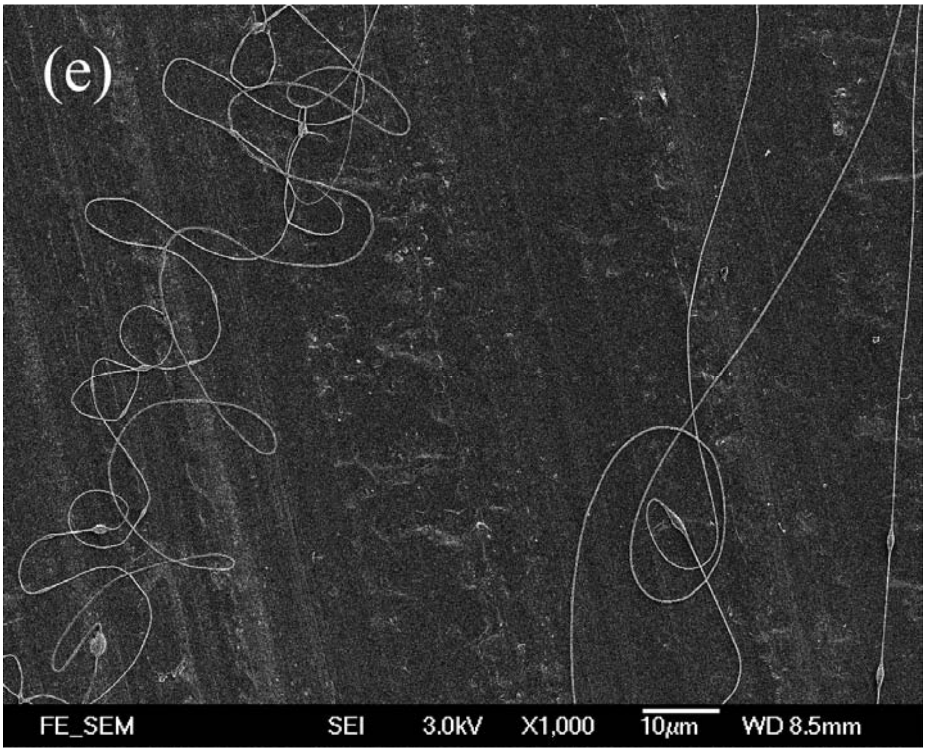
(e)
FE_SEM
SEI
3.0kV
X1,000
10μm
WD 8.5mm

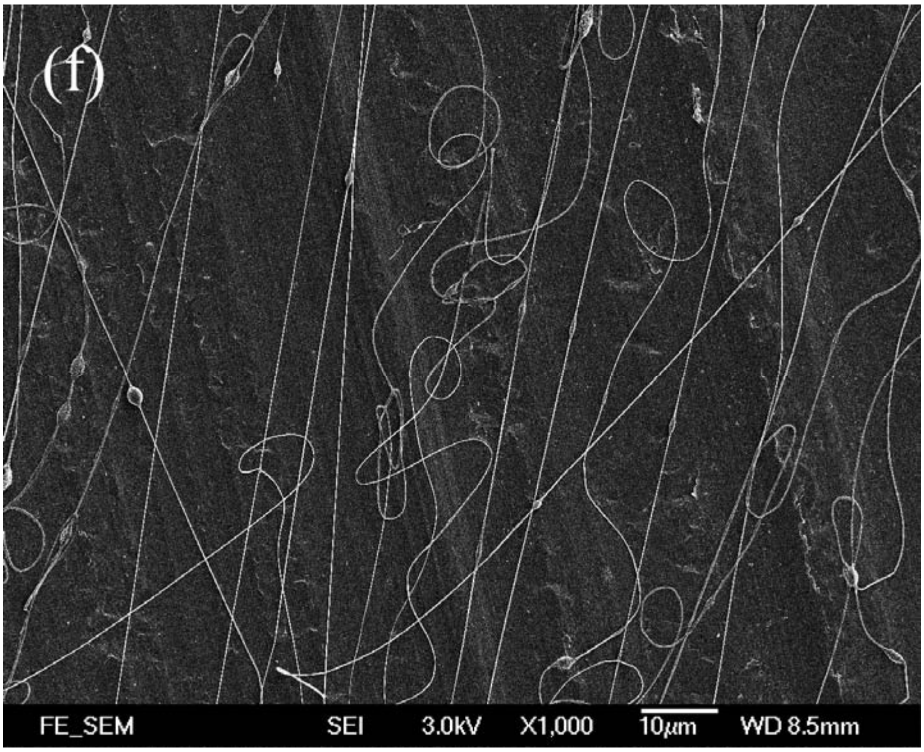
(f)
FE_SEM
SEI
3.0kV
X1,000
10μm
WD 8.5mm

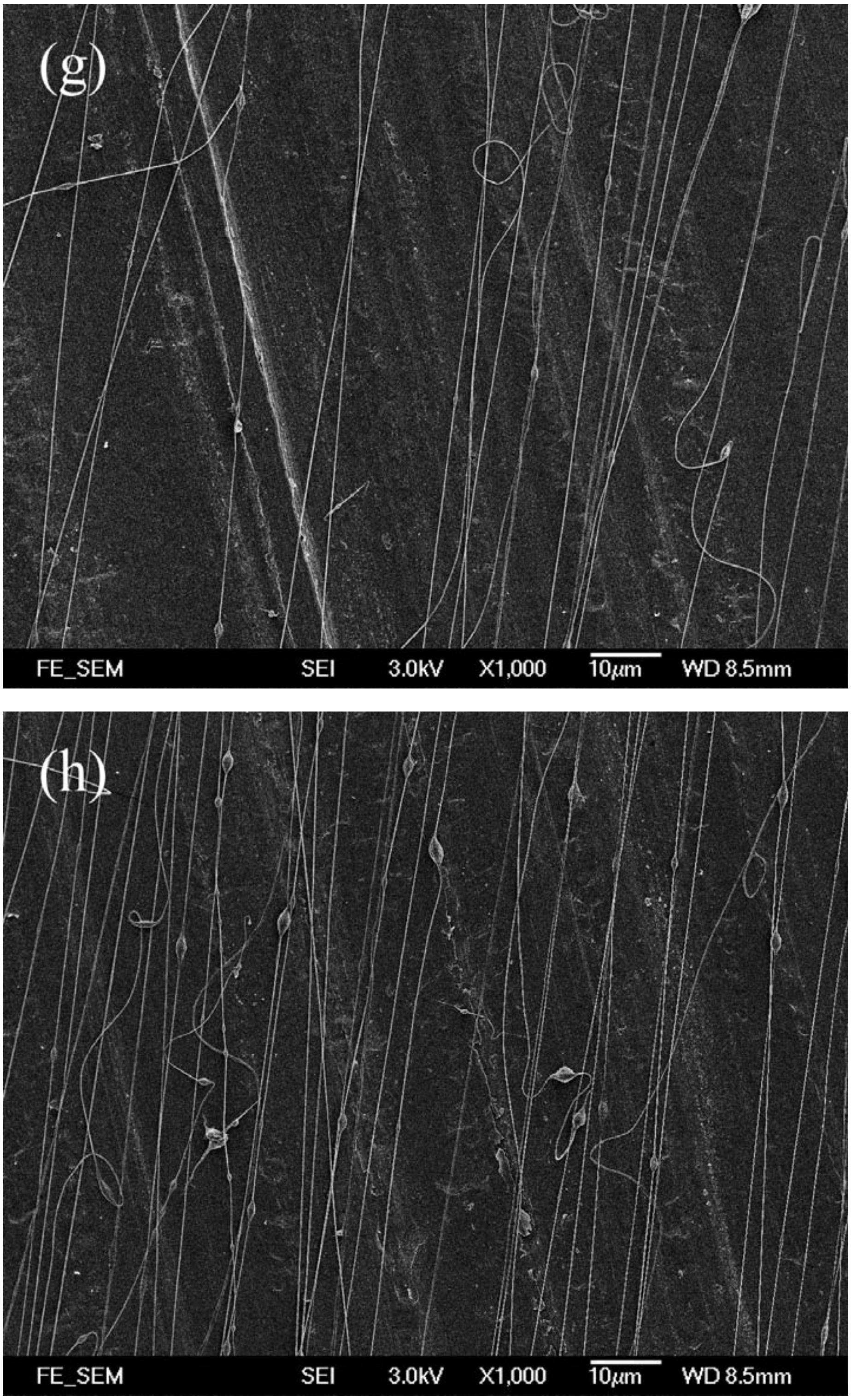

Fig. 3.6 SEM pictures of PMMA fibers collected by rotating disc collector at different distance from center: (a) 1, (b) 5, (c) 8, (d) 10, (e) 15, (f) 18, (g) 25 and (h) 35mm. The collector was rotating at 3600 rpm.

3.3 Conclusion

In the project, smooth and thin fibers are desired. In order to achieve such good quality of fibers, parameters for controlling the electrospinning process have been studied in details. By investigating the effects on different solvents, concentration and molecular weight of polymer, and the applied voltage for electrospinning, the optimized polymer solution and processing condition of electrospinning were determined. Solutions of around 7 wt% of PMMA with molecular weight of 350,000 in NMP solvent could be used in electrospinning to obtain smooth fibers of diameter in 200nm range.

In addition, aligned nanofibers are preferable for characterization and analysis. Therefore, the rotating speed of collector has also been tried. From the observation of morphology of the fibers, linear speed above 9 ms^{-1} in our setup is required to obtain good orientation.

Studying of electrospinning process helps to control the morphology of electrospun fibers, and experience is also necessary for optimizing other electrospun polymers like PEO that will be discussed in the next chapter.

Chapter 4

PEO/carbon black Nanofibers

In this chapter, properties of PEO/carbon black composite fibers prepared by electrospinning will be discussed. PEO is known as an electrolytic polymer which is similar to liquid electrolyte capable to conduct electricity via ions transportation. PEO thus has been used for studying electrospinning process due to its relatively high conductivity in addition to the good fiber formation quality. In the first part of this study, crystalline structure and degree of orientation of electrospun pure PEO nanofibers will be introduced. Following this is the study of PEO mixed with carbon black powders for electrospinning. The morphology and characteristic of PEO/carbon black fibers prepared in various conditions will be presented. Lastly, the electrical properties of the composite fibers will be investigated. It reveals the effect of the conducting carbon black powders in the composite nanofibers. Before going into details, a brief review on the conventional polymer/carbon black bulk composite films, concerning the conductivity dependence of the sample on the concentration of carbon black added will be introduced.

4.1 Conventional Polymer/carbon black Composites

Carbon black powders are widely used in making conductive polymer composites. An insulating polymer blended with the carbon black powders will have a change in conductivity; in general the more carbon black is added, the larger is the conductivity. If the volume fraction of the carbon black is over the threshold of percolation, the composite will become a conductor-like material. Fig. 4.1 shows the conductivity of a PEO/carbon black composite film sample which changes with the increase of volume fraction of carbon black powders. This experiment was done by other member in our research group. The conductivity was obtained by measuring the D.C. current-voltage characteristics of those samples; the voltage was ranged between -1 V and 1V. From the log scale used in the y-axis, it can be seen that the conductivity increases almost two orders of magnitude with just about 10% carbon black added. From the literature (Elimat, 2006), it has been reported the A.C. conductivity of PMMA/carbon black composite shows similar dependence. These results prove that carbon black inside bulk polymers including PEO can enhance the conductivity of the composites. Carbon black is known as conductive materials and when they are filled into polymer, conducting paths increases and thus conductivity increases. In summary, the conductivity of conventional bulk polymer/carbon black composites increases as more carbon black particles are added.

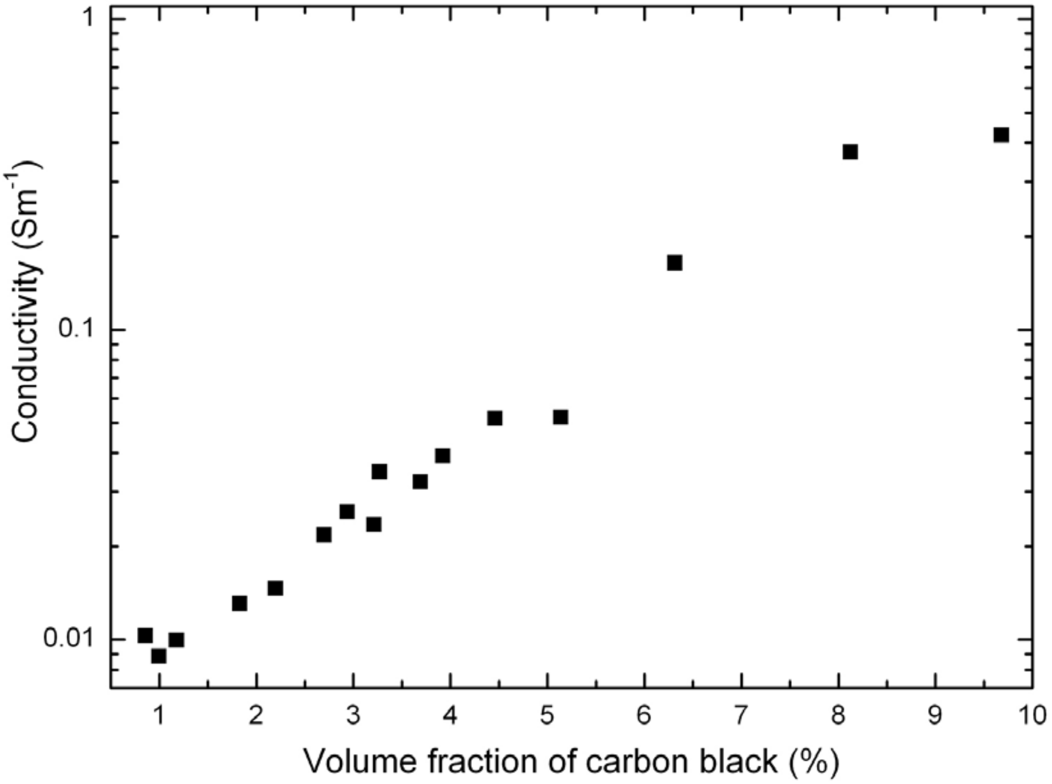

Fig. 4.1 Conductivity of PEO/carbon black film sample versus volume fraction of carbon black powders.

4.2 Experimental

4.2.1 Solution Preparation

Polyethylene oxide (PEO) (M_w=1,000,000) was purchased from Sigma-Aldrich. The carbon black particles were provide by 南方化工染料有限公司 with a trade name 華光導電炭黑; the average particle size is about 50 nm and a conductivity of about 3 Scm^{-1}. They were used as-received without further purification.

The solvent was a mixture of water (60 wt%) and ethanol (40 wt%). 3 wt% of PEO was dissolved into the solvent by rigorous stirring at room temperature. Various amounts of carbon black were added (0.1, 1, 2 and 4 wt% with relative to PEO powders) were added in the polymer solution by further stirring for one hour and ultrasonication for 30 minutes.

4.2.2 Electrospinning Process

In producing PEO/carbon black composite fibers, a positive 10kV was connected to the tip for electrospinning. A grounded rotating cylinder collector (Fig. 2.3b) wrapped with an aluminum foil was used and the rotating speed was 2900 rpm. The diameter of the cylinder is 6 mm thus producing a tangential velocity of 9 ms^{-1} at the cylinder surface. Distance between the tip and collector was 12 cm. The amount of solutions for electrospinning was controlled to 0.4 ml in order to maintain a similar amount of fibers through-put. 1 ml of solution was used to deposit the fibers for XRD measurement. After the deposition, samples were collected and dried at 40˚C for 24 hours.

4.2.3 Electrical Measurements

A.C. Conductivity

A.C. conductivity of nanofibers was determined by using a lock-in amplifier. The lock-in amplifier gave 1 V sinusoidal voltage (V) on the sample which was connected in series with a resistor of resistance R. The circuit diagram is given in Fig. 4.2. In this circuit, R was properly selected to have a reasonable large voltage drop on it, in the present study it was set to 10 MΩ. The sample can be regarded as a capacitive component in this circuit. The voltage across the resistor (V_R) was measured by the Lock-in amplifier. According to the circuit diagram, the ratio of V_C and V_R is proportional to the impedance ratio of the two components as given in equation 4.1 as follow:

$$\frac{V_C}{V_R} = \frac{I \cdot (Z' + iZ'')}{I \cdot R} \qquad (4.1)$$

Where Z' and Z'' are the real and imaginary parts of the impedance of the sample since $V_C = V - V_R$, thus

$$\frac{V - V_R}{V_R} = \frac{Z' + iZ''}{R} \tag{4.2}$$

If V_R is expressed in its real part V_{RX} and imaginary part V_{RY} as:

$$V_R = V_{RX} + iV_{RY} \tag{4.3}$$

and V_{RX} and V_{RY} can be obtained from the Lock-in output voltage components of 90° out of phase. Substitute equation 4.3 into equation 4.2 and evaluate Z' and Z'', the impedance can then be calculated from the following two equations respectively:

$$Z' = R\left[\frac{VV_{RX}}{[V_R]^2} - 1\right] \quad (4.4) \text{ and}$$

$$Z'' = \frac{-VV_{RY}R}{[V_R]^2} \quad (4.5).$$

Thus a Cole-Cole plot of the sample's impedance can be obtained.

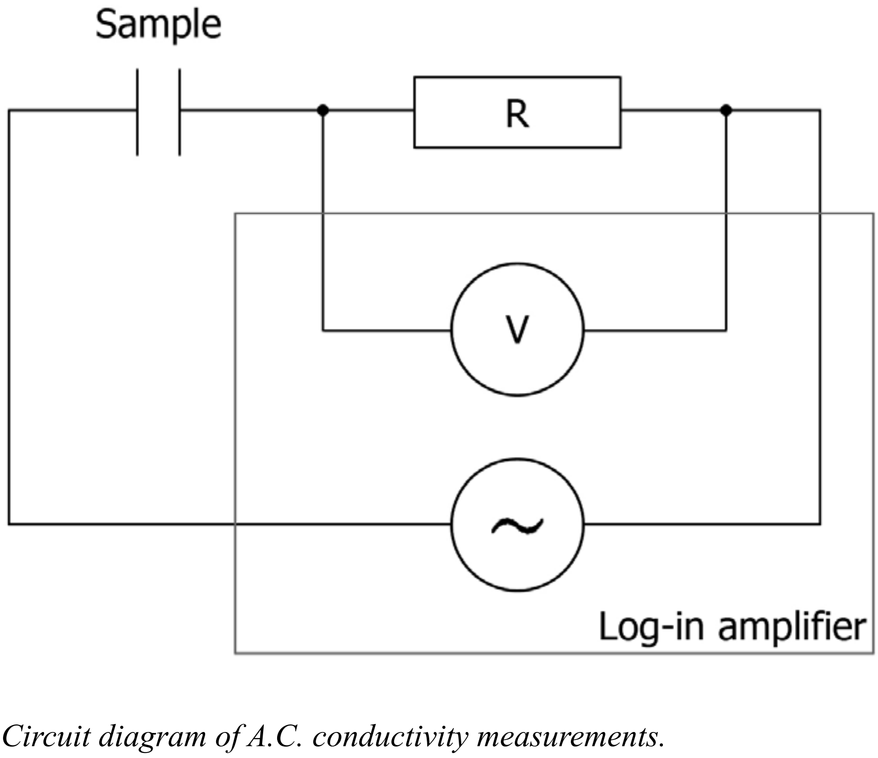

Fig. 4.2 Circuit diagram of A.C. conductivity measurements.

D.C. Current-voltage (IV) Characteristics

The D.C. conductance of the samples can be estimated from their relationship of current and voltage. Keithley 6517A electrometer is used to measure the IV characteristics with its built-in voltage source, the voltage was applied onto the samples and the current is recorded by the computer via the electrometer.

In measuring the IV curves of PEO/carbon black fibers and films, measurements were scanned from -50 to 50 V in a 2 V step.

4.3 Results and Discussion

4.3.1 XRD Analysis

PEO is a semicrystalline polymer of crystallinity usually higher than 50% in bulk samples. Its molecular conformation is a (7/2) helix. The unit cell of PEO is basically of a monoclinic structure (Kirk & Othmer, 1991). Interestingly, if PEO is under stretching, its conformation may be changed to planer zig-zag and the unit cell becomes triclinic. Therefore it is worth to conduct an investigation of the crystal structure of PEO nanofibers which is likely to have been stretched during electrospinning. Fig. 4.3 shows the XRD of bulk PEO sample, the peaks of crystal planes (120) and (112) are at $2\theta = 19.2^\circ$ and 23.4° respectively.

Fig. 4.4 shows the θ-2θ scans of the highly aligned PEO fiber sample collected by the cylinder; the direction of the fibers was made at an angle (ψ) with respect to the X-ray plane of incidence. A clear observe of the XRD intensity changes with ψ can be found in Fig. 4.5 and the schematic diagram is given in Fig. 2.1. ψ changes from 66° to 92° in steps of 2°. Two peaks are observed at $2\theta = 19.2^\circ$ and 23.4° respectively. The intensity of the former peak begin to increase from $\psi = 66^\circ$ and reaches the maximum at $\psi = 90^\circ$. On the contrary, the intensity of the latter peak increases from $\psi = 86^\circ$ and reaches the maximum at $\psi = 70^\circ$. Similar results had also been reported by other research group

(Deitzel, Kleinmeyer, Hirvonen, & Beck Tan, 2001a).

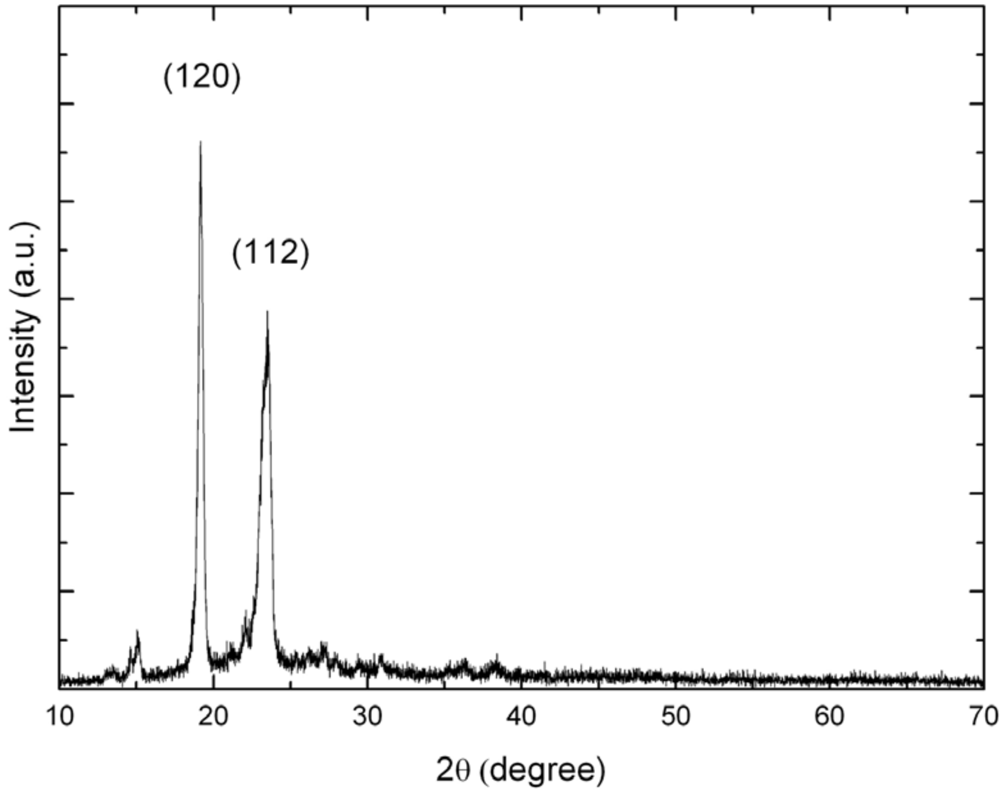

Fig. 4.3 XRD of bulk PEO, θ–2θ scans (from 2θ =10° to 70°)

Concerning the crystal structure of PEO fibers, diffraction peaks found at 2θ = 19.2° and 23.4° verify the helical symmetry of PEO (Fig. 4.6). The schematic diagram shown in Fig. 4.7 illustrates the crystal structure of PEO, the crystallographic unit cell contains four molecular chains and is monoclinic with a = 7.96 Å, b = 13.11 Å, c = 19.39 Å and β = 124°48′. The polymer chain in crystalline state contains seven structural units, CH_2CH_2O, and two helical turns per period, 19.3 Å (Bailey & Koleske, 1976). It is noted that (120) and (112) crystal planes are responsible for the peaks at 2θ = 19.2° and 23.4° respectively (Deitzel, Kleinmeyer, Hirvonen, & Beck Tan, 2001a). In addition, there is no observable diffraction peaks found in the XRD profiles which can be used to verify the existence of planer zigzag conformation (Takahashi, Sumita, & Tadokoro, 1973).

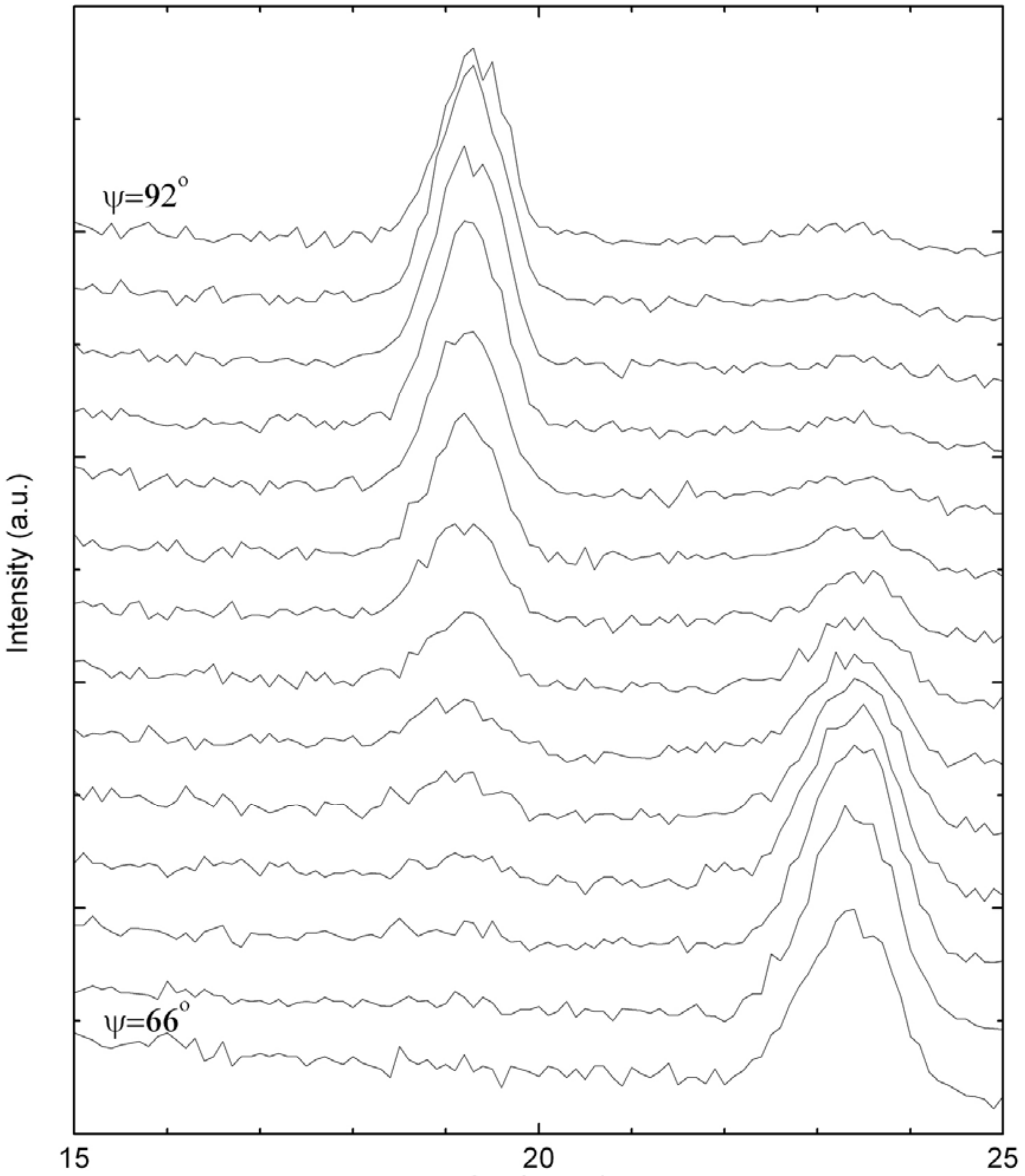

Fig. 4.4 XRD of pure PEO electrospun nanofibers, θ–2θ scans (from 2θ = 15° to 25°) with different angles of fiber direction (from ψ = 66° to 92°).

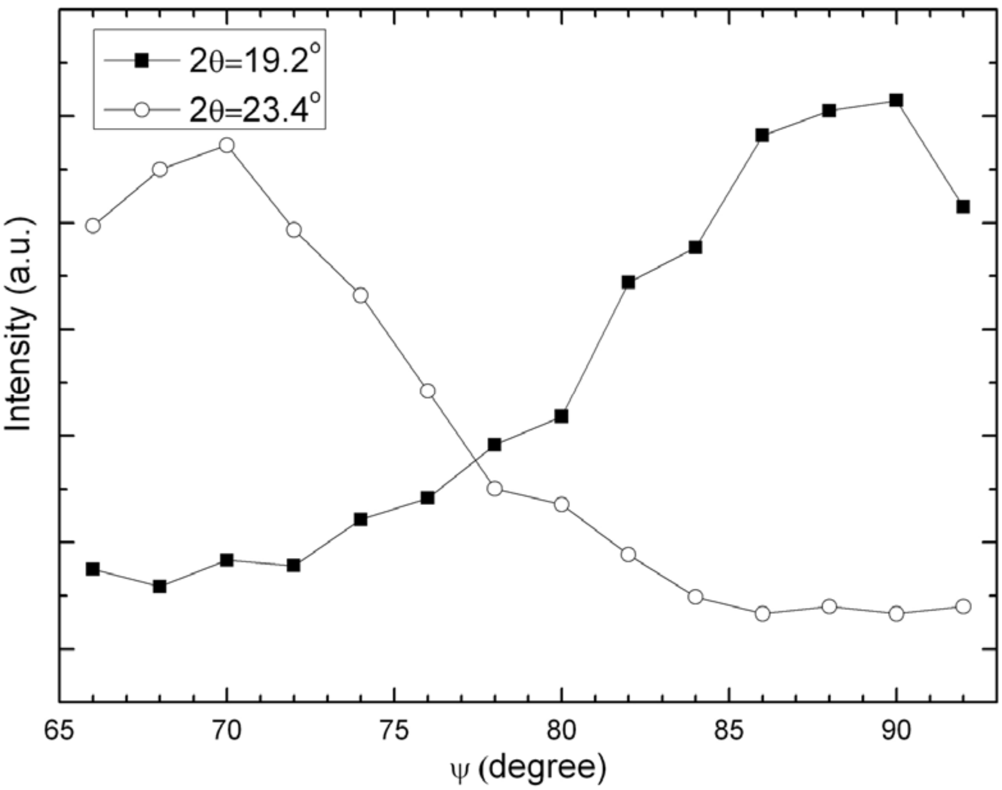

Fig. 4.5 XRD of pure PEO electrospun nanofibers, shows ψ from 66° to 92° at 2θ = 19.2° and 23.4°. The data points are picked from θ–2θ scans (from 2θ = 15° to 25°) as shown in Fig. 4.4.

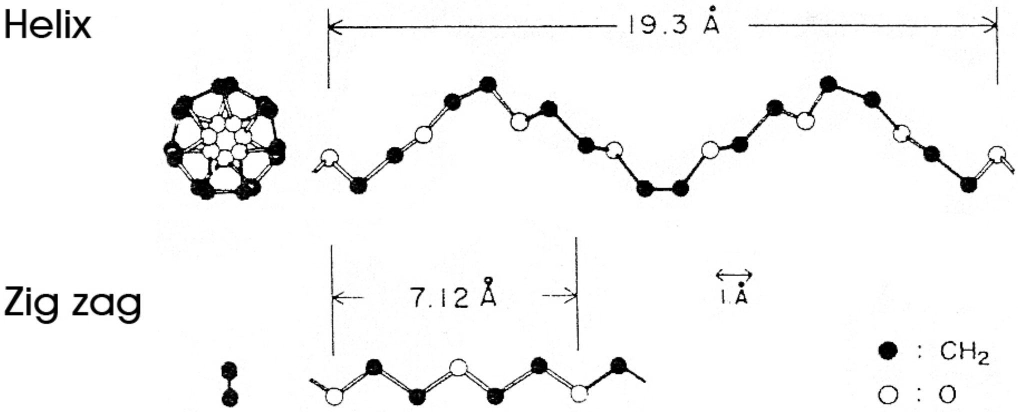

Fig. 4.6 Two of known conformations of the PEO molecule (Takahashi et al., 1973).

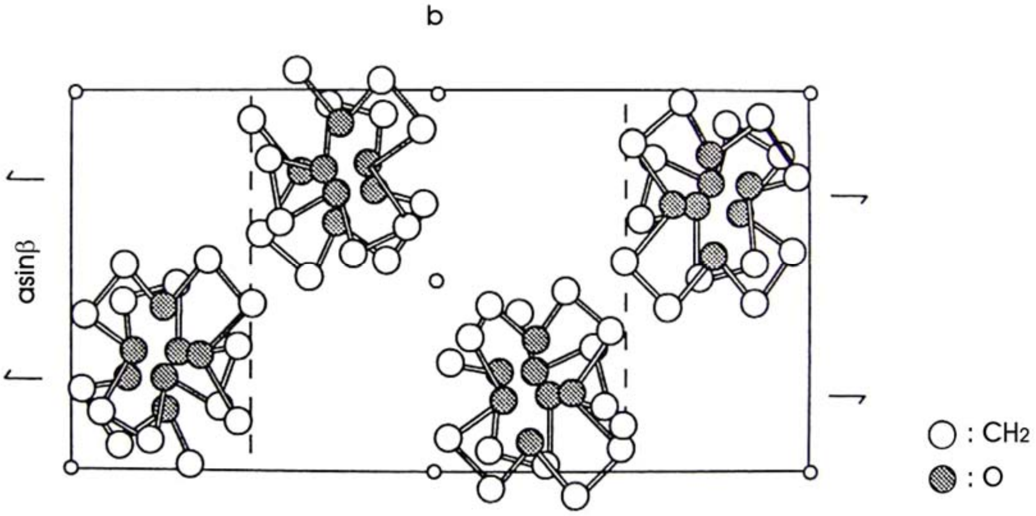

Fig. 4.7 Crystal structure of PEO (Takahashi & Tadokoro, 1973).

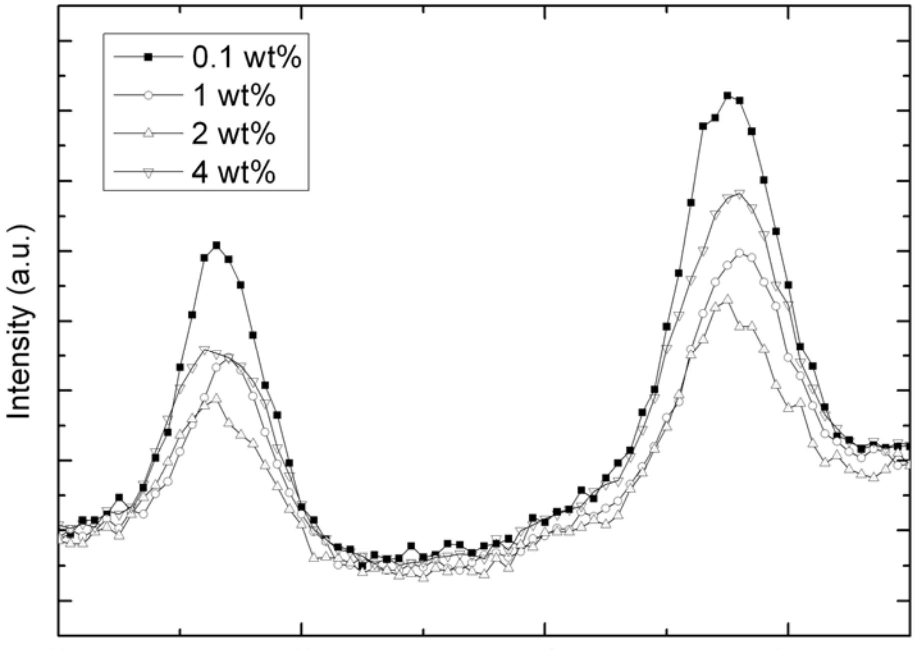

Fig. 4.8 XRD of randomly aligned PEO/carbon black electrospun nanofibers (0.1, 1, 2 and 4 wt% of carbon black was added), θ–2θ scans (from 2θ = 15° to 25°).

The degree of orientation of the electrospun fiber revealed by XRD has been calculated according to equation 2.3 and equation 2.4.

In the present case, the (120) crystal plane is convenient to be used for finding orientation parameter (f) as the diffraction intensity reaches maximum at $\psi = 90^{\circ}$. By approximating the integrals into summation and making use of the diffraction intensity results given in the XRD profiles, f can be estimated and the value is 0.94. This result implies a high degree of orientation of the electrospun PEO nanofibers using rotating cylinder collector.

It should be noted that XRD of aligned fiber mat of PEO/carbon black samples collected by the rotating disc reveals no discernable peaks; this fact indicates that the collective diffraction intensity of the aligned PEO/carbon black fibers is not large enough to a measurable level. This may due to the smaller amount of fibers as the presence of carbon black retards the production of fibers in electrospinning which will be further discussed in Section 4.3.3 . Therefore, the degree of orientation of PEO/carbon black fibers cannot be determined as there are only a small amount of fibers satisfy the Bragg's diffraction condition. However, XRD of PEO/carbon black fibers have still been carried out by collecting those fibers from a large area of the collector as to increase the number of fibers.

Fig. 4.8 shows the θ–2θ scans of the PEO/carbon black fiber samples. Solid conclusion cannot be drawn on the difference of the diffraction intensity as the intensity is small and the amount of fibers in each samples vary. However, the XRD shows the crystalline phase of PEO still exists with the presence of carbon black.

4.3.2 FTIR Spectra

A study of the IR absorption of neat PEO and PEO/carbon black fibers has been performed by FTIR. This result will reveal the microstructure of the electrospun PEO and its composite fibers. Fig. 4.9a to c show the FTIR spectra of neat PEO and PEO/carbon black nanofibers of various carbon black concentrations, from which two configurations of PEO molecules, trans and helical structures can be identified (Fig. 4.6).

Absorption peaks appeared in the spectra shown in Fig. 4.9b at 962, 1241 and 1341cm^{-1} are resulted from the trans configuration of PEO molecules, while the peaks of 948, 1060, 1149, 1280 and 1358cm^{-1} in Fig. 4.9c revealed the vibrational absorption of helical configuration (Marcos, Orlandi, & Zerbi, 1990). The former set of absorption bands is more prominent (Fig. 4.9a) which indicates that the electrospun fibers are in favor of trans configuration. This has been further confirmed with the polarized FTIR as shown in Fig. 4.9b and c, it was measured with the electric vector of the polarized IR beam parallel to fiber direction, the trans peaks are dominant. As the electric vector was rotated perpendicular to the fiber direction as shown in Fig. 4.9c, the helix absorption bands emerged but of lower intensity. From the polarized IR spectra, it is clear that trans structure were more favorable to be formed along the fiber direction, which implies electrospinning process could align the polymer chains.

However, it is interesting to compare the results obtained from XRD and FTIR studies. It is evident that from FTIR result, most of the chains are found in trans formation, but it cannot be observed in XRD, one of the possible explanation is that the molecular chains in trans configuration are most likely amorphous. The helical structure identified by XRD is also verified in FTIR. It suggests that electrospinning helps to align the molecules along the fiber direction that also could minimize crystallization of PEO due to the fast drying during the jet flying in the air.

On the other hand, the main absorption peak intensities of PEO/carbon black composite fiber decrease with the increase of carbon black concentration, this phenomenon occur in all the three measurements shown in Fig. 4.9. This can be explained by the increasing scattering of carbon black powders in the composite samples. In addition, the FTIR spectra of two orthogonal electric vectors direction became more alike when more carbon black powders were added; it suggests that carbon black particles in the fibers suppress the molecular orientation and/or formation of the helical structure. This may be due to the morphology change of PEO/carbon black fibers that brings from the carbon black particles, details on the morphology will be discussed in the next section.

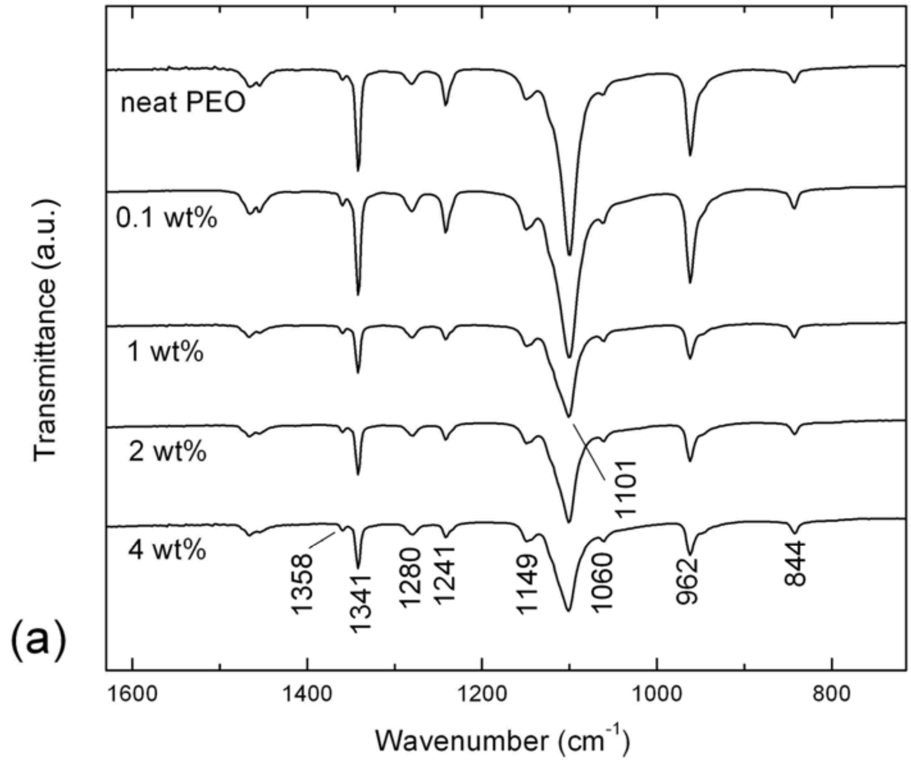

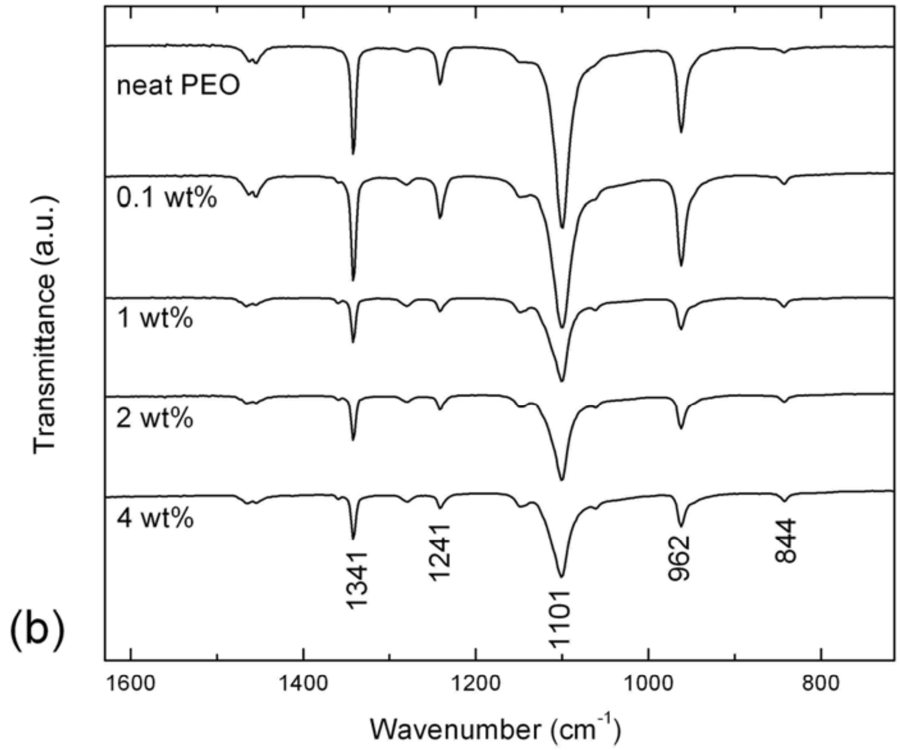

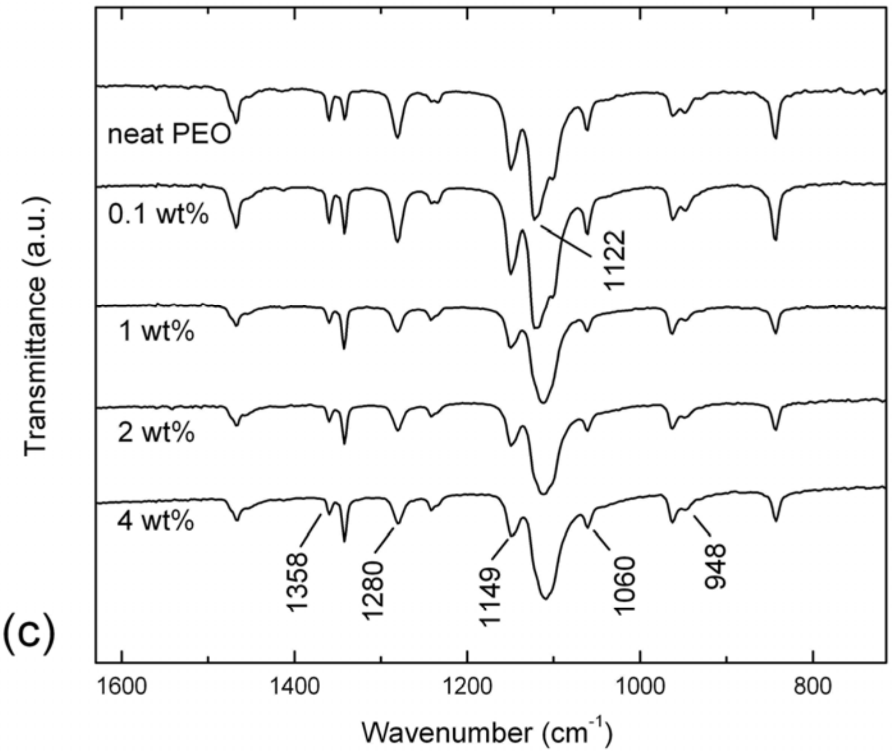

Fig. 4.9 Infrared spectra of PEO/carbon black nanofibers with different amount of carbon black: (a) no polarizer, (b) electric vector of polarized beam parallel and (c) perpendicular to fiber direction.

4.3.3 Morphology of Electrospun Fibers

In study the morphology of the PEO/carbon black fibers, both the transmission electron microscope and scanning electron microscope had been employed. Fig. 4.10a to e show the SEM pictures of the PEO/carbon black nanofibers with no carbon black; 0.1, 1, 2, 4 wt% carbon black respectively. The diameter of pure PEO fibers is around 150 nm and the size remained the same when carbon black is added. Beads are formed when fibers contain more than 1 wt% of carbon black particles. It may be due to the uneven distribution of carbon black particles as they agglomerated in the PEO solution and affect the distribution of electrostatic charges in the jet of fibers.

Fig. 4.11a and b show two TEM pictures of PEO/carbon black electrospun fibers. The pictures clearly show that the carbon black is not evenly distributed along the PEO fibers. They aggregate, and through electrospinning, some can be separated into small groups (Fig. 4.11b); however, large clusters of carbon black (Fig. 4.11a) cannot be eliminated.

Carbon black powders are difficult to disperse uniformly in the solution even using surfactants. However, the founding shows that during electrospinning, carbon black powders are able to be further dispersed within certain extent. During electrospinning, the polymer jet is being stretched and the carbon black particles inside will also be stretched by the jet. Since carbon black is also a charge carrier, repulsive electrostatic force will also help to disperse.

As a matter of fact, more carbon black in the solution would retard the formation of the jet thus the production of fibers in electrospinning. Solutions with more than 4 wt% of carbon black could not be electrospun. It is believed that this is mainly related to the poor ability of dispersion and electrospinning of carbon black. Electrospinning requires polymer chains to flow continuously to the tip of syringe. However, the clusters of carbon black inside the polymer solution cannot be dispersed thus they jam the syringe.

The more the carbon black particles added, the harder the polymer solution can flow inside syringe.

In summary, the quality of pure PEO fibers, in terms of size distribution and beam formation, is comparatively better than the fibers with addition of carbon black. The size of the fibers varies significantly with the appearance of beads as more carbon black is added.

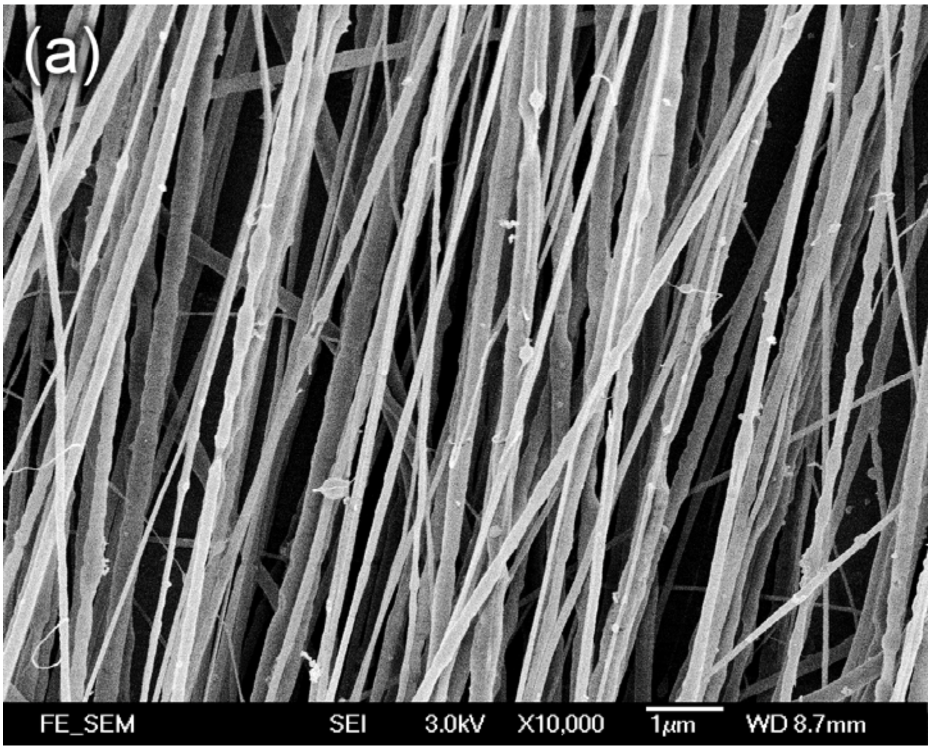

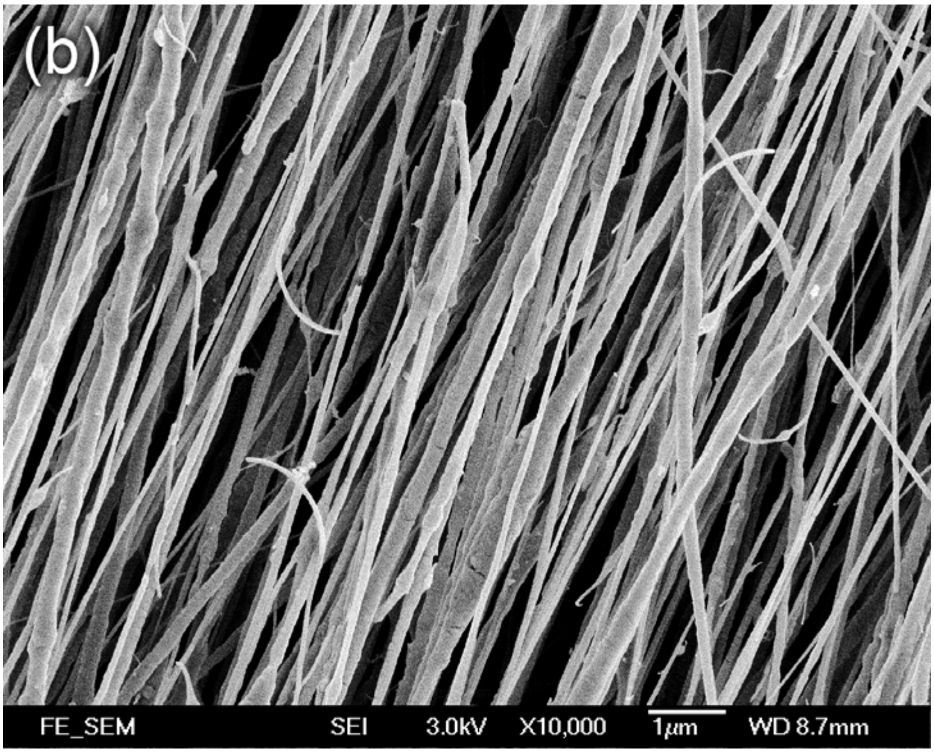
(b)
FE_SEM
SEI
3.0kV
X10,000
1µm
WD 8.7mm

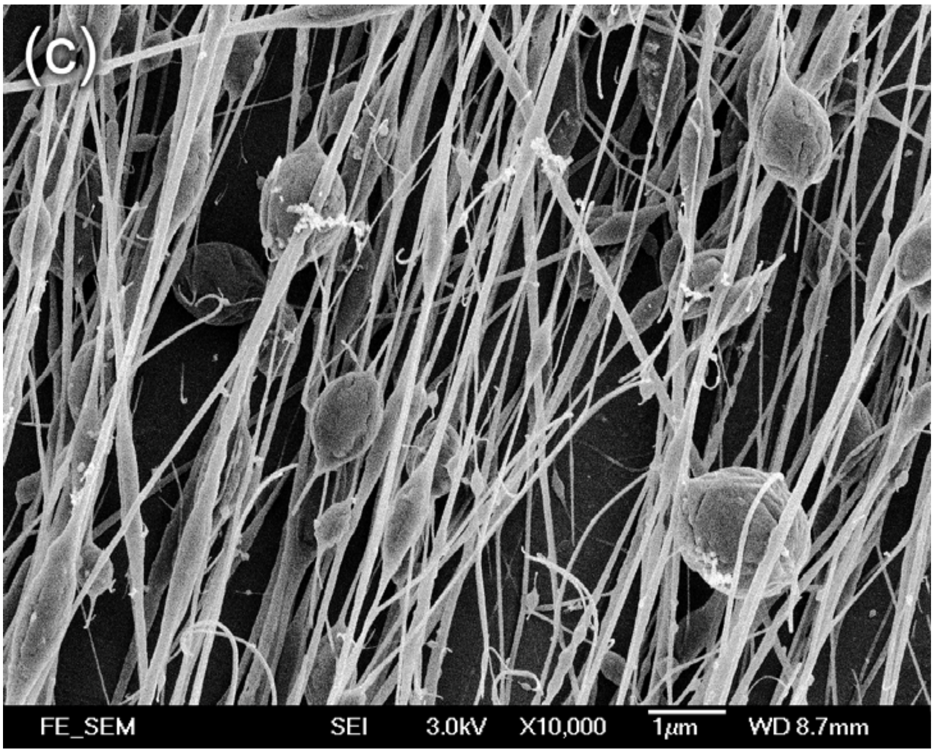
(c)
FE_SEM
SEI
3.0kV
X10,000
1µm
WD 8.7mm

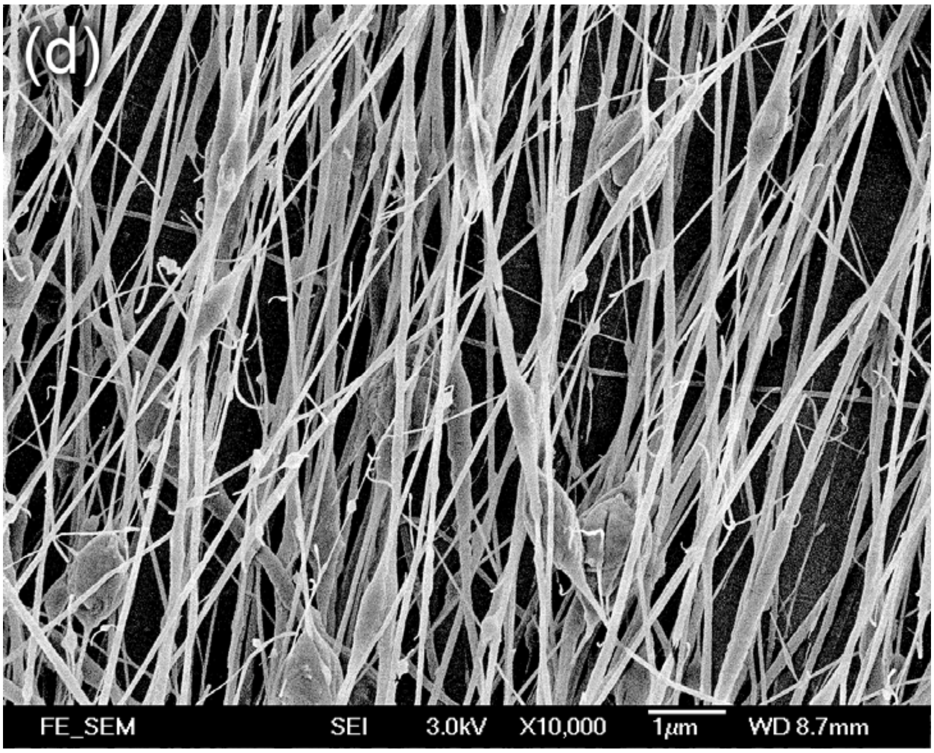

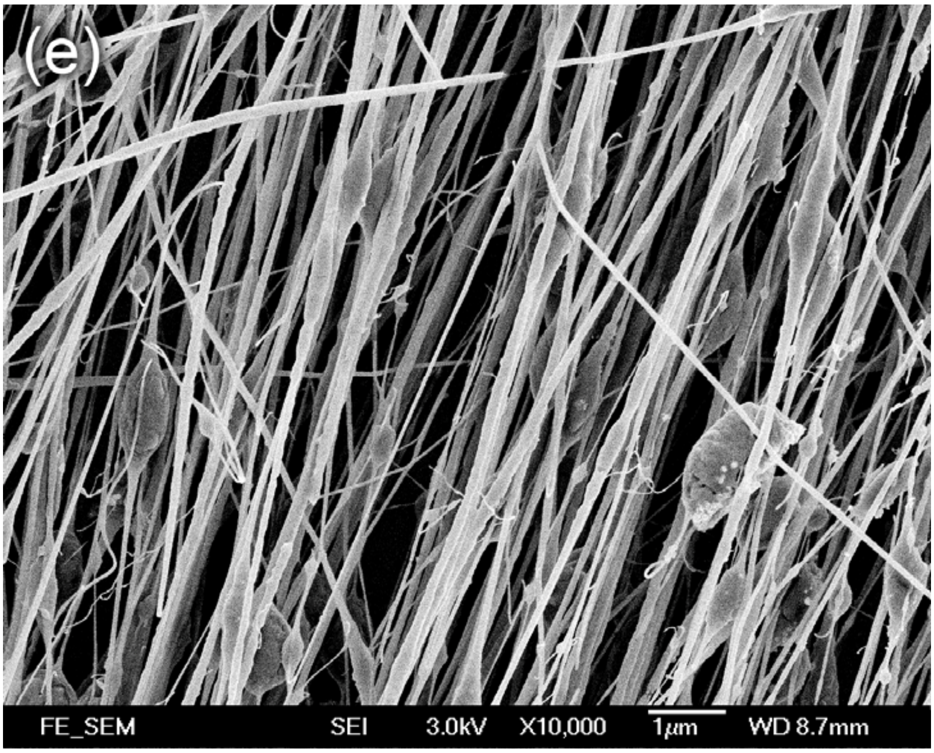

Fig. 4.10 SEM pictures of PEO/carbon black nanofibers with different amount of carbon black (a) neat PEO, (b) 0.1 wt%, (c) 1 wt%, (d) 2 wt% and (e) 4 wt%.

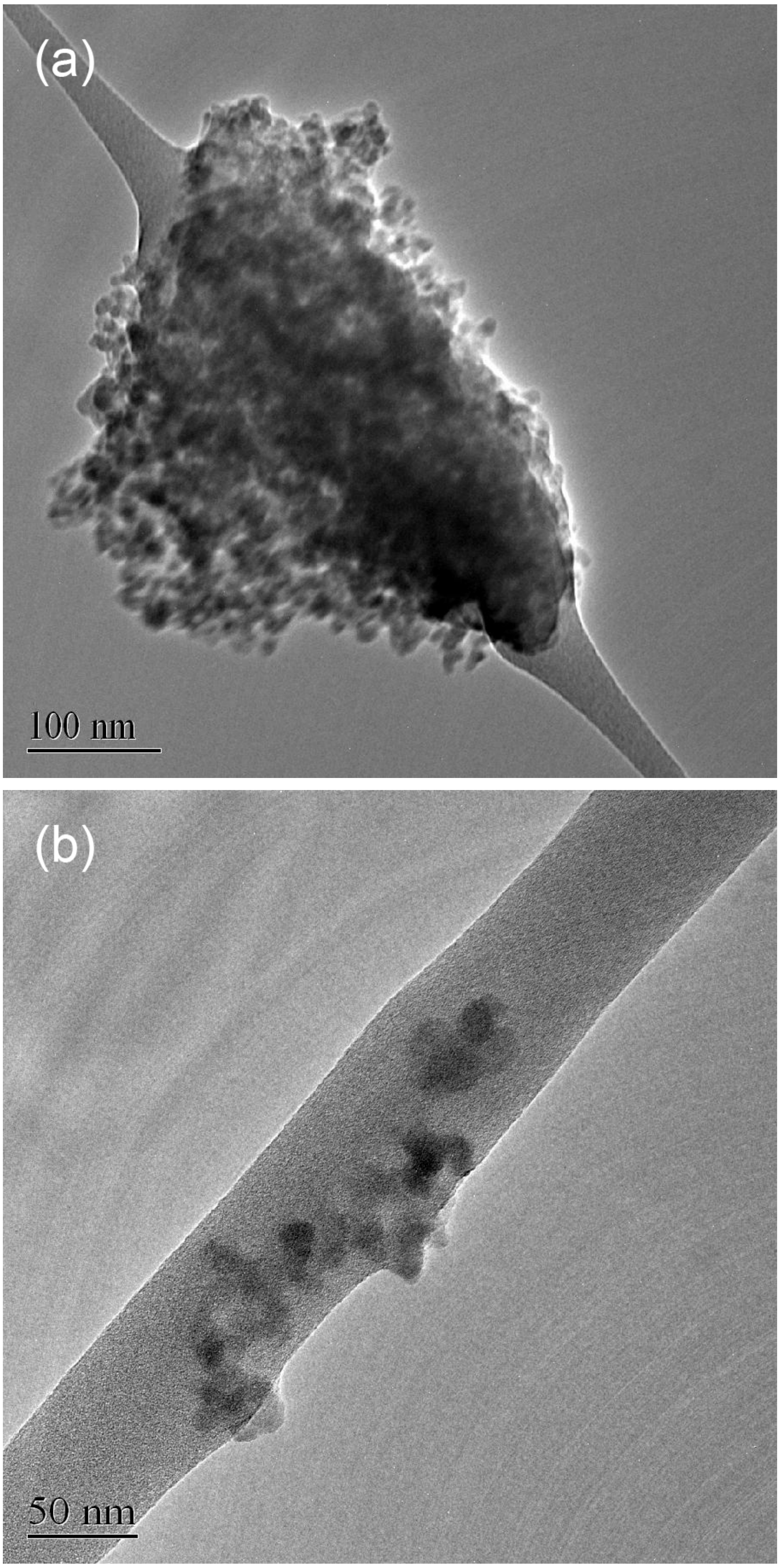

Fig. 4.11 TEM images of PEO/carbon black fibers with a cluster of carbon black: (a) larger and (b) smaller than the fiber diameters.

4.3.4 Electrical Measurements

Electrical properties of electrospun PEO/carbon black composite nanofibers are worth studying due to its nanometer size and the quasi-one dimensional construction. Electrospinning is able to disperse carbon black and distributed them into the PEO fibers. Nanofibers increase the surface area to volume ratio, which is expected to shorten the reaction time for sensing application and also to boost up the responding magnitude.

A.C. Conductivity

The A.C. measurements were carried out at 1 V rms applied voltage across the sample in series with a 10 MΩ resistor. Five samples of PEO/carbon black fibers have been measured and Fig. 4.12 shows their Cole-Cole plots. Three points per order of magnitude from 100 kHz to 0.1 Hz were obtained. Due to the large fluctuation of signals at low frequencies, data points of PEO/carbon black fibers at low frequency (down to 10 mHz) are disregarded.

Neat PEO fibers exhibit the Debye dielectric semicircle with a spike occurs at 0.1 Hz and the impedance is about 180 GΩ. Semicircles of the rest of composite samples could not be completed even at 0.1 Hz; and the curves at the high frequency end rise almost linearly, it implies that the composite fiber show almost no dielectric loss. On the other hand, PEO/carbon black fibers are like an insulator, the impedances increase with the amount of carbon black. Only a small amount of carbon black (0.1 wt%). The Cole-Cole plot of which shows no semi-circle feature even at a very low frequency (0.1 Hz). All of the observations indicate that, on the one hand these composite fibers do not show Debye dielectric properties, and on the other hand, carbon black particles are not favorable if conducting fibers are required.

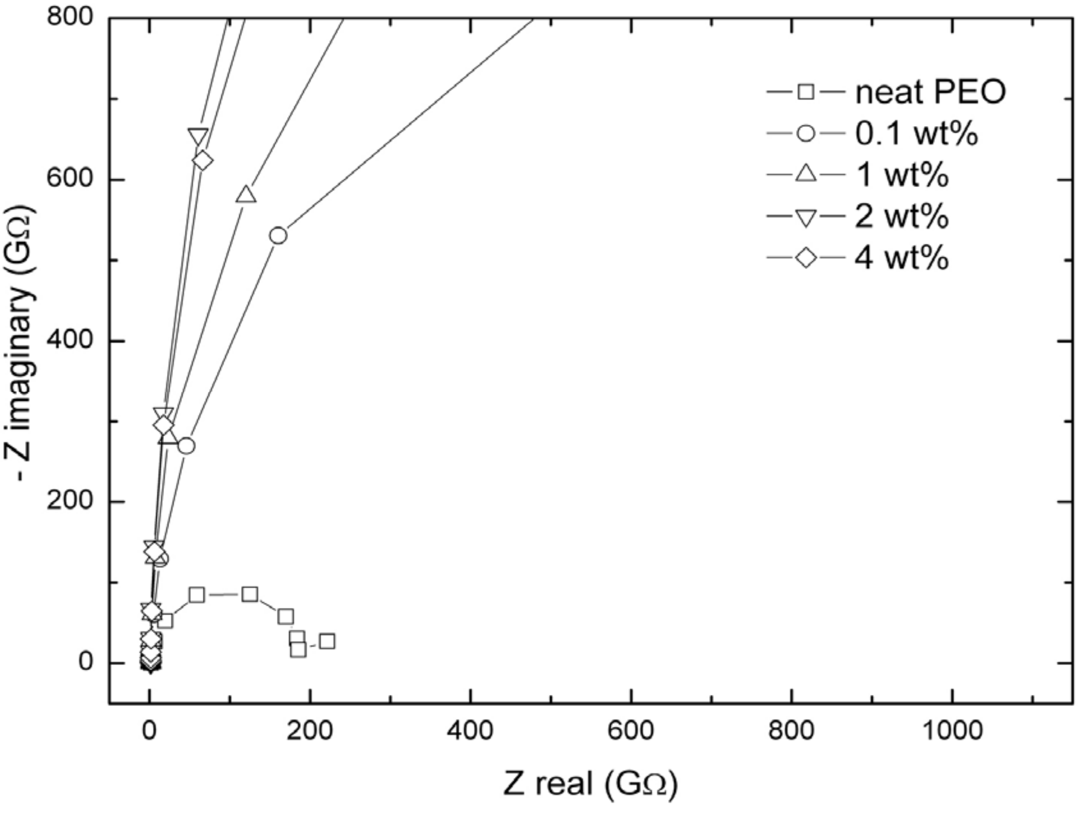

Fig. 4.12 Impedance spectra of PEO/carbon black nanofibers with different amount of carbon black.

Moreover, at the high frequency end, the slope of the curve of 4 wt% carbon black dropped when comparing with the 2 wt% one. This result is not conclusive which may be due to the error caused by the tremendous value of impedance.

D.C. Current-voltage (IV) Characteristics

The D.C. measurements were scanned from -50 to 50V in 2V step (Fig. 4.13a and b). As the measured current range is large between samples, semi-log scale of IV plot (Fig. 4.13b) was used. At a very low applied voltage, linear IV characteristics of the composite fibers are observed as shown in Fig. 4.13a, the resistances of the samples were estimated. The relation between resistance and the concentration of carbon black of the samples is shown in Fig. 4.14.

It can be seen that the sample resistances increase with carbon black concentration, the lower the current they are able to carry. It indicates that the electrical conduction ability of the composite fibers is suppressed with the addition of small amount of carbon black, same as those observed in the A.C. measurements. These results in general contradict the results obtained for bulk composite samples.

A possible explanation of this phenomenon is proposed in the following. The lower conductance with more carbon black in the fiber is due to the different conduction mechanisms between carbon black and PEO. The comparable size between the carbon black particles and the PEO nano-sized diameter also plays a role in this abnormal trend of conductance. The major charge carriers of carbon black are electrons but the major current conduction in PEO is accomplished by ion diffusion (Bailey & Koleske, 1976).

When there is no or only a very small amount of carbon black which is not enough to aggregate in PEO nanofibers as shown in Fig. 4.15, the only way for current flow is the ions in PEO. However, as more carbon black are introduced into the nanofibers, which will block the conducting path of ions. The ions cannot get across carbon black as they do in bulk PEO/carbon black samples. On the other hand, since carbon black is a good conductor, the electric field would be screened due to its existence in the fiber. As a result, at a long distance away from the electrodes, the electric field is reduced and not large enough to drive the ions. Thus, the bundle of PEO/carbon black nanofibers becomes more like an insulator.

It is found that the quasi-one dimensional construction of the nanofibers is able to impede carbon black from percolation even its concentration as high as 4 wt% which is enough to form percolation in bulk samples. However, a research group (Kessick & Tepper, 2006) has reported that by adding about 19 wt% of carbon black, percolation can be occurred in micron-sized fibers.

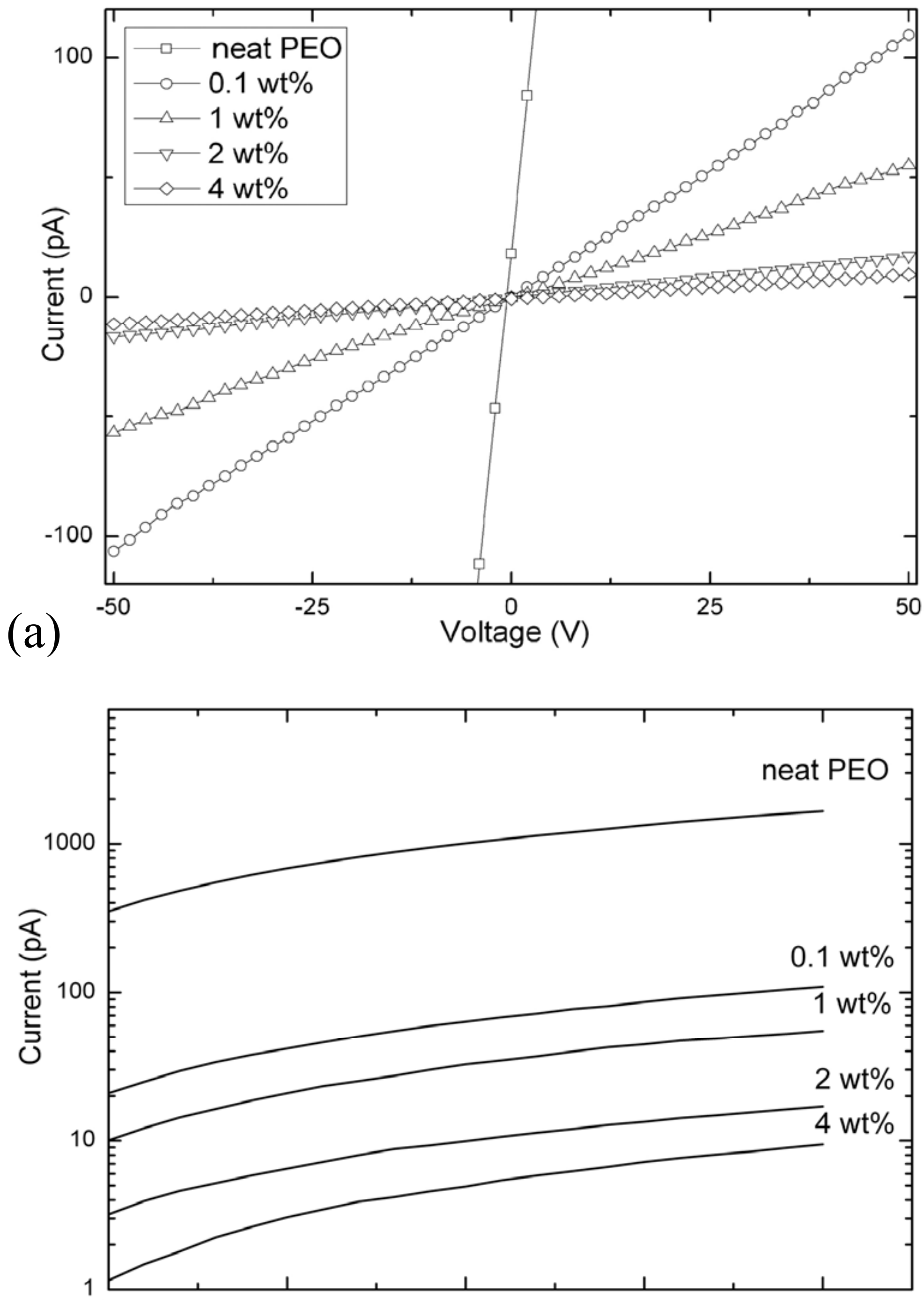

Fig. 4.13 Current-voltage (IV) curves of PEO/carbon black nanofibers with different amount of carbon black. (a) linear scale from -50 V to 50V, (b) semi-log scale from 10 V to 50V.

Concerning the effect of the morphology of fibers, it is believed that the formation of beads and the orientation of fibers did not affect much the electrical properties of the samples. Though the changes of electrical signals were dramatic, the amount of fibers was comparable and there were no significant change in the morphology of fibers.

To conclude, carbon black particles are not able to enhance the conductivity of PEO/carbon black composite nanofibers prepared by electrospinning but they reduced the electrical conduction up to 4 wt% of which is added.

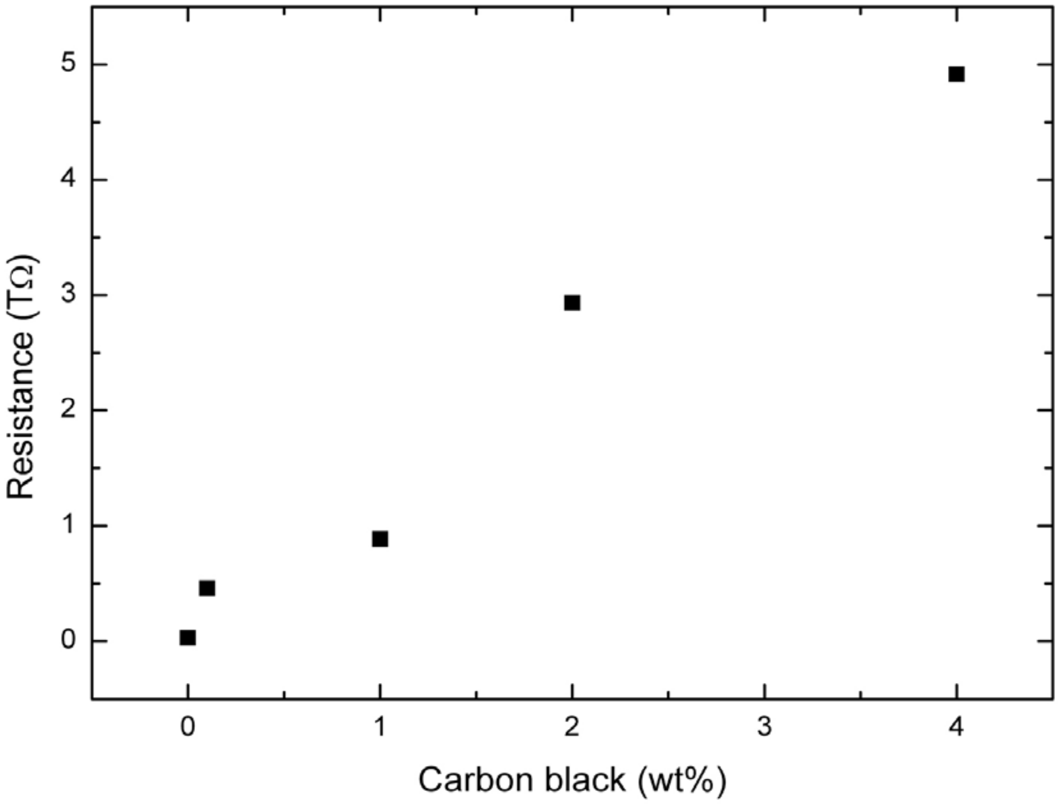

Fig. 4.14 Estimated value of resistance of PEO/carbon black fibers in various amount of carbon black.

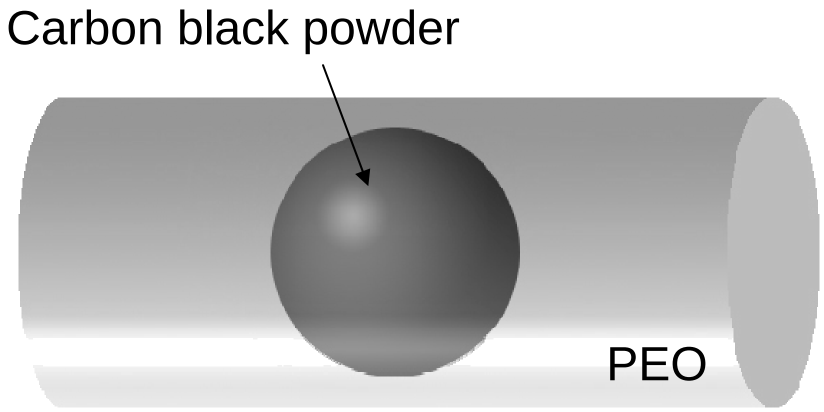

Fig. 4.15 Schematic diagram of PEO/carbon black composite nanofibers.

4.4 Conclusion

The objective of studying PEO/carbon black composite fibers is to investigate the influence of the conducting particles inside the fibers.

It is found that electrospinning process helps to minimize crystallization of PEO; PEO molecular chains in trans configuration are mostly amorphous. However, crystalline helical structure is still observable as revealed by XRD. Also, by employing the XRD of the crystalline phase of PEO, the degree of orientation of the electrospun fibers can be determined; its Hermans' orientation parameter f is about 0.94, which means the degree of orientation is decent. The fact also indicates the polymer chains of PEO are able to be aligned along fiber direction.

By adding different amount of carbon black in PEO solution, composite fibers were electrospun and collected. Carbon black would influence the morphology of the fibers, beads are easily formed and the distribution of fiber diameters is broadened. The effect may also be contributed to the decrease in electrical performance (higher resistance) of composite fibers.

From the IV characteristics of the samples, their resistances are estimated. With more carbon black, the sample resistance increases linearly. This is contrary to the conventional bulk composite samples as more carbon black will increase the conductivity. The addition of conducting particles which are of size similar to fiber diameter will not help to increase electrical properties. This could be explained by the different conduction mechanisms: the electronic conduction of the particles and ionic conduction of the matrix in the composite fibers.

Chapter 5

PMMA/PANi(AMPS) Fibers for Alcohol Sensing

In this chapter, the electrical response of PMMA/PANi(AMPS) fibers to alcohol molecules will be reported. PANi is conducting polymer and is sensitive to alcohol; by blending it together with PMMA, nanofibers can be produced by electrospinning. PMMA has been taken as a carrier of PANi since PANi does not have long polymer chain for electrospinning. AMPS was applied for doping in PANi in order to enhance electrical conductivity of PANi. Two kinds of measurements have been taken in order to test the responding time and the sensitivity of the blend fibers with different weight percentage of PANi.

5.1 Experimental

5.1.1 Solution Preparation

Poly(methyl methacrylate) (PMMA) (M_w=350,000), Polyaniline (PANi) (emeraldine base, M_w=10,000) (molar mass = 214.3) and 2-Acrylamido-2-methyl-1-propanesulfonic acid (AMPS) (molar mass = 207.25) were purchased from Sigma-Aldrich. The solvent 1-Methyl-2-pyrrolidone (NMP) was purchased from

International Laboratory USA.

7 wt% of PMMA was dissolved into NMP together with PANi and AMPS by stirring at 40 ˚C for 12 hours. Different amount of PANi were added (5, 12 and 16 wt% with relative to PMMA) and AMPS was added where the molar mass ratio of PANi:AMPS = 1:1.

5.1.2 Electrospinning Process

Regarding the fabrication of PMMA/PANi(AMPS) nanofibers, positive 8kV was applied in electrospinning. The rotating cylinder collector (Fig. 2.3b) was set to a speed of 2900 rpm. Distance between the tip and collector was 17cm. 0.4ml of solution was deposited for the production of each sample.

After electrospinning, samples were dried at 40˚C for 24 hours.

5.1.3 Film Samples

Apart from the blend nanofibers, three film samples have been made for comparing the performance between nanofibers and bulk samples. Three concentrations (5, 12, 20 wt% relative to PMMA) of PANi were added where the molar mass ratio of PANi:AMPS = 1:1, the same as fibers.

The solutions were casted onto a glass plate and dried at 50 ˚C for 24 hours. The thickness of the films is about 180 μm.

5.1.4 Alcohol Sensing Measurements

Methanol, ethanol and isopropanol are the three kinds of alcohol that were used in the following two experiments.

In order to measure the electrical response of PMMA/PANi(AMPS) fibers and films to various concentrations of alcohols molecules, sample was placed inside a 17-litre chamber that filled up with nitrogen. There is a fan inside the chamber to accelerate the evaporation of alcohol (Fig. 5.1). By applying a D.C. voltage across the samples, the current passing through was measured. Alcohol was introduced into the chamber continually in every 15 minutes so as to increase the concentrations stepwise.

Various volumes of alcohols were introduced into the chamber: 0.5, 1, 1.4, 1.6, 1.8 and 2 ml, which are equal to concentrations: 29, 59, 82, 94, 106 and 118 ppm respectively.

The film samples only go through the experiment for ethanol. 50 V was applied on all of the fibers samples and film sample of 5 wt% PANi. 1 V was applied for the film of 12 and 20 wt% PANi. This change of applied voltage is necessary as the current goes through those particular samples is too high to measure if 50 V is applied on them.

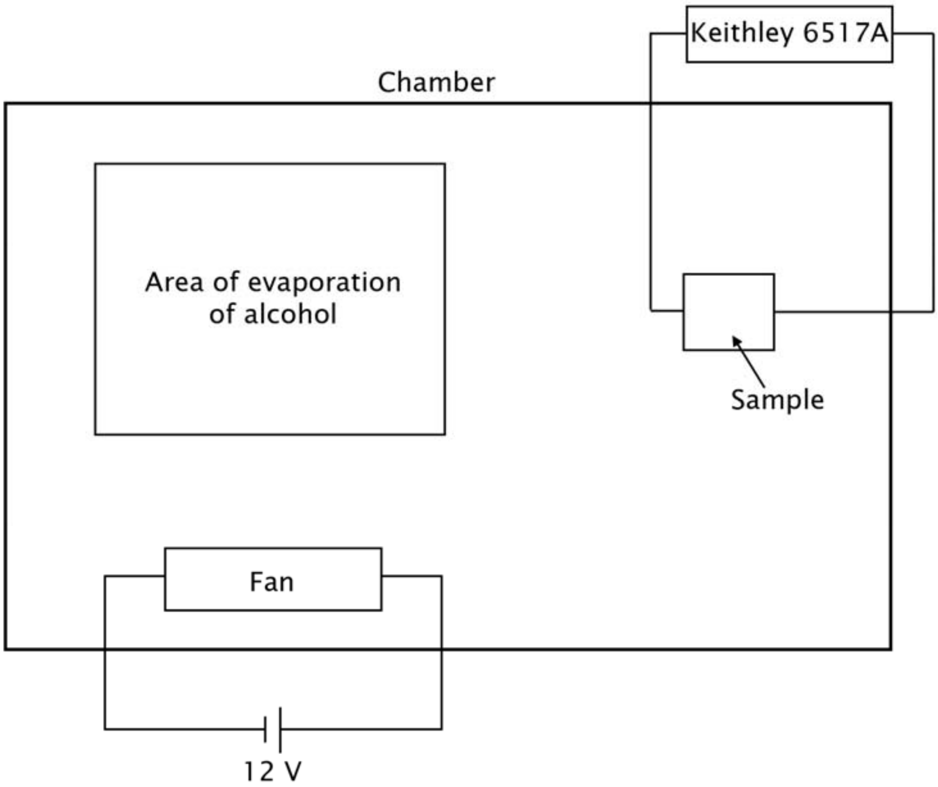

Fig. 5.1 Schematic diagram of the setup for alcohol sensing test.

Regarding the response time of the fibers, another experiment has been conducted. Nitrogen gas was introduced to a flask of ethanol and to the sample (Fig. 5.2). When nitrogen was bubbled into ethanol with the flow rate of 10 ml/s, saturated ethanol vapor was filled into nitrogen and flowed onto the samples. This process was switched on and off every 100 s. The fan would help to provide fresh air to the sample and thus no alcohol was around when there was no flow of nitrogen; the location of the fan and the sample are similar to that for alcohol sensing test as shown in Fig. 5.1 with a distance of 20 cm apart. The same voltages were applied across the samples as previous in the test of concentration.

All of the samples were only used for one kind of alcohol for eliminating the influence of different alcohols.

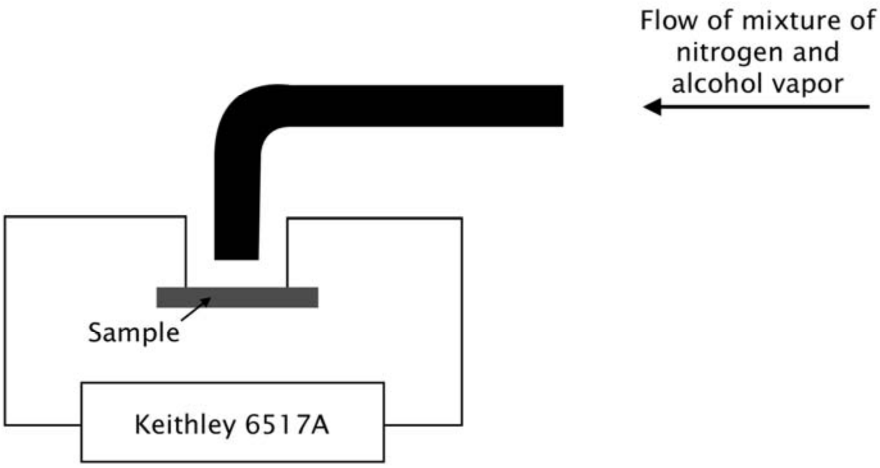

Fig. 5.2 Schematic diagram of alcohol flow test.

5.2 Results and Discussion

5.2.1 FTIR Spectra

FTIR has been utilized for the investigation of the AMPS doped PANi, and the PMMA/PANi(AMPS) nanofibers.

Fig. 5.3 shows the infrared absorption spectra of powders of PANi, AMPS and their blend. The absorption spectrum of PANi(AMPS) powders is different from the spectra of the original materials. Although the spectrum of the PANi is similar to the spectrum of the doped PANi, most of absorption peak shapes are distorted. There is chemical reaction after they were dissolved and blended in NMP solvent. The results shown AMPS was applicable for doping PANi. However, Yang et al. reported that AMPS was able to be removed by solvents like ammonia and could be substituted by other acids (J. Yang, Burkinshaw, Zhou, Monkman, & Brown, 2003).

Fig. 5.4 shows the infrared spectra of the blend fibers of different weight percentages of PANi(AMPS) of PMMA up to 16 wt% and also PANi(AMPS) powders. It was observed that the blend fibers had no obvious evidence that there were chemical reaction between PMMA and PANi(AMPS). With more PANi(AMPS) inside the fibers, the representative peaks were more significant. Strong peaks of PANi(AMPS) were still distinguishable.

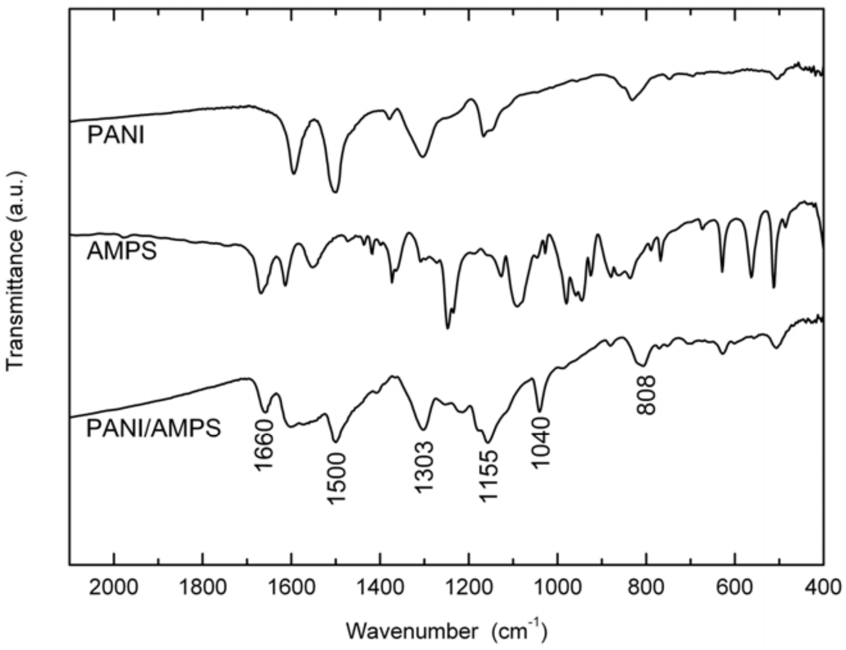

Fig. 5.3 Infrared spectra of powders of PANi, AMPS and blend of PANi and AMPS.

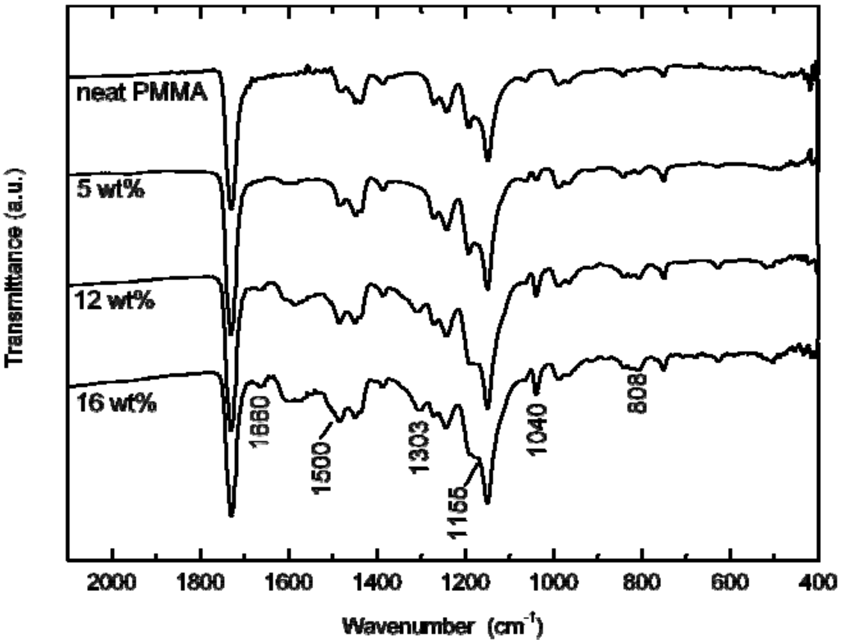

Fig. 5.4 Infrared spectra of PMMA/PANi(AMPS) nanofibers with different amount of PANi(AMPS) in PMMA.

5.2.2 Morphology

In the study of PMMA/PANi(AMPS) nanofibers for alcohol sensing, different amount of PANi(AMPS) were added. Fig. 5.5a to e show the SEM pictures of the fibers of pure PMMA; 5, 12, 16 and 20 wt% of PANi(AMPS) respectively. It is observed that by adding 5 wt% of PANi(AMPS) into PMMA (Fig. 5.5b), the electrospun fibers are thinner that the diameter decrease roughly from 200 nm to 100nm. However, as more PANi(AMPS) is added (12 and 16 wt%) into PMMA (Fig. 5.5c and d), the diameter of fibers increase gradually to about 150nm.

When 20 wt% of PANi(AMPS) is introduced into PMMA, the electrospun fibers is deformed, fibers were stuck together as the solvent dissolved them back. Besides, during electrospinning process, it is observed that jets are hard to emerge from the syringe. Those factors made the blend fibers with high percentage of PANi(AMPS) could not be test for alcohol sensing, since the number of fibers was not sufficient.

It is believed that the good electrical conductivity of PANi(AMPS) was the contributing factor of tiny fibers with 5 wt% PANi. Doped PANi has high conductivity which increase the number of charge carriers and thus enhance the columbic force in the jet during electrospinning.

However, the polymer chains of PANi are very short compare with PMMA; with more PANi inside the solution, it weakened the ability to electrospin. The presence of PANi of short molecular chains, the viscosity of the solution drops as there are fewer chain entanglements of PMMA. Thus, surface tension became significant, diameter of fibers increased. This is the reason of producing thinker fibers with 12 wt% and 16 wt% PANi. Also, thicker fibers means longer drying time is required for them; since the time required may be not enough, the fibers will deform and leads to the failure of fiber networks with 20 wt% PANi.

In summary, the morphology of fibers on or below 16 wt% of PANi was smooth and alike, electrical measurements for alcohol sensing on them were possible.

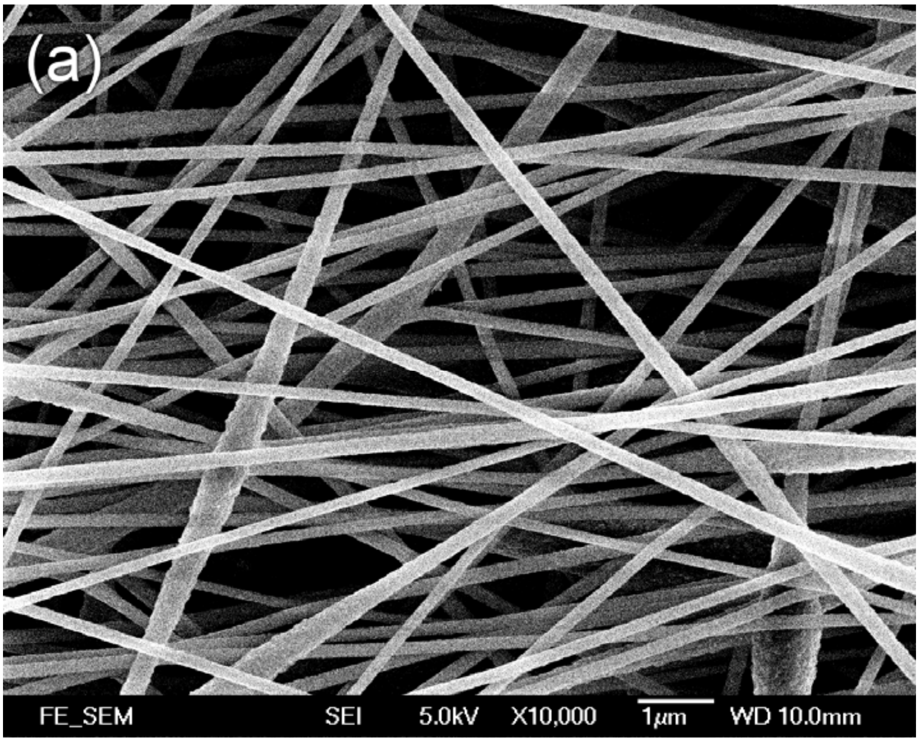

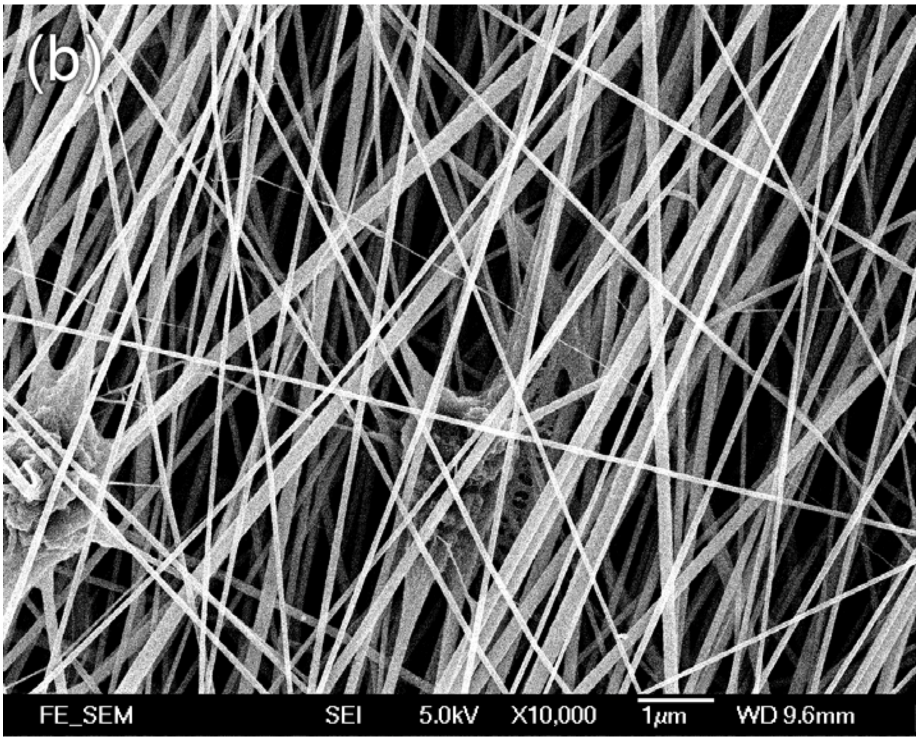
(b)
FE_SEM
SEI
5.0kV
X10,000
1μm
WD 9.6mm

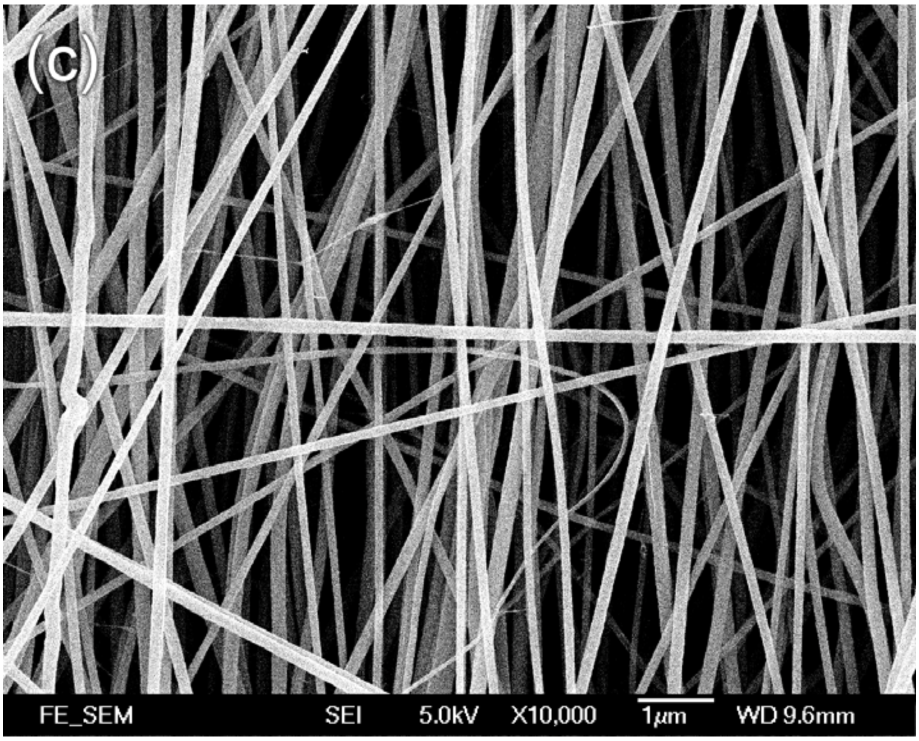
(c)
FE_SEM
SEI
5.0kV
X10,000
1μm
WD 9.6mm

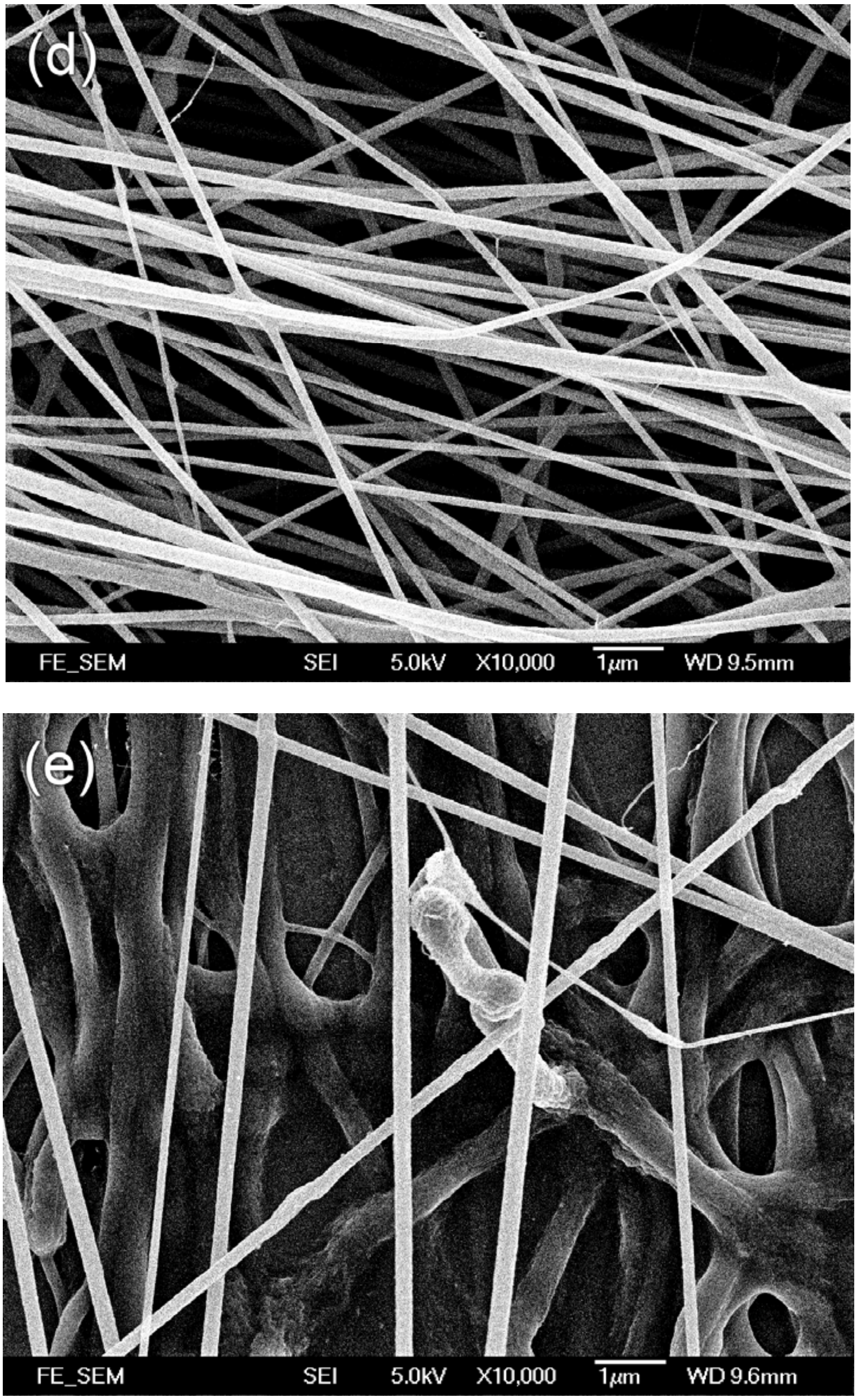

Fig. 5.5 SEM pictures of PMMA/PANi(AMPS) nanofibers with different weight percentage of PANi in PMMA: (a) neat PMMA, (b) 5 wt%, (c) 12 wt%, (d) 16 wt% and (e) 20 wt%.

5.2.3 Alcohol Sensing Measurements

Electrical resistance of PMMA/PANi(AMPS) fibers and film samples were measured in response to the alcohol vapor. The magnitude of resistance change and its response time subject to the exposure of different alcohols and the concentrations of alcohol vapor were determined.

Alcohol Concentration Test

The normalized resistance (R/R_o) of PMMA/PANi(AMPS) fibers and films are used for easy comparison between the responses of the samples, where R is the measured resistance and R_o is the initial resistance at no alcohol vapor is introduced. Fig. 5.6a, b and c show the normalized resistance of the samples of 5, 12 and 16 wt% of PANi(AMPS) respectively in the three different alcohol vapor of increasing concentration. The fibers with 5 wt% PANi(AMPS) (Fig. 5.6a) exhibit a monotonic change with alcohol concentrations. The resistance drops as the concentration of alcohol increases and becomes unstable when the concentration of alcohol is above 100 ppm. In addition, from the slope of the curves, it can be seen that the samples are more sensitive to isopropanol, but less sensitive to ethanol and then methanol.

On the other hand, response of the fibers with 12 and 16 wt% of PANi(AMPS) (Fig. 5.6b and c) are quite different compared with the one with 5 wt% PANi(AMPS), their resistances increase on the contrary to the 5 wt% samples when alcohols are added. In

Fig. 5.6b, it shows that the resistance of the sample increases monotonically with the increasing concentration of methanol, but the sample resistance increases in the first 30 ppm ethanol then decrease with higher concentration. Similarly, the sample resistance increases up to 60 ppm of isopropanol then decrease with higher concentration. In Fig. 5.6c, it can be found that the sample resistance increase up to 60 ppm of alcohols but then fluctuate largely except in methanol vapor. Fig. 5.7a, b and c re-plot the normalize resistance of samples against alcohol concentrations but in view of the three kinds of alcohol. From Fig. 5.7a, it is clear that in the same methanol concentration sample with the least (5 wt%) PANi(AMPS) exhibit a larger change in resistance, it drops about 50% in 90 ppm of methanol in comparison with the other two samples which increase, but not decrease, only about 10%. We shall explain the change in resistance mechanism in the following paragraph. Fig. 5.7b and c show the response curves of the samples in ethanol and isopropanol atmosphere respectively. The 5 wt% sample gives the most stable response, it resistance drops steadily with the increasing concentration of alcohols. On the contrary, the other two samples (12 and 16 wt%) respond to the increasing concentration of alcohols in a peculiar way, the resistances of which increase in low concentration then decrease in the higher concentrations.

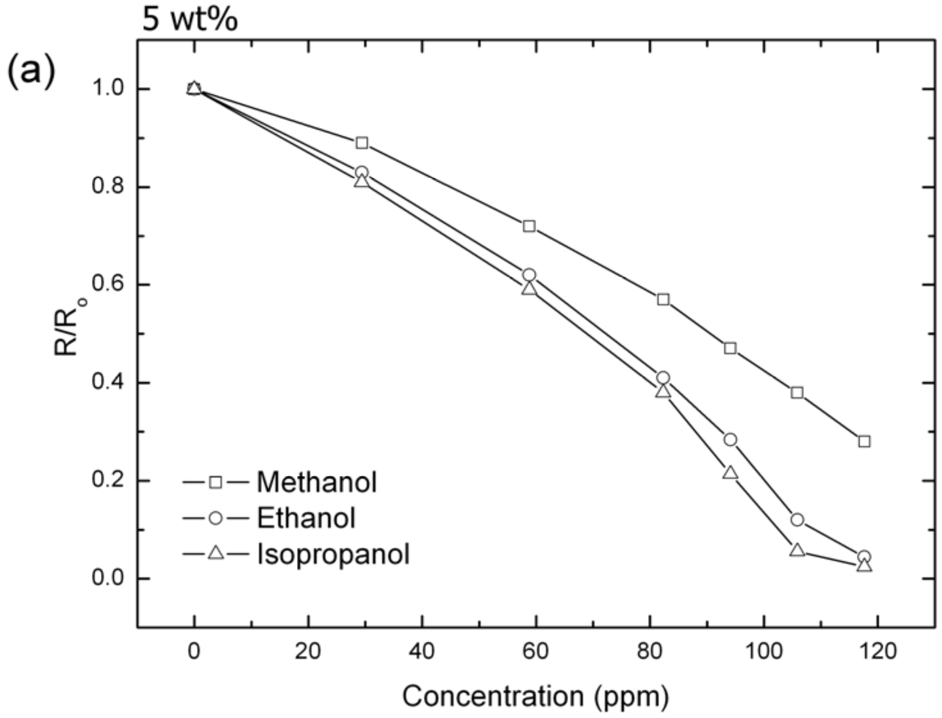
5 wt%
(a)
R/R$_o$
1.0
0.8
0.6
0.4
0.2
0.0
0
20
40
60
80
100
120
Concentration (ppm)
Methanol
Ethanol
Isopropanol

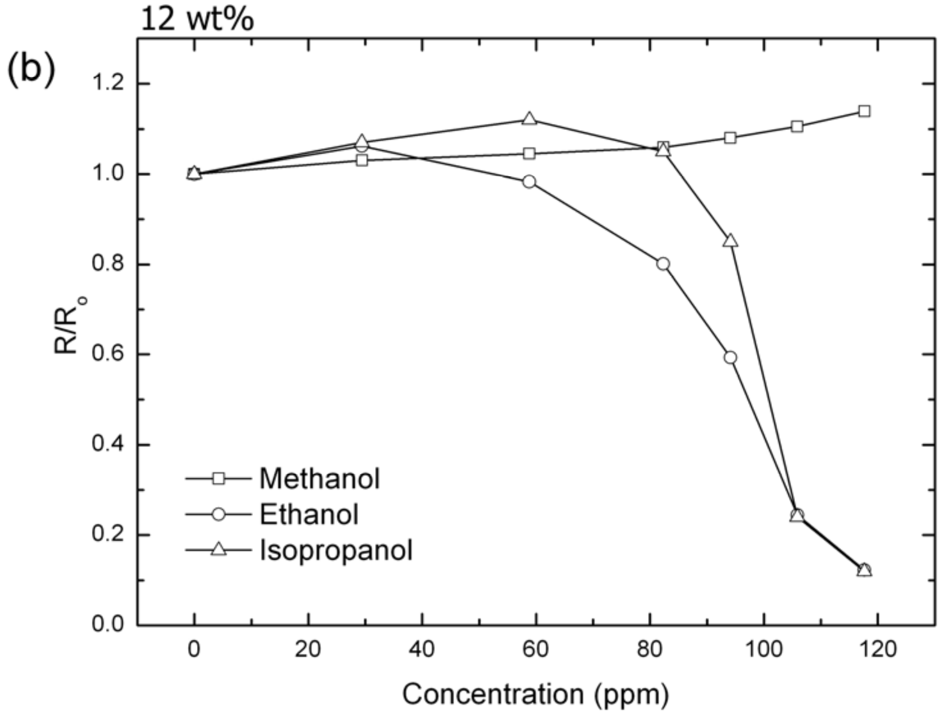
12 wt%
(b)
R/R$_o$
1.2
1.0
0.8
0.6
0.4
0.2
0.0
0
20
40
60
80
100
120
Concentration (ppm)
Methanol
Ethanol
Isopropanol

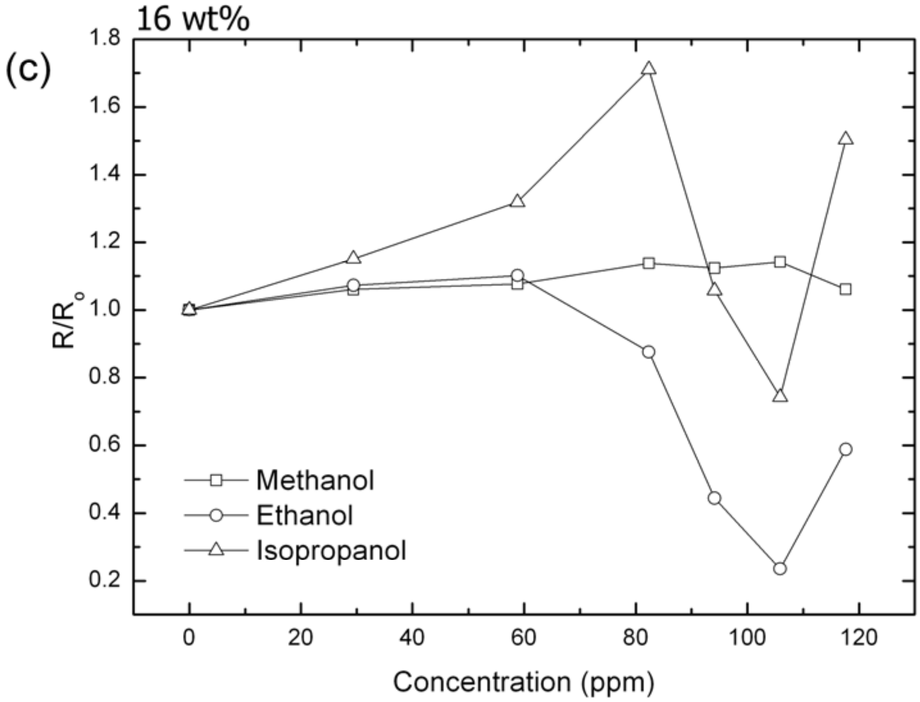

Fig. 5.6 Normalized resistance of PMMA/PANi(AMPS) nanofibers with different amount of PANi: (a) 5 wt%, (b) 12 wt% and (c) 16 wt% in alcohol vapor environment.

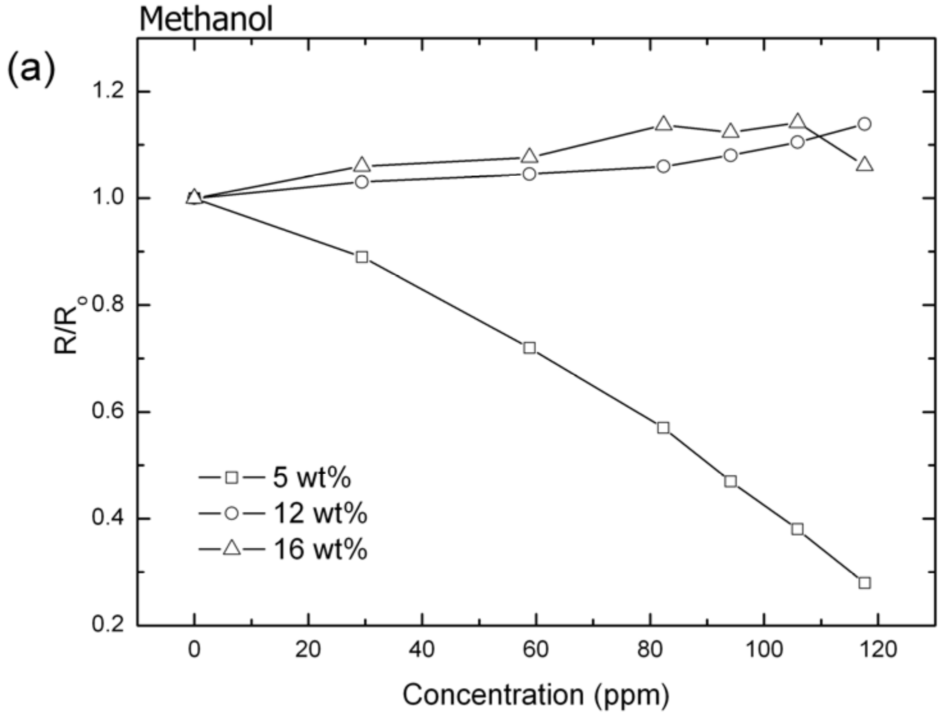

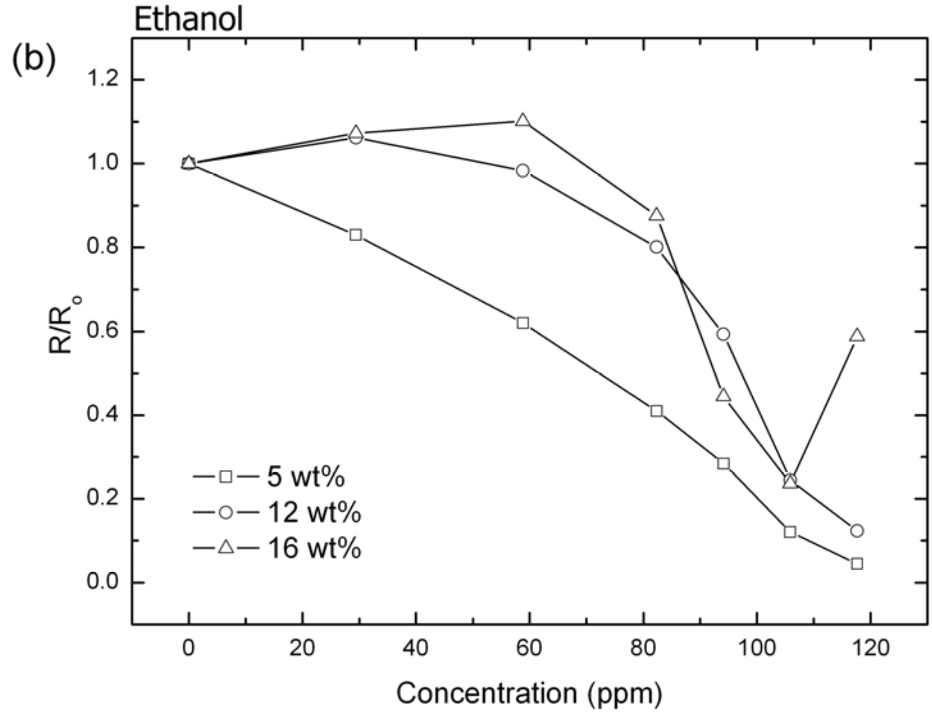

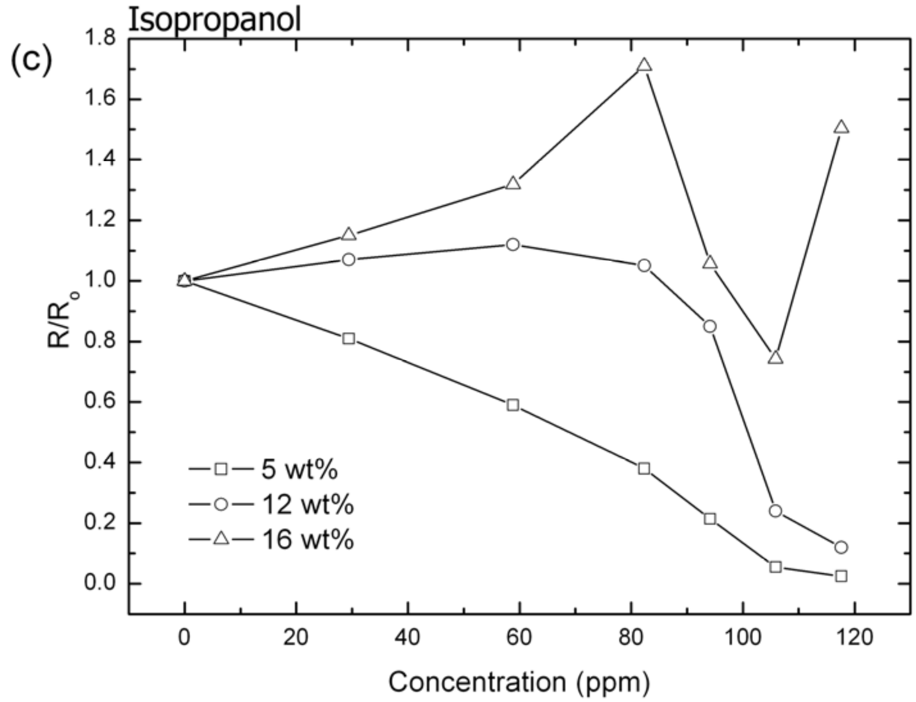

Fig. 5.7 Normalized resistance of PMMA/PANi(AMPS) nanofibers with different amount of PANi in alcohol environment: (a) methanol, (b) ethanol and (c) isopropanol.

Apart from electrospun fibers samples, the alcohol sensing tests were also conducted for three solution casted film samples of which the PANi(AMPS) in PMMA are 5, 12 and 20 wt% respectively. Fig. 5.8 shows the resistance response curves of the films in ethanol. The resistance of 5 wt% sample slightly increases in 30 ppm then decreases in higher concentration. The resistances of 12 and 20 wt% samples increase all the way in ethanol where the latter one has a larger response which is quite different in comparison with the fibers. Nevertheless, the 5 wt% fiber sample gets a 50% drop in resistance in 70 ppm ethanol as shown in Fig. 5.7b; it is more sensitive than the 5 wt% film sample of which a 50% drop in resistance requires 90 ppm ethanol as revealed in Fig. 5.8. This could be due to the higher surface area to volume ratio of the electrospun fibers in comparison with the film sample.

Regarding the change of sample resistance in response to the alcohol vapor, it can be understood from two mechanisms that lead to different effects on the resistance of the samples. Firstly, the PANi(AMPS) as the conducting phase of the fiber its resistance will decrease upon the exposure to alcohols. It is due to the interaction of hydrogen bonding of the alcohols with the PANi. In the emeraldine base PANi, it is likely to bridge the PANi chains via the hydrogen bonding provided by the alcohols. However, for emeraldine salt such as the AMPS doped PANI, the nitrogen atoms in the chains are protonated thus are not available for hydrogen bonding with the alcohol molecules.

Instead of bridging the PANi chains, the alcohol molecules appear to serve as the separator pushing the PANi chains apart, thus uncoiling the chains and resulting in an enhancement of charge transport or a decrease in resistance (Pinto et al., 2008; Tan & Blackwood, 2000). This would also lead to a volume change of the PANi. Secondly, PMMA as an insulator serves as the matrix phase of the samples. It will swell upon the exposure to alcohols as a result of physisorption. The swollen matrix will separate the conducting phase apart causing an increase in resistivity of the blend fibers. However, the absorbed alcohol molecule in PMMA will provide charge carriers which in turn decrease PMMA's resistivity.

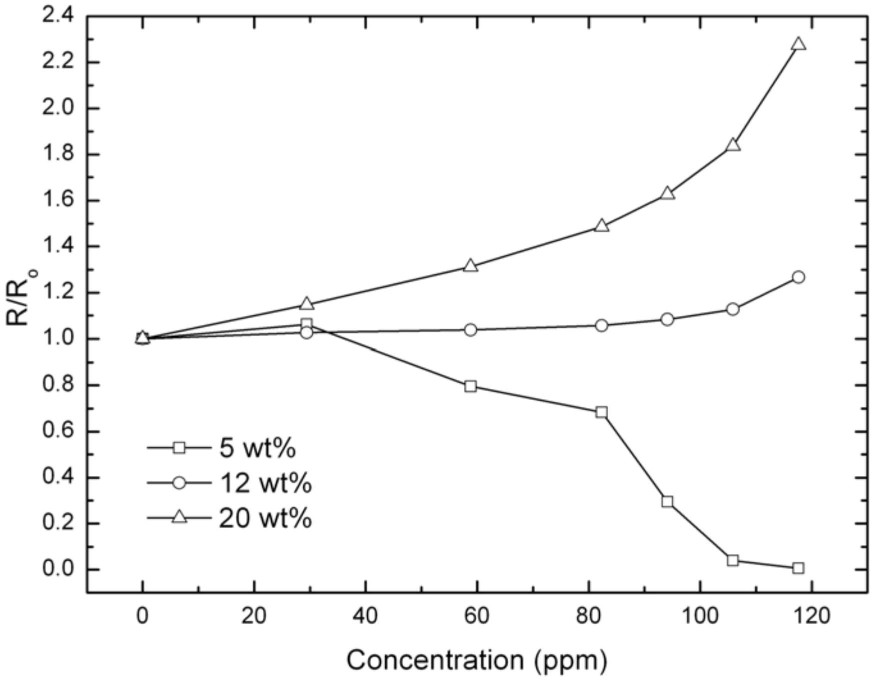

Fig. 5.8 Normalized resistance of PMMA/PANi(AMPS) film with different amount of PANi in ethanol environment.

Table 5.1 Resistance of PMMA/PANi(AMPS) samples with different concentrations of PANi(AMPS).

Fiber sample/ wt%	Resistance/ Ω
5	175 G
12	24 G
16	53 G
Film sample/ wt%	
5	153 G
12	35 k
20	4.7 M

From the resistance given in the Table 5.1 shown above, the film samples with 12 and 20 wt% AMPS doped PANi are in percolation of which their resistances are five orders of magnitude lower than the 5 wt% sample. It helps to explain the behavior of the film samples as shown in Fig. 5.8. For the unpercolated 5 wt% film sample, the conducting phase decreases in resistance with the absorption of alcohol, and the insulating matrix PMMA become less resistive as the introduction of alcohol molecules, thus the overall resistance of the sample decreases with the increasing alcohol concentration. For the percolated film samples, since the conducting phase is mostly connected throughout the whole sample, the overall resistance is small. As it exposes to alcohols, the insulating matrix swells in which some parts of the conducting phase become disconnecting. It leads to the resistance increasing which is in magnitude overwhelmingly larger the resistance decreasing of the matrix with the absorbed alcohol, thus the percolated film samples exhibit resistance increasing with alcohol absorbing. The more connecting paths in percolated sample, the more disconnecting path as a result of matrix swelling which explains the larger change in normalized resistance of the 20 wt% sample.

On the other hand, in the electrospun fiber samples, their resistances given in Table 5.1 reveal that the samples have not reach percolation, even though they have the similar weight fractions of the conducting phase with the film samples. This could be understood by the quasi-one dimensional structure of the nanosized fibers. The conducting phase in the nanofiber is confined along the fiber axis to form connecting paths, but it may have been broken during stretching in the electrospinning process. However, similar reasoning as those given to explain the behavior of film samples can still be applied to explain the results as shown in Fig. 5.7a. The methanol reduces the resistance of the 5 wt% fibers but increases the resistances of 12wt% and 16wt% fibers. Although the two samples of more conducting phase are not in percolation, some of the connecting paths will still be discontinued in the swollen samples. Fig. 5.7b and c reveal some more interesting results. Resistances of the 12 and 16 wt% fiber samples increase upon exposure to ethanol and isopropanol but then decrease drastically at higher concentration of the alcohols. This can be attributed to the swelling of matrix phase at the first place then comes to the swelling of the conducting phase exposing to more alcohols. This leads to the reconnection of the discontinued conducting path in the swollen matrix. The resistance of the fiber samples therefore decreases upon the exposure to more alcohols. The phenomenon cannot be observed in the case of methanol because of its smaller molecular size.

Alcohol Flow Test

Apart from testing the response magnitude of PMMA/PANi(AMPS) fibers to different concentrations of various alcohols, the response time and the stability of the samples have also been studied. Only ethanol was used in these set of tests. An ethanol vapor flow was introduced to the samples for 100 s and switched off for another 100 s, during this stage the sample was exposed to air in the normal condition, and then the whole test was repeated again.

Fig. 5.9a and b show results of the response time tests of the blend fibers and the film samples respectively. As shown in Fig. 5.9a, the resistance of the 5 wt% fibers decreases sharply when they are exposed to ethanol followed by a slow decreasing which indicates a reaching of saturation of the ethanol in the fiber. When the ethanol is switched off in the first cycle, the resistance of the fiber sample switches back to normal value almost instantly. This fast switching can only be observed for few cycles only then showing almost no response to the alcohol. Contrary to the 5 wt% sample, the 12 and 16 wt% samples exhibit a reverse performance, both sample resistances rise upon the exposure to ethanol and drop when switch back to air. These results are similar to those observed in the concentration test as shown in Fig. 5.7b. At low concentration, the resistance of 5 wt% sample drops while the other two samples rise. On the other hand, unlike the 5 wt% sample, 12 and 16 wt% samples show steadily switching behavior between ethanol and air for many cycles. From the switching characteristics of both samples, it can be seen that the rise of the normalized resistance is fast but has to take longer time to reach equilibrium, whereas the removal of ethanol incurs a fast drop of resistance and reach equilibrium almost in a few seconds. Fig. 5.9b shows the normalized resistance change of film samples upon the exposure to ethanol and then back to air. All of the three samples exhibit an increase in resistance with ethanol and then switch back to the equilibrium values in air, this feature is particularly clear for the 20 wt% sample film, although the rise time is slow. The 12wt% sample appears differently in the switching feature. Its resistance keeps on increasing in air and rise sharply up exposure to ethanol but then decreases slowly even in the ethanol atmosphere until it is switched off, the resistance then drops sharply to a point where the resistance keeps on increasing again in air. It should be noted that the magnitude of this peculiar switching feature is negligible small although it can be repeated many cycles. Another point about the 5 wt% film sample, despite the grand trend of decreasing resistance to the ethanol of high concentration (Fig. 5.8), there is a slightly increase in resistance at concentration below 30 ppm which is consistence with the result shown in Fig. 5.9b of 5 wt% sample in the first two switching cycles.

In summary, the results are complicated to strictly compare the response time and stability among the samples. However, when we compare two samples, 16 wt% fibers and 20 wt% film samples, it can be seen that when there is large amount of PANi(AMPS), response time can be speed up from over 100 s to about 30 s. Therefore, it is believed that the fiber construction can shorten the response time at high concentration of conducting phase.

Regarding the stability of the samples, samples with more PANi(AMPS) are more stable in general.

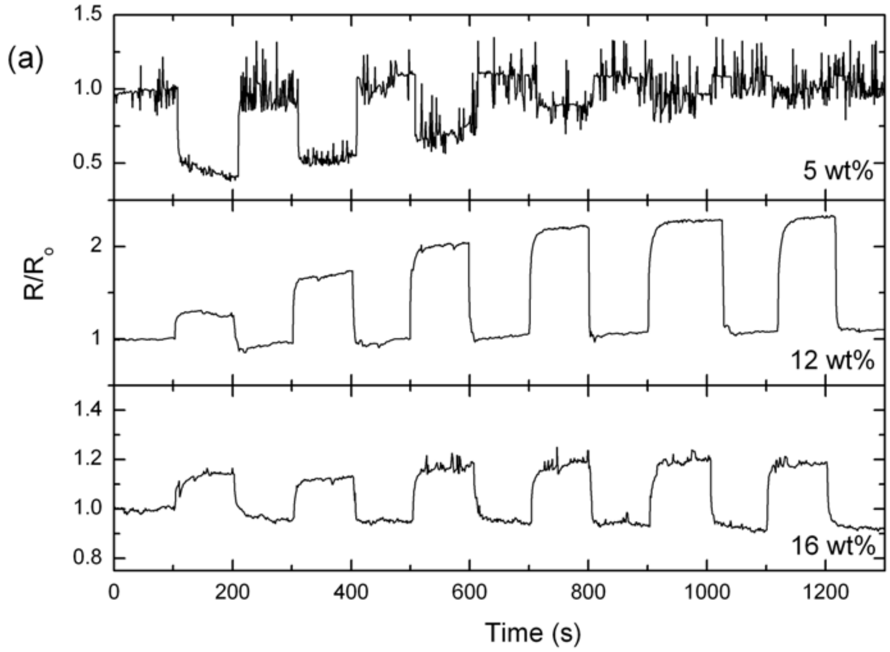

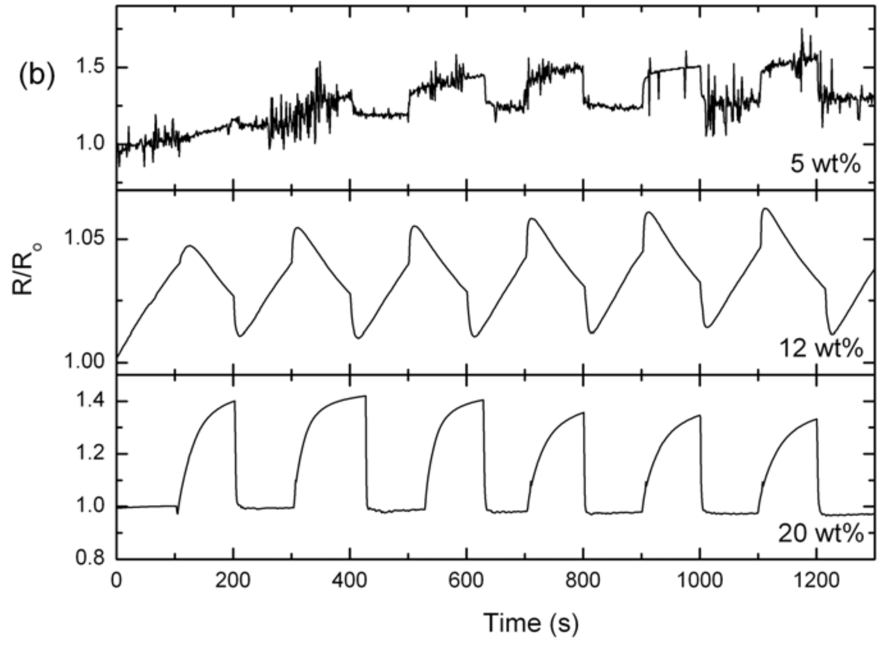

Fig. 5.9 Electrical responds (normalized resistance) of PMMA/PANi(AMPS): (a) fibers and (b) films, in different weight percentage of PANi, to ethanol flows. Flows first occurred at 100 s for 100 s and stopped for another 100 s, six cycles were completed.

5.3 Conclusion

The objective of studying PMMA/PANi(AMPS) blend fibers is to investigate the electrical responses of them to alcohol molecules. As the surface area to volume ratio increases dramatically after electrospun into nanofibers, the electrical responses of the blend fibers have been compared with the blend films.

The FTIR spectra revealed that blending in AMPS into PANi with molar mass ratio of 1:1, PANi can be successfully doped. Also, by blending in PMMA to the PANi(AMPS), doped PANi(AMPS) still exists and it seems that there is no chemical reaction in between.

The electrospun blend fibers of 5, 12 and 16 wt% of PANi(AMPS) were fabricated successfully and can be used for alcohol vapor tests. However, it is found that 20 wt% of PANi(AMPS) would hinder the formation of fiber forming in the electrospinning process. It suggests the short molecular chain of PANi is the major factor.

Alcohol sensing measurements including concentration test and flow test were performed. Base on the findings, two mechanisms upon PMMA and PANi(AMPS) are suggested for the interesting changes of the resistances. Regarding the response time, all of the samples performed similarly. However, the response time of 20 wt% film is particularly slow. It is believed that electrospun fibers with high concentrations of

PANi(AMPS) can speed up the response time due to the large surface area to volume ratio. Regarding the stability of the samples, samples with more PANi(AMPS) are more stable in general.

Chapter 6

Conclusion

The purpose of this project is to make use of electrospinning to fabricate functional polymer fibers. The major advantage of electrospun fibers is the very large surface area to volume ratio, which is believed that the response can be fast if they act as a sensor.

In the first part of study, electrospinning process is investigated for optimizing the fiber size and suppressing the bead formation. Different solutions of PMMA have been tested including different solvents, concentration and molecular weight of polymer electrospinning conditions, and electrospinning conditions including voltage and charge polarity. On the other hand, rotating collector was introduced to deposit aligned fibers and aligned electrospun nanofibers have been made successfully when the surface velocity beyond 6 ms^{-1}. The above study is essential for optimizing fiber diameter and morphology, and for maximizing electrical responds in the latter part of the study.

Study of PEO/carbon black composite fibers is performed in order to reveal the influence of the conducting particles inside electrospun fibers. In conventional cases, conducting particles in polymer can increase conductivity of the matrix as the number of conducting paths increase. However, carbon black in electrospun fibers of quasi-one dimensional structure causes a linear increase in resistance, which suggests carbon black screens the electric field to weaken the movement of ions in PEO phase and also the different conduction mechanisms between carbon black and PEO. The result implies conducting particles in comparable size of electrospun fibers may not be able to decrease the resistance of the composite fibers.

In addition, the PEO fibers prepared by electrospinning are studied. Polarized FTIR and XRD reveals the PEO molecular chains are able to be aligned along fiber direction in trans configuration and mostly amorphous. However, crystalline helical structure is still observable, and with its help, the degree of orientation of the electrospun fibers can be determined where its Hermans' orientation parameter is about 0.94, which is decent.

Lastly, PMMA/PANi(AMPS) blend fibers has been studied, which is aimed to investigate the nanofibers response with respect to various alcohol molecules: such as the methanol, ethanol and isopropanol respectively. It was found that PMMA fibers contains on or below 16 wt% PANi(AMPS) can be successfully electrospun. With more PANi(AMPS) such as 20 wt%, the fibers mat cannot be made as PANi(AMPS) hinder the formation of fiber forming in the electrospinning process.

Concerning the alcohol sensing measurements, two series of experiments: alcohol concentration test and flow test is performed. Two mechanisms are suggested for the interesting changes of the resistances upon two phases: PMMA and PANi(AMPS). When the blend fibers expose to alcohols, PMMA swells that leads to the increase in resistance; on the contrary, alcohols also bring in charge carriers that makes the resistance decrease. On the other hand, PANi(AMPS) uncoil the chains upon the exposure to alcohols that makes a decrease in resistance. In addition, the results of alcohol flow test suggest the nanofibers' morphology could help to shorten the response time when the concentration of PANi(AMPS) is high (i.e. 20 wt%). Regarding the stability of the samples, samples with more PANi(AMPS) are more stable in general.

The experiment on alcohol vapor sensing suggests conducting polymer blend made from electrospinning process is able to give electrical response upon the exposure to chemical vapor. Although the results in the alcohol flow test reveal the uncertainty of the electrical signals, we believe the electrospun fibers can still shorten the response time in sensor application. Nevertheless, the study of PMMA/PANi(AMPS) blend fibers at higher concentration of conducting phase is desirable for sensor applications. As a gas sensor, the particular patterns of the resistance change, related to alcohols, of the blend fibers can also play a part in electronic nose (ENose) as to speed up the response during monitoring the air quality (Ryan et al., 2004).

Reference

Alfrey, T. (1947). The influence of solvent composition on the specific viscosities of polymer solutions. *Journal of Colloid Science, 2*(1), 99-114.

Alfrey, T., Bartovics, A., & Mark, H. (1942). The effect of temperature and solvent type on the intrinsic viscosity of high polymer solutions. *Journal of the American Chemical Society, 64*(7), 1557-1560.

Armand, M. B. (1987). Current state of PEO-based electrolyte. In J. R. MacCallum, & C. A. Vincent (Eds.), *Polymer electrolyte reviews* (pp. 1). New York: Springer.

Athawale, A. A., & Kulkarni, M. V. (2000). Polyaniline and its substituted derivatives as sensor for aliphatic alcohols. *Sensors and Actuators B: Chemical, 67*(1-2), 173-177.

Bailey, F. E., Jr., & Koleske, J. V. (1976). *Poly(ethylene oxide)*. New York: Academic Press, INC.

Baumgarten, P. K. (1971). Electrostatic spinning of acrylic microfibers. *Journal of Colloid and Interface Science, 36*(1), 71-79.

Berry, J. P. (1990). Electrostatically produced structures and methods of manufacturing. *US Patent,* (4965110)

Bornat, A. (1987). Production of electrostatically spun products. [Production of electrostatically spun products.] *US Patent,* (4689186)

Buchko, C. J., Chen, L. C., Shen, Y., & Martin, D. C. (1999). Processing and microstructural characterization of porous biocompatible protein polymer thin films. *Polymer, 40*(26), 7397-7407.

Chen, Z., Foster, M. D., Zhou, W., Fong, H., Reneker, D. H., Resendes, R., et al. (2001). Structure of poly(ferrocenyldimethylsilane) in electrospun nanofibers. *Macromolecules, 34*(18), 6156-6158.

Chipara, M., Hui, D., Notingher, P. V., Chipara, M. D., Lau, K. T., Sankar, J., et al. (2003). On polyethylene–polyaniline composites. *Composites Part B: Engineering, 34*(7), 637-645.

Croce, F., Appetecchi, G. B., Persi, L., & Scrosati, B. (1998). Nanocomposite polymer electrolytes for lithium batteries. *Nature, 394*(6692), 456-458.

Dalton, P. D., Grafahrend, D., Klinkhammer, K., Klee, D., & Möller, M. (2007). Electrospinning of polymer melts: Phenomenological observations. *Polymer, 48*(23), 6823-6833.

Deitzel, J. M., Kleinmeyer, J. D., Hirvonen, J. K., & Beck Tan, N. C. (2001a). Controlled deposition of electrospun poly(ethylene oxide) fibers. *Polymer, 42*(19), 8163-8170.

Deitzel, J. M., Kleinmeyer, J. D., Hirvonen, J. K., & Beck Tan, N. C. (2001b). Controlled deposition of electrospun poly(ethylene oxide) fibers. *Polymer, 42*(19), 8163-8170.

Deitzel, J. M., Kleinmeyer, J., Harris, D., & Beck Tan, N. C. (2001). The effect of processing variables on the morphology of electrospun nanofibers and textiles. *Polymer, 42*(1), 261-272.

Demir, M. M., Yilgor, I., Yilgor, E., & Erman, B. (2002). Electrospinning of polyurethane fibers. *Polymer, 43*(11), 3303-3309.

Drozin, V. G. (1955). The electrical dispersion of liquids as aerosols. *Journal of Colloid Science, 10*(2), 158-164.

Elimat, Z. M. (2006). AC electrical conductivity of poly(methyl methacrylate)/carbon black composite. *Journal of Physics D: Applied Physics, 39*(13), 2824-2828.

Feng, L., Li, S., Li, H., Zhai, J., Song, Y., Jiang, L., et al. (2002). Super-hydrophobic surface of aligned polyacrylonitrile nanofibers. *Angewandte Chemie - International Edition, 41*(7), 1221-1223.

Fennessey, S. F., & Farris, R. J. (2004). Fabrication of aligned and molecularly oriented electrospun polyacrylonitrile nanofibers and the mechanical behavior of their twisted yarns. *Polymer, 45*(12), 4217-4225.

Fong, H., Chun, I., & Reneker, D. H. (1999). Beaded nanofibers formed during electrospinning. *Polymer, 40*(16), 4585-4592.

Fong, H., & Reneker, D. H. (1999). Elastomeric nanofibers of styrene-butadiene-styrene triblock copolymer. *Journal of Polymer Science Part B: Polymer Physics, 37*(24), 3488-3493.

Fong, H., & Reneker, D. H. (2001). Electrospinning and formation of nanofibers. In D. R. Salem (Ed.), *Structure formation in polymeric fibers* (pp. 225-246). Munich: Hanser.

Formhals, A. (1934). Process and apparatus for preparing artificial threads. *US Patent,* (1975504)

Gary, F. M. (1997). *Polymer electrolytes*. Cambridge: Royal Society of Chemistry.

Gurtovenko, A., & Blumen, A. (2005). *Generalized gaussian structures: Models for polymer systems with complex topologies*

Hamlett, C. A. E., Jayasinghe, S. N., & Preece, J. A. (2008). Electrospinning nanosuspensions loaded with passivated au nanoparticles. *Tetrahedron, 64*(36), 8476-8483.

Hesse, M., Meier, H., & Zeeh, B. (1997). *Spectroscopic methods in organic chemistry* (A. Linden, M. Murray Trans.). New York: Georg Thieme Verlag Stuttgart.

Huang, Z., Zhang, Y. Z., Kotaki, M., & Ramakrishna, S. (2003). A review on polymer nanofibers by electrospinning and their applications in nanocomposites. *Composites Science and Technology, 63*(15), 2223-2253.

Jarusuwannapoom, T., Hongrojjanawiwat, W., Jitjaicham, S., Wannatong, L., Nithitanakul, M., Pattamaprom, C., et al. (2005). Effect of solvents on electro-spinnability of polystyrene solutions and morphological appearance of resulting electrospun polystyrene fibers. *European Polymer Journal, 41*(3), 409-421.

Ji, S., Li, Y., & Yang, M. (2008). Gas sensing properties of a composite composed of electrospun poly(methyl methacrylate) nanofibers and in situ polymerized polyaniline. *Sensors and Actuators B: Chemical, 133*(2), 644-649.

Jonassen, N. (2002). Electrostatics.

Kameoka, J., Orth, R., Yang, Y., Czaplewski, D., Mathers, R., Coates, G. W., et al. (2003). A scanning tip electrospinning source for deposition of oriented nanofibres. *Nanotechnology,* (10), 1124.

Kasai, N., & Kakudo, M. (2005). *X-ray diffraction by macromolecules*. Berlin Heidelberg New York: Springer.

Kessick, R., & Tepper, G. (2006). Electrospun polymer composite fiber arrays for the detection and identification of volatile organic compounds. *Sensors and Actuators B: Chemical, 117*(1), 205-210.

Kinlen, P. J., Liu, J., Ding, Y., Graham, C. R., & Remsen, E. E. (1998). Emulsion polymerization process for organically soluble and electrically conducting polyaniline. *Macromolecules, 31*(6), 1735-1744.

Kirk, R. E., & Othmer, D. F. (1991). In Kroschwitz J. I., Howe-Grant M. (Eds.), *Kirk-othmer encyclopedia of chemical technology* (4th ed.). New York: Wiley.

Larrondo, L., & St. John Manley, R. (1981a). Electrostatic fiber spinning from polymer melts. I. experimental observations on fiber formation and properties. *Journal of Polymer Science: Polymer Physics Edition, 19*(6), 909-920.

Larrondo, L., & St. John Manley, R. (1981b). Electrostatic fiber spinning from polymer melts. II. examination of the flow field in an electrically driven jet. *Journal of Polymer Science: Polymer Physics Edition, 19*(6), 921-932.

Larrondo, L., & St. John Manley, R. (1981c). Electrostatic fiber spinning from polymer melts. III. electrostatic deformation of a pendant drop of polymer melt. *Journal of Polymer Science: Polymer Physics Edition, 19*(6), 933-940.

Lee, J. S., Choi, K. H., Ghim, H. D., Kim, S. S., Chun, D. H., Kim, H. Y., et al. (2004). Role of molecular weight of atactic poly(vinyl alcohol) (PVA) in the structure and properties of PVA nanofabric prepared by electrospinning. *Journal of Applied Polymer Science, 93*(4), 1638-1646.

Li, D., Wang, Y., & Xia, Y. (2004). Electrospinning nanofibers as uniaxially aligned arrays and layer-by-layer stacked films. *Advanced Materials, 16*(4), 361-366.

Lin, Q., Jho, J., & Yee, A. F. (1993). Effect of drawing on structure and properties of a liquid crystalline polymer and polycarbonate *in-situ* composite. *Polymer Engineering & Science, 33*(13), 789-798.

Liu, G., Ding, J., Qiao, L., Guo, A., Dymov, B. P., Gleeson, J. T., et al. (1999). Polystyrene-block-pory(2-cinnamoylethyl methacrylate) nanofibers - preparation, characterization, and liquid crystalline properties. *Chemistry - A European Journal, 5*(9), 2740-2749.

Ma, P. X., & Zhang, R. (1999). Synthetic nano-scale fibrous extracellular matrix. *Journal of Biomedical Materials Research, 46*(1), 60-72.

Manuel Stephan, A., & Nahm, K. S. (2006). Review on composite polymer electrolytes for lithium batteries. *Polymer, 47*(16), 5952-5964.

Marcos, J. I., Orlandi, E., & Zerbi, G. (1990). Poly(ethylene oxide)-poly(methyl methacrylate) interactions in polymer blends: An infra-red study. *Polymer, 31*(10), 1899-1903.

Martin, C. R. (1996). Membrane-based synthesis of nanomaterials. *Chemistry of Materials, 8*(8), 1739-1746.

Matthews, J. A., Wnek, G. E., Simpson, D. G., & Bowlin, G. L. (2002). Electrospinning of collagen nanofibers. *Biomacromolecules, 3*(2), 232-238.

Matveeva, E. S. (1996). Residual water as a factor influencing the electrical properties of polyaniline. the role of hydrogen bonding of the polymer with solvent molecules in the formation of a conductive polymeric network. *Synthetic Metals, 79*(2), 127-139.

Mitchell, G. R., & Windle, A. H. (1988). Orientation in liquid crystal polymers. (pp. 115-175)

Mit-uppatham, C., Nithitanakul, M., & Supaphol, P. (2004). Ultrafine electrospun polyamide-6 fibers: Effect of solution conditions on morphology and average fiber diameter. *Macromolecular Chemistry and Physics, 205*(17), 2327-2338.

Norris, I. D., Shaker, M. M., Ko, F. K., & MacDiarmid, A. G. (2000). Electrostatic fabrication of ultrafine conducting fibers: Polyaniline/polyethylene oxide blends. *Synthetic Metals, 114*(2), 109-114.

Ondarçuhu, T., & Joachim, C. (1998). Drawing a single nanofibre over hundreds of microns. *Europhysics Letters, 42*(2), 215-220.

Pinto, N. J., Ramos, I., Rojas, R., Wang, P., & Johnson Jr., A. T. (2008). Electric response of isolated electrospun polyaniline nanofibers to vapors of aliphatic alcohols. *Sensors and Actuators B: Chemical, 129*(2), 621-627.

Rafique, J., Yu, J., Yu, J., Fang, G., Wong, K. W., Zheng, Z., et al. (2007). Electrospinning highly aligned long polymer nanofibers on large scale by using a tip collector. *Applied Physics Letters, 91*(6), 063126.

Ramakrishna, S., Fujihara, K., Teo, W. E., Lim, T. C., & Ma, Z. (2005). *An introduction to electrospinning and nanofibers* World Scientific.

Reimer, L. (1998). In Hawkes P. W. (Ed.), ***Scanning electron microscopy*** *physics of image formation and microanalysis* (2nd ed.). Berlin Heidelberg New York: Springer-Verlag.

Reneker, D. H., & Chun, I. (1996). Nanometre diameter fibres of polymer, produced by electrospinning. *Nanotechnology, 7*(3), 216-223.

Reneker, D. H., & Fong, H. (Eds.). (2005). *Polymeric nanofibers*. Washington, DC: American Chemical Society.

Reneker, D. H., & Yarin, A. L. (2008). Electrospinning jets and polymer nanofibers. *Polymer, 49*(10), 2387-2425.

Reneker, D. H., Yarin, A. L., Fong, H., & Koombhongse, S. (2000a). Bending instability of electrically charged liquid jets of polymer solutions in electrospinning. *Journal of Applied Physics, 87*(9), 4531-4547.

Reneker, D. H., Yarin, A. L., Fong, H., & Koombhongse, S. (2000b). Bending instability of electrically charged liquid jets of polymer solutions in electrospinning. *Journal of Applied Physics, 87*(9), 4531-4547.

Reneker, D. H., Yarin, A. L., Fong, H., & Koombhongse, S. (2000c). Bending instability of electrically charged liquid jets of polymer solutions in electrospinning. *Journal of Applied Physics, 87*(9 I), 4531-4547.

Ryan, M. A., Zhou, H., Buehler, M. G., Manatt, K. S., Mowrey, V. S., Jackson, S. P., et al. (2004). Monitoring space shuttle air quality using the jet propulsion laboratory electronic nose. *Sensors Journal, IEEE, 4; 4*(3), 337-347.

Scrosati, B. (Ed.). (1993). *Applications of electroactive polymers*. London: Chapman & Hall.

Segal, E., Tchoudakov, R., Narkis, M., Siegmann, A., & Yen, W. (2005). Polystyrene/polyaniline nanoblends for sensing of aliphatic alcohols. *Sensors and Actuators B: Chemical, 104*(1), 140-150.

Shacklette, L. W. (1994). Dipole and hydrogen-bonding interactions in polyaniline: A mechanism for conductivity enhancement. *Synthetic Metals, 65*(2-3), 123-130.

Shin, M. K., Kim, Y. J., Kim, S. I., Kim, S. K., Lee, H., Spinks, G. M., et al. (2008). Enhanced conductivity of aligned PANi/PEO/MWNT nanofibers by electrospinning. *Sensors and Actuators B: Chemical, 134*(1), 122-126.

Simons, H. L. (1966). Process and apparatus for producing patterned non-woven fabrics. *US Patent,* (3280229)

Son, W. K., Youk, J. H., Lee, T. S., & Park, W. H. (2004). The effects of solution properties and polyelectrolyte on electrospinning of ultrafine poly(ethylene oxide) fibers. *Polymer, 45*(9), 2959-2966.

Spivak, A. F., & Dzenis, Y. A. (1999). A condition of the existence of a conductive liquid meniscus in an external electric field. *Journal of Applied Mechanics, Transactions ASME, 66*(4), 1026-1028.

Sundaray, B., Subramanian, V., Natarajan, T. S., & Krishnamurthy, K. (2006). Electrical conductivity of a single electrospun fiber of poly(methyl methacrylate) and multiwalled carbon nanotube nanocomposite. *Applied Physics Letters, 88*(14), 143114.

Sundaray, B., Subramanian, V., Natarajan, T. S., Xiang, R., Chang, C. C., & Fann, W. S. (2004). Electrospinning of continuous aligned polymer fibers. *Applied Physics Letters, 84*(7), 1222-1224.

Svetlicic, V., Schmidt, A. J., & Miller, L. L. (1998). Conductometric sensors based on the hypersensitive response of plasticized polyaniline films to organic vapors. *Chemistry of Materials, 10*(11), 3305-3307.

Takahashi, Y., Sumita, I., & Tadokoro, H. (1973). Structural studies of polyethers. IX. planar zigzag modification of poly(ethylene oxide). *Journal of Polymer Science: Polymer Physics Edition, 11*(11), 2113-2122.

Takahashi, Y., & Tadokoro, H. (1973). Structural studies of polyethers, (-(CH2)m-O-)n. X. crystal structure of poly(ethylene oxide). *Macromolecules, 6*(5), 672-675.

Tan, C. K., & Blackwood, D. J. (2000). Interactions between polyaniline and methanol vapour. *Sensors and Actuators B: Chemical, 71*(3), 184-191.

Taylor, G. (1964). Disintegration of water drops in an electric field. *Proceedings of the Royal Society of London. Series A. Mathematical and Physical Sciences, 280*(1382), 383-397.

Theron, S. A., Zussman, E., & Yarin, A. L. (2004). Experimental investigation of the governing parameters in the electrospinning of polymer solutions. *Polymer, 45*(6), 2017-2030.

Tripatanasuwan, S., Zhong, Z., & Reneker, D. H. (2007). Effect of evaporation and solidification of the charged jet in electrospinning of poly(ethylene oxide) aqueous solution. *Polymer, 48*(19), 5742-5746.

Uyar, T., & Besenbacher, F. (2009). Electrospinning of cyclodextrin functionalized polyethylene oxide (PEO) nanofibers. *European Polymer Journal, 45*(4), 1032-1037.

Varesano, A., Carletto, R. A., & Mazzuchetti, G. (2009). Experimental investigations on the multi-jet electrospinning process. *Journal of Materials Processing Technology, 209*(11), 5178-5185.

Vonnegut, B., & Neubauer, R. L. (1952). Production of monodisperse liquid particles by electrical atomization. *Journal of Colloid Science, 7*(6), 616-622.

Wannatong, L., Sirivat, A., & Supaphol, P. (2004). Effects of solvents on electrospun polymeric fibers: Preliminary study on polystyrene. *Polymer International, 53*(11), 1851-1859.

Whitesides, G. M., & Grzybowski, B. (2002). Self-assembly at all scales. *Science, 295*(5564), 2418-2421.

Wilson, S. A., Jourdain, R. P. J., Zhang, Q., Dorey, R. A., Bowen, C. R., Willander, M., et al. (2007). New materials for micro-scale sensors and actuators: An engineering review. *Materials Science and Engineering: R: Reports, 56*(1-6), 1-129.

Windle, A. H. (1982). Measurement of molecular orientation and structure in non-crystalline polymers by wide angle X-ray diffraction. In I. M. Ward (Ed.), *Developments in oriented polymers-1* (pp. 1-46). London: Applied Science Publishers.

Yang, F., Murugan, R., Wang, S., & Ramakrishna, S. (2005). Electrospinning of nano/micro scale poly(L-lactic acid) aligned fibers and their potential in neural tissue engineering. *Biomaterials, 26*(15), 2603-2610.

Yang, J., Burkinshaw, S. M., Zhou, J., Monkman, A. P., & Brown, P. J. (2003). Fabrication and characteristics of 2-acrylamido-2-methyl-1-propanesulfonic acid-doped polyaniline hollow fibers. *Advanced Materials, 15*(13), 1081-1084.

Yarin, A. L., Koombhongse, S., & Reneker, D. H. (2001). Bending instability in electrospinning of nanofibers. *Journal of Applied Physics, 89*(5), 3018-3026.

Zong, X., Kim, K., Fang, D., Ran, S., Hsiao, B. S., & Chu, B. (2002). Structure and process relationship of electrospun bioabsorbable nanofiber membranes. *Polymer, 43*(16), 4403-4412.